

The University of Hull

**Real-time Detection of Auditory
Steady-State Brainstem Potentials
Evoked by Auditory Stimuli**

Being a thesis submitted for the Degree of PhD

in the University of Hull

by

LAM AUN CHEAH

MEng Electronic Engineering (Hull)

July 2010

Acknowledgements

This thesis has greatly benefited from the efforts and support of many people whom I like to thank. First and foremost, I would like to begin my acknowledgements by expressing my deepest gratitude to my principle supervisor Dr. Ming Hou for his heuristic teaching and guidance in every aspect of the thesis. I would also like to thank him for his friendship and suggestions, providing support and encouragement throughout my PhD research. He has always given me opportunities and flexibilities to explore new ideas, while assisting me to make critical decisions whenever the project was at a crossroad. I would also like to thank my associate supervisor Dr. Jim M Gilbert, for his time and guidance during the countless number of impromptu meetings over the duration of my PhD.

I am thankful to Prof. Ronald J Patton from Control and Intelligent Systems Engineering (C&ISE) for his valuable suggestions towards the project and Prof. Michael J Fagan from the Centre of Medical Engineering and Technology (CMET) for granting me access into his laboratory facilities. Acknowledgements also go to Mr. Peter Haugton from the Audiology Department of Hull Royal Infirmary for his medical expertises.

Many thanks go out to my fellow group members, Dr. Supat Klinkhieo and Dr. Cahit Perkgoz from Control and Intelligent Systems Engineering (C&ISE) for their academic expertise and good friendships. I gratefully acknowledge the financial support of my PhD study from the Engineering Department of The University of Hull.

I am indebted to my parents for their unconditional love, encouragement and support over my entire tertiary education. Last but not least, I would like express my appreciation to my lovely fiancé, Xiao Yan Dai for her understanding, patience, love and support during all these years.

Abstract

The auditory steady-state response (ASSR) is advantageous against other hearing techniques because of its capability in providing objective and frequency specific information. The objectives are to reduce the lengthy test duration, and improve the signal detection rate and the robustness of the detection against the background noise and unwanted artefacts.

Two prominent state estimation techniques of Luenberger observer and Kalman filter have been used in the development of the autonomous ASSR detection scheme. Both techniques are real-time implementable, while the challenges faced in the application of the observer and Kalman filter techniques are the very poor SNR (could be as low as -30dB) of ASSRs and unknown statistics of the noise. Dual-channel architecture is proposed, one is for the estimate of sinusoid and the other for the estimate of the background noise. Simulation and experimental studies were also conducted to evaluate the performances of the developed ASSR detection scheme, and to compare the new method with other conventional techniques. In general, both the state estimation techniques within the detection scheme produced comparable results as compared to the conventional techniques, but achieved significant measurement time reduction in some cases. A guide is given for the determination of the observer gains, while an adaptive algorithm has been used for adjustment of the gains in the Kalman filters.

In order to enhance the robustness of the ASSR detection scheme with adaptive Kalman filters against possible artefacts (outliers), a multisensory data fusion approach is used to combine both standard mean operation and median operation in the ASSR detection algorithm. In addition, a self-tuned statistical-based thresholding using the regression technique is applied in the autonomous ASSR detection scheme. The scheme with adaptive Kalman filters is capable of estimating the variances of system and background noise to improve the ASSR detection rate.

Table of Contents

List of Figures	vii
List of Tables	x
Glossary	xi
Chapter 1	1
Introduction	1
1.1 Motivation of Research	1
1.2 Hearing and Hearing Impairment	3
1.2.1 Human Auditory System	3
1.2.2 Classification of Hearing Loss	5
1.3 Hearing Detection and Intervention	7
1.3.1 Essentiality of Early Detection	7
1.3.2 Overview on Hearing Test	8
1.3.3 Follow-up Intervention	10
1.4 Key Challenges	11
1.5 Research Objectives	12
1.6 Thesis Outline and Contributions	13
1.7 Author's Publication List	15
1.7.1 Publications in Preparation	15
Chapter 2	16
An Overview on Auditory Steady-State Responses	16
2.1 Introduction	16
2.2 Theoretical Overview of ASSR	16
2.2.1 History and Terminology	16
2.2.2 Physiological Model	17
2.2.3 Stimulus Paradigms	18
2.2.4 Recording and Analysis Techniques	23
2.3 Clinical Applications	27
2.4 Concluding Remarks	27
Chapter 3	29
Preliminary Study of ASSR using Observer Approach via BIOPAC	29
3.1 Introduction	29
3.2 Observer-based Sinusoid Detector	30
3.2.1 Sinusoid Extraction	31
3.2.2 Variable Estimation	33

3.2.3	Thresholding	35
3.2.4	ASSR Detection Scheme	36
3.3	Simulation Study	38
3.3.1	Gain Tuning	38
3.3.2	Noisy Sinusoidal Signal (Low SNR)	39
3.4	Experimental Validation Study	40
3.4.1	Experimental Setup	41
3.4.2	Fundamental Frequency and its Harmonics	42
3.4.3	Intensity	43
3.4.4	Modulating Frequency	43
3.4.5	Relax and Non-relax	45
3.4.6	Types of Modulation Tones	45
3.4.7	Comparison between ASSR Detection Methods	46
3.5	Concluding Remarks	49
Chapter 4	51
On-line Detection of ASSR via Adaptive Kalman Filter	51
4.1	Introduction	51
4.2	Kalman Filtering	52
4.3	Adaptive Kalman Filtering	58
4.3.1	Background	58
4.3.2	Development of On-line Adaptive ASSR Detector	59
4.3.3	Simulation Results	68
4.4	Experimental Results	71
4.5	Concluding Remarks	75
Chapter 5	76
Improving the Robustness of ASSR Detection via Multiple Filters Fusion	76
5.1	Introduction	76
5.2	Artefact-Robust Detection	77
5.2.1	Background	77
5.2.2	Artefact-Robust Detection of ASSR via Statistical Operators	79
5.3	Multisensor Data Fusion Strategy	82
5.3.1	Overview	82
5.3.2	Kalman Filter-based Fusion Method	82
5.3.3	Development of Fusion-based ASSR Detector	84
5.3.4	Simulation Results	86
5.4	Experimental Results	91
5.5	Concluding Remarks	93
Chapter 6	94

Automatic ASSR Detection Scheme via Regression Modelling	94
6.1 Introduction	94
6.2 Automatic ASSR Detection.....	95
6.2.1 Regression Analysis	95
6.2.2 Simple Regression Linear	96
6.2.3 Development of Automatic ASSR Detector via Linear Regression	99
6.3 Outlier-Robust Automatic ASSR Detection.....	104
6.3.1 Background	104
6.3.2 Robust Regression.....	106
6.4 Evaluation.....	107
6.4.1 Simulation Results	107
6.4.2 Experimental Results	110
6.5 Concluding Remarks	114
Chapter 7.....	115
Conclusions and Future Research Intentions	115
7.1 Summary and Conclusion.....	115
7.2 Future Research Direction.....	119
References	121

List of Figures

Figure 1.1: Schematic of peripheral auditory system (Seikel <i>et al.</i> , 2000).....	3
Figure 1.2: Central auditory pathways (Bess and Humes, 1995).....	4
Figure 1.3: Positions of the base and apex ends relative to different frequencies (in Hz) in basilar membrane (adapted from Sherwood, 1993).....	4
Figure 1.4: Cross section of the cochlear (Seikel <i>et al.</i> , 2000).	5
Figure 1.5: A typical audiogram template for hearing test (adapted from Yetter, 2006). 6	
Figure 1.6: Cochlear implant devices (Clark, 2003).	11
Figure 2.1: A simple model for comprehensive rectification (Picton, 2006).....	18
Figure 2.3: Example of measurement of signal and noise at different ASSR frequencies (adapted from Picton <i>et al.</i> , 2003a).....	20
Figure 2.4: Examples of stimuli used in evoking ASSR (Picton <i>et al.</i> , 2003a).....	22
Figure 2.5: Time and frequency spectra of multiple ASSR stimuli (Stapells <i>et al.</i> , 2004).	23
Figure 2.6: International 10-20 standard of electrode placement (Sharbroug <i>et al.</i> , 1991).	24
Figure 2.7: Example of multiple ASSRs recorded corresponding to multiple stimuli (Staples <i>et al.</i> , 2004).	26
Figure 3.1: Architectural block diagram of the sinusoid detector.....	31
Figure 3.2: On-line ASSR detection scheme acquiring AEP via BIOPAC system.	36
Figure 3.3: Simulation results of (i) clean sinusoid (ii) noisy sinusoid (iii) noise.	37
Figure 3.4: The detection rate in identifying the presence of sinusoid via amplitude and power-based approaches (a) and (b) $SNR \approx 6dB$ (c) $SNR \approx -30dB$	37
Figure 3.5: Tuneable gain parameters to improve the sinusoid responses (a) $SNR \approx 6$ dB	39
Figure 3.6: Detection rates of the different SNR scenarios.	40
Figure 3.7: Schematic of the experiment setup for ASSR experiment (adapted from Luts, 2005).	42
Figure 3.8: Responses to various intensity stimuli.	43
Figure 3.9: Responses to 40Hz ASSR in relaxing and non-relaxing conditions.	44
Figure 3.10: Responses to 90Hz ASSR in relaxing and non-relaxing conditions.	44
Figure 3.11: ASSR responses to various types of modulation at 90 Hz modulated.	46

Figure 3.12: ASSR detection rate (a) using observer-based thresholding approach, (b)–(e) normal averaging plus FFT.....	48
Figure 4.1: Comparative between KF and observer-based detectors via (a) amplitude response and (b) detection rate.....	57
Figure 4.2: Amplitude responses between both AKF algorithms in (a) SNR= 20dB and (b) SNR= -20dB.	65
Figure 4.3: Autocorrelation plot for various test scenarios.....	66
Figure 4.4: Schematic of the proposed on-line adaptive ASSR detection scheme.	67
Figure 4.5: Output responses from process noise signals of (a) SNR 0dB and (b) SNR= -30dB.....	69
Figure 4.6: Comparative performance between optimal KF and AKF in detecting noisy sinusoid in SNR \approx -30dB.....	70
Figure 4.7: Identifying the existence and non-existence of a sinusoid in a low SNR environment (SNR \approx -30dB).	71
Figure 4.8: Determination of the existence and non-existence of ASSR.....	72
Figure 4.9: Comparison between standard the ASSR (single harmonic) and combined ASSR (multiple harmonics) detection rate responses.....	73
Figure 4.10: Comparison of performances between observer-based and AKF-based ASSR detectors.	74
Figure 5.1: Decentralization fusion architecture: State-vector fusion.	83
Figure 5.2: Centralization fusion architecture: Measurement fusion.....	83
Figure 5.3: Schematic of the adaptive ASSR detection scheme via MSDF.	85
Figure 5.4: Synthesized noisy sinusoidal signal corrupted with outliers.	87
Figure 5.5: Variance of measurement noise of sample mean and sample median operators.....	89
Figure 5.6: Error difference $\Delta e(\%)$ between different statistical operators.....	89
Figure 5.7: Comparative responses between detection using different operators via (a) amplitude response and (b) their mean square error.	91
Figure 5.8: Detection rate response between different operators.....	91
Figure 5.9: Comparative responses between fused and non-fused algorithms in ASSR detection.....	92
Figure 6.1: Schematic of the automatic ASSR detection scheme.....	100
Figure 6.2: Generic example of displaying regression frequency domain plot into time domain response.....	101

Figure 6.3: Schematic of objective of multiple ASSRs detection scheme.....	103
Figure 6.4: Schematic of objective of multiple ASSRs detection scheme (scaled version).....	104
Figure 6.5: Relationship between thresholding and linear regression detection rate responses.	108
Figure 6.6: Comparative performances between linear and robust regression methods in detection of outlier-free noisy sinusoid and with contamination of outliers.....	109
Figure 6.7: ASSR determination via linear regression and by thresholding.....	111

List of Tables

Table 3.1: Multiple stimuli parameters.	47
Table 3.2: Comparison between various detection methods for multiple ASSRs stimuli (without artefact rejection).	47
Table 3.3: Comparison between various detection methods for multiple ASSRs stimuli (with artefact rejection at $80\mu\text{V}$).	48
Table 4.1: Parameters setting for KF and observer-based detectors.	57
Table 4.2: Parameters setting of ASSR detector.	65
Table 5.1: Parameters setting of the synthesized outliers.	86
Table 5.2: Error e (%) between outliers present against outliers absent.	87
Table 6.1: Generic values used for demonstration of the example in Figure 6.2.	101
Table 6.2: Comparison between proposed method and other conventional methods. ...	113

Glossary

Mathematical Notation

$ \cdot $	Absolute value
$E[\cdot]$	Expectation value

Abbreviations

ABR	Auditory Brainstem Response
AEP	Auditory Evoked Potentials
AKF	Adaptive Kalman Filter
AM	Amplitude Modulation
AM^m	Exponential Modulation
ASSR	Auditory Steady-State Response
CI	Confident Interval
dB	Decibels
dB(A)	Decibels A weighted
EEG	Electroencephalogram
EFM	Exponential-Frequency Modulation
EMG	Electromyography
FFR	Frequency-Following Response
FFT	Fast Fourier Transform
FM	Frequency Modulation
HL	Hearing Level
Hz	Hertz
IRLS	Iterative Reweighted Least Square
JCIH	American Joint Committee on Infant Hearing
KF	Kalman Filter
LTI	Linear Time Invariant
MM	Mixed Modulation
MSDF	Multisensor Data Fusion
MSE	Mean Square Error
NHS	National Health Service
NHSP	Newborn Hearing Screening Programme
OAE	Otoacoustic Emission

OLS	Ordinary Least Square
SAM	Sinusoidal Amplitude Modulated
SNR	Signal-to-Noise Ratio
SPL	Sound Pressure Level
UNHS	Universal Newborn Hearing Screening

1 . Introduction

To begin with this introductory chapter, motivations are given for the techniques that will be developed in the forthcoming chapters of the thesis. In Section 1.2, an overview of the human auditory system and a brief classification of impairment are presented. Section 1.3 describes the essentials of having early hearing detection and the follow-up rehabilitation treatments. It includes fitting hearing aids and cochlear implants. Both subjective and objective hearing assessment techniques to obtain hearing thresholds estimation will also be described in Section 1.3.

Main challenges encountered are stated in Section 1.4, and with Section 1.5 presenting the research objectives of this thesis. The methodologies chosen for the thesis will also be briefly described in Section 1.5. An outline and an overview of the different chapters of the thesis will be given in Section 1.6.

1.1 Motivation of Research

The ability to hear and process sounds is crucial for an appropriate development of speech, language and cognitive abilities. However, at least one in a thousand worldwide and around 840 newborns each year in the UK suffer from permanent bilateral hearing loss (The Hearing Research Trust, 2005). Therefore, early diagnosis and rehabilitation are vital to reduce the handicap of hearing loss in those children. If the outcome of the initial hearing screening test is abnormal, the infant is to be referred for further hearing threshold diagnosis. However, the standard behavioural observation assessments are not

applicable for infants. This is because of the nature of these hearing assessments which require reliable responses from the subjects. Thus, objective audiometric techniques appear to be suitable options for hearing assessments which are able to quantify test results more objectively and not influenced by sleep or sedation of the subject. As a result, the objective audiometric techniques are vital to the “difficult-to-test” population, which mainly consists of infants, children and patients with disabilities (Fulton and Lloyd, 1969; Picton, 1991)

Nowadays the most commonly used objective audiometric techniques for young infants are otoacoustic emissions (OAE), click-evoked audiology brainstem response (ABR) and auditory steady-state response (ASSR). The OAE approach is to test cochlear status (mainly hair cell function) founded by Kemp (1979), and it is only limited for hearing screening purposes because of its frequency-specificity that is not correlated with threshold of the observed subject and also not observable at hearing losses for 40dB HL and higher (Luts and Wouters, 2004). Meanwhile, click-evoked ABR is generally used for hearing screening and hearing threshold estimation but the technique is limited in identifying the degree of hearing loss and providing essential frequency specific information required for any rehabilitation treatment, for instance, fitting a hearing aid or surgical need for a cochlear implant (Luts *et al.*, 2006). In response to the shortcomings of these techniques, the ASSR was developed to provide vital frequency-specific hearing threshold estimation that is highly correlated with the standard behavioural observation assessments and to perform within an acceptable duration of time typically at approximately 60 minutes (Luts and Wouters, 2004; Ahn *et al.*, 2007).

The ASSR also has its drawbacks. Since the ASSR is a faint auditory evoked responses (AEP), the technique is very susceptible to noise and artefacts which disrupt the measurement and pro-long the recording time. Recent studies revealed that a reliable ASSR based hearing threshold estimation for adults are approximately an hour and could last for hours if tested on newborns (Luts and Wouters, 2004). This thesis will introduce several approaches with the aim to reduce ASSR measurement time and to increase its robustness against background noise and artefacts.

1.2 Hearing and Hearing Impairment

Hearing is one of humans' five senses, and commonly refers to the ability to detect sound. Surprisingly, humans extract more information from sound than any other senses. Although human primates are known as visually oriented animals, speech and music carry more of culture and societal meaning than sight or other senses. Moreover, humans suffer more from deafness than with other sensory losses (Clopton and Viogt, 2006). This section provides a brief survey of essential parts of the auditory system and the classification of hearing impairments.

1.2.1 Human Auditory System

The human auditory system can be divided into two main sections, the peripheral auditory system (including outer ear, middle ear and inner ear) (see Figure 1.1) and the central auditory pathways (see Figure 1.2) (Yost, 2000).

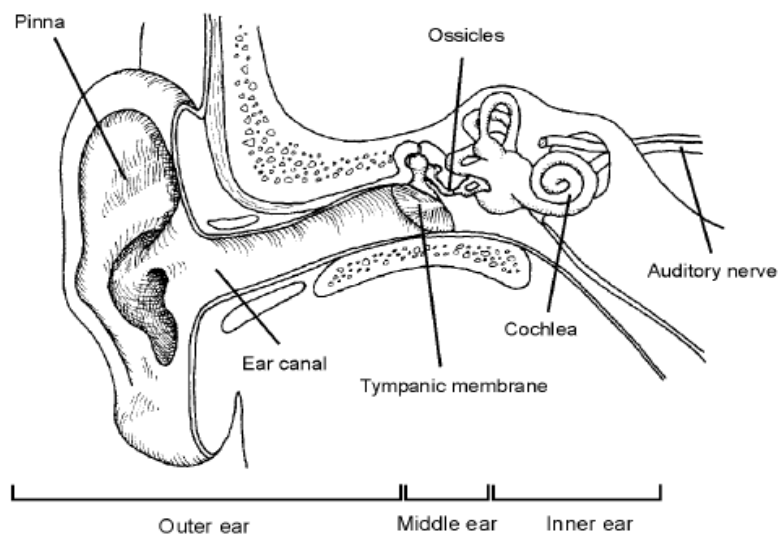


Figure 1.1: Schematic of peripheral auditory system (Seikel *et al.*, 2000).

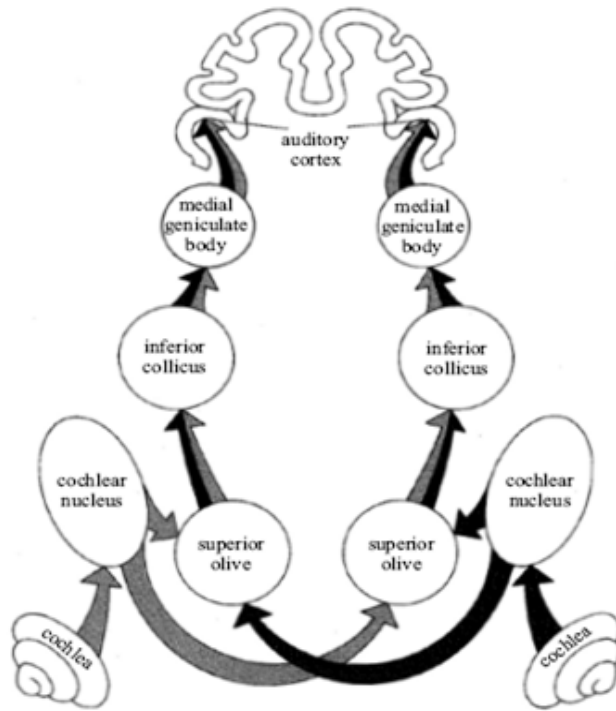


Figure 1.2: Central auditory pathways (Bess and Humes, 1995).

Human hearing process consists of a sequence of complex sound transformations as the sound travels through peripheral auditory system and central auditory pathways. The sound energy enters the outer ear through the ear canal and causes the tympanic membrane to vibrate, thus the acoustical energy is converted into mechanical energy. The mechanical vibration energy is then transmitted by the ossicles (human's smallest bones, i.e. *malleus*, *incus* and *stapes*) in the middle ear to the oval window. This induces motion in the fluids of the cochlear, also known as auditory filter bank (see Figure 1.3) (Moore, 2003). This would then causes a wave-like movement of the basilar membrane and its surrounding structures (see Figure 1.4).

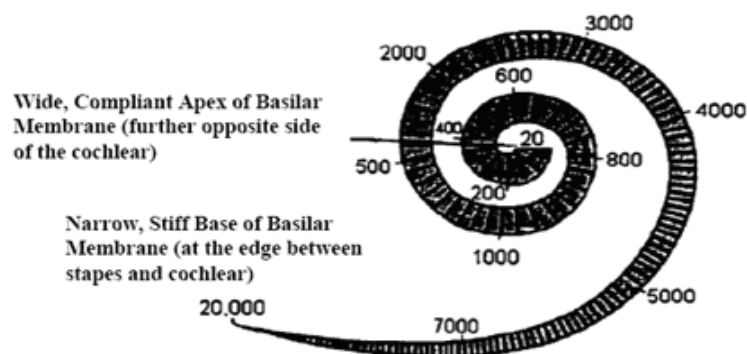


Figure 1.3: Positions of the base and apex ends relative to different frequencies (in Hz) in basilar membrane (adapted from Sherwood, 1993).

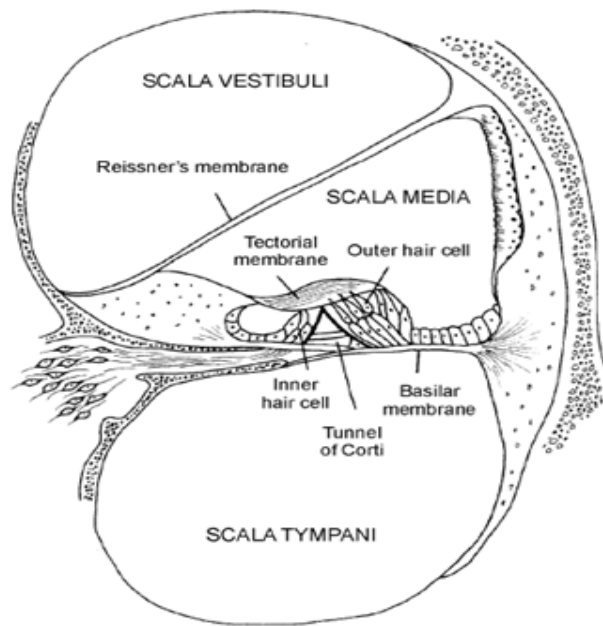


Figure 1.4: Cross section of the cochlear (Seikel *et al.*, 2000).

With this mechanism, the hair cells are moved relative to the tectorial membrane and the hairs on top of the hair cells are then bent. The displacement of the hairs leads to excitation of the hair cells and thus creates the generation of actions potentials in the neurons of the auditory nerve (Pickles, 1988; Northern and Downs, 1991). Therefore, the mechanical vibrations are transformed into electrical events and then transmitted to the central auditory pathways by the auditory nerve. However, both the cochlear and the auditory nerve represent only the first initial stages of information extraction of auditory signal. Electrical events are transmitted to neurons at higher levels of the central auditory pathways for further extraction of information, and the responses of these neurons are more complex yet not well defined so far (Nolte, 1988). These pathways are not be discussed in this thesis, but detailed information can be found in Clopton and Viogt (2006).

1.2.2 Classification of Hearing Loss

Hearing loss can be classified into three attributes, which are the degree, type and configuration of the hearing loss. The degree of hearing loss refers to the severity of the loss (range of intensities that one able to hear) and commonly groups into, normal hearing (0—25dB HL), mild hearing loss (26—45dB HL), moderate hearing loss (46—70dB HL), severe hearing loss (71—90dB HL), and profound hearing loss (above 90dB HL), as shown in Figure 1.5. The hearing level (HL) suffix is a relative scale with

its zero defined by the standard audiograms of a group of normal hearing young adults (International Organization for Standardization, 1998).

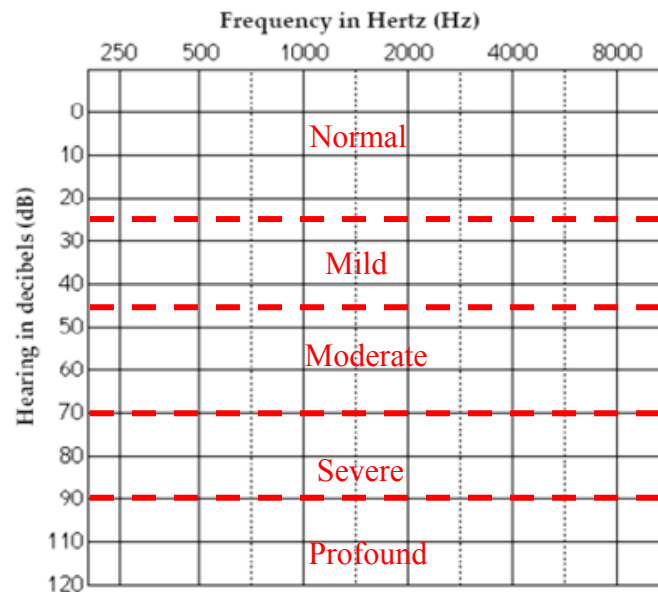


Figure 1.5: A typical audiogram template for hearing test (adapted from Yetter, 2006).

Next, classification of the type of hearing loss is based on the auditory anatomical location of the impairment. If the sound is attenuated (sound level reduced) through the outer and middle ear, conductive hearing loss occurs. On the other hand, if the inner ear or the auditory nerve pathway is damaged, common sounds are not only attenuated but also distorted, thus sensorineural hearing loss is present. However, only conductive hearing loss can be corrected by medicine or surgery, but sensorineural hearing loss is permanent and neither medication nor surgery is effective. The last type of hearing loss is called mixed hearing loss, which occurs with a combination of both conductive and sensorineural hearing losses (Hall, 1992; Haughton, 2002).

Lastly, the configuration of hearing loss often refers to the extent of the hearing loss in particular frequency ranges. In general, possible configurations are high-frequency/low-frequency hearing loss, flat hearing loss and a cookie-bite configuration. A bilateral hearing loss refers to that both ears are affected, while unilateral hearing loss means just one ear is affected. In a symmetrical hearing loss, the degree and configuration is the same in each ear, in contrast with asymmetrical hearing loss (Hall, 1992; Haughton, 2002).

1.3 Hearing Detection and Intervention

This section discusses the importance of early hearing diagnosis (or screening) and with appropriate follow-up intervention for hearing impaired subjects. An early detection is vital particularly for children, because language development will be delayed if the hearing problem is not remedied. On the other hand, hearing loss can cause adults feeling socially isolated and compromise personal achievements. This section also describes two possible rehabilitation approaches, i.e. fitting hearing aids and cochlear implants.

1.3.1 Essentiality of Early Detection

At least one in a thousand newborns worldwide suffers from permanent bilateral hearing loss (Mason and Herrmann, 1998; Dalzell *et al.*, 2000). Hearing loss in children is a silent, hidden handicap. If undetected and untreated, it can lead to delayed speech and language development, learning, social and emotional problems (Northern and Downs, 1991). The development of the auditory nervous relies partly on auditory input, while language acquisition in human requires a critical period of good hearing capacity which spans the frequency range of human speech (between 300–3000 Hz). The critical period is from birth until approximately 12 months of age. The longer auditory language stimulation is delayed because of an undetected hearing loss, the less efficient will be the language facility, because there is a critical period for the development of language (Northern and Downs, 1991). Moreover, the study conducted by Yoshinaga-Itano *et al.* (1998) demonstrated that significant better language development is associated with identification of hearing screening and intervention within 6 months of age.

Since undetected hearing loss has crucial impacts on the development of language abilities and communicative competence of infants or young children, American Joint Committee on Infant Hearing (JCIH) was established and is responsible in making recommendations concerning the early identification of children at-risk for hearing loss and newborn hearing screening (Joint Committee on Infant Hearing, 2000). In 2000, the committee endorsed screening of all neonates' hearing using objective physiologic measures named Universal Newborn Hearing Screening (UNHS). The recommendations of the UNHS are summarised as:

- All infants should undergo hearing screening before 1 month of age.

- An appropriate audiological and medical diagnosis should be made before age of 3 months if one failed the previous stage of hearing screening.
- All infants with confirmed permanent hearing loss should receive multidisciplinary intervention by age of 6 months.

The screening procedures suggested in UNHS consist of a combined non-invasive objective approach using both OAE and ABR testing. In general, the ABR test is a measurement of the response to sounds from the lowest part of the brain (the brainstem). The auditory system is stimulated by a brief acoustic signal via air (with earphones) or bone (with bone vibrator) conduction. The resulting neuro-electric activity is then recorded by surface electrodes placed on the head, and its response is accessed based on the identification of the components within the waves, their morphology and the measurement of absolute and interwave latencies (University of Michigan Health System, 2003). Unlike the ABR, the acoustic emissions are sounds generated by the outer hair cells in the cochlear of a person with normal hearing or with mild hearing loss. The OAE are measured by a probe (small microphone) which is placed in the ear canal after direct acoustic stimulation from the probe and perceived by the cochlear (University of Michigan Health System, 2003). In the United Kingdom, the UNHS equivalent hearing screening assessment is carry out under the National Health Service (NHS) under Newborn Hearing Screening Programme (NHSP). The screening protocol is similar to the UNHS and all infants are scheduled to be screened before the first 5 weeks from their birth and to receive appropriate rehabilitation support within the following six months (NHS, 2008).

1.3.2 Overview on Hearing Test

There are generally two approaches to test hearing, subjective and objective hearing tests. Subjective testing requires a behavioural response from the subject. These tests are done in the test booth by watching the baby's responses to sound or by playing a "Listening game" with the child. There are three subjective hearing test methods (University of Michigan Health System, 2003):

- Behavioural observation audiometry (from birth to seven months).
- Visual reinforcement audiometry (from seven until thirty months).
- Conditional play audiometry (thirty months and above).

On the other hand, objective hearing tests (e.g. OAE, ABR and ASSR) do not require responses or cooperation from the child. In many situations, these infants may be unwilling or unable to participate in any of the conventional behavioural (subjective approaches) auditory tests at their early age. Although the ABR and OAE have been well established in both clinical and research areas for at least 20 years, there are limitations within these hearing tests (Brookhouser *et al.*, 1990; Hall, 1992 and 2000; Luts *et al.*, 2004). The limitations are:

- Lack of frequency specific information for click-evoked (transient) ABR especially below 1000 Hz, which is required in determining the configuration of hearing loss. Although tone-burst ABR could overcome the problem, it is still difficult to record and observe at near threshold levels (particularly at lower frequencies).
- The subjective nature of assessing responses of ABR, which requires visual detection of waveform peaks, latencies and morphology by highly experienced examiner to undertake and interpret the results accurately. Thus, ABR cannot be classified as 100% objective test.
- Only limited information can be provided by either click-evoked or tone-burst ABR for hearing loss greater than 90dB HL. Therefore, it could be hard to discriminate severe-to-profound threshold for hearing impaired children and to provide accurate advice when it comes to hearing aid fitting or cochlear implant.
- A lengthy test duration is required by the ABR due to multiple recordings at various intensity levels and at multiple frequencies to estimate the degree of hearing loss.
- Since OAE testing does not correlate to behavioural thresholds and only use to indicate the normality function of outer hair cell. Therefore, limited information is available about the configuration, type or degree of hearing loss.

In recent years, the ASSR had gained considerable attention and some excitement by audiologists, especially those who are involved in the assessment and subsequent hearing aid fitting for very young infants with hearing disability. It is believed, compared to commonly clinically used objective AEP methods (i.e. the click-evoked ABR), that the ASSR has some interesting features (Aoyagi *et al.*, 1994; Cone-Wesson *et al.*, 2002a; Stueve and O'Rourke, 2003; Swanepoel and Hugo 2004):

- More frequency specific auditory stimulus in activating the desired part of cochlear to produce response.
- Information is available on profound levels (greater than 90dB HL) of hearing impairment, thus making the procedure of fitting a hearing aid less challenging.
- Fully objective detection method could be applied compared with the visual inspection method needed by ABR.
- Minimally affected by sedation as compared to ABR, which is crucial in some cases.
- Further reduction of test time by simultaneous multiple stimulus presentation (i.e. multiple ASSR stimuli).

1.3.3 Follow-up Intervention

The decision on whether a hearing aid or a cochlear implant to be fitted as part of the rehabilitation depends on the initial hearing screening assessment, to provide sufficiently accurate information about the hearing loss so that hearing evaluation can be graphically represented by an audiogram. As described in Section 1.3.2, these can be carried out by either subjective or objective approaches. Some permanent hearing impairment cases can be treated through surgery or medication. Alternatively, the use of a hearing aid and a cochlear implant can be implemented. A hearing aid is commonly use in cases of mild to severe hearing loss, records sound signals in the acoustic environment through one or more microphones (Dillon, 2001). These sound signals are often a mixture of a speech and unwanted noise. The recorded signals are then amplified by a loudspeaker according to the user specific hearing thresholds to the user ear canal (Dillon, 2001).

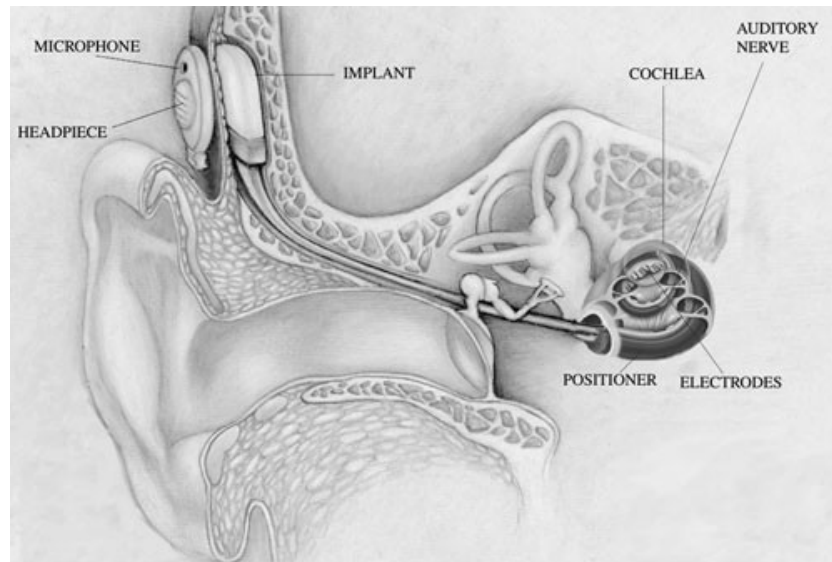


Figure 1.6: Cochlear implant devices (Clark, 2003).

On the other hand, a cochlear implant is used to bypass the hair cell by stimulating the auditory nerve directly for cases of profound hearing loss or deafness. The implant may restore the perception for the subject who has much severe hearing loss, but the auditory nerve is still intact (Clark, 2003). A cochlear implant device (see Figure 1.6) consists of a microphone that picks up sound from the environment, a signal processor which selects sounds picked up and transforms them into electrical signals, a transmission system that transmits the electrical signals to the implanted electrodes, and an electrode or an electrode array (multiple electrodes) is inserted into the cochlea to collect the impulses from the stimulator and sends them to the auditory nerve (Loizou, 1998). Detailed description on functionality of these instruments will not be covered in this thesis.

1.4 Key Challenges

The interest to implement ASSR as an essential part of hearing diagnostic assessment has increased significantly worldwide, with recent experimental studies demonstrated that the ASSR technique can estimate a frequency specific hearing threshold faster than ABR technique. Unfortunately, the technique is very susceptible to background noise and artefacts that disrupt the measurement. This is because ASSR signal is a very weak AEP response with extremely low signal-to-noise ratio (SNR). It is embedded in strong background noise mainly represented by electroencephalogram (EEG). Besides, with the implementation of the present ASSR detection method that involves artefacts rejection protocol, signal averaging and the use of fast Fourier transform (FFT) with

employment on statistical test, this can be a very lengthy test procedure in conducting a reliable hearing test for infants or young children. This is because the infant needs to be asleep or otherwise sedated in order to reduce the background noise level and to avoid any interruption by the infant during the test to minimise the occurrence of artefacts. Further delay can be caused by discarding the recorded epochs that contaminated with artefacts, because this is vital in order to ensure the reliability of the latter processing stages (i.e. averaging, FFT and statistical test). In addition, extra waiting time is required in order to have sufficient recorded data available for averaging and FFT to ensure meaningful output resolution. Moreover, by combining averaging and FFT, it therefore cannot be operated in real-time principally. It is believed that, a less complex medical instrument will be welcomed by hospitals globally and could also be an alternative solution for the expansion of the adoption of UNHS globally, especially in developing countries.

1.5 Research Objectives

To address problems stated in Section 1.4, this study has aimed to develop an on-line automatic ASSR detection scheme based on the state estimation techniques. These algorithms should improve the time efficiency of the screening assessment and still be capable of providing accurate thresholds estimation without test-controlled environments (i.e. using a test booth). These objectives have been achieved with the following activities:

- To investigate the use of state estimation techniques, such as Luenberger observer and Kalman Filter (KF), in estimating single/multiple ASSRs (Chapter 3 and 4).
- To introduce an observer-based thresholding approach (ASSR decision making) via amplitude-based and power-based evaluation (Chapter 3).
- To extract ASSR signals from AEP (low SNR) using adaptive Kalman filter (AKF), and develop an on-line adaptive ASSR detection scheme based upon thresholding approach (Chapter 4).
- To investigate the use of artefact-resilient method such as median operator, to improve the robustness of the ASSR detector against possible artefacts within the AEP (Chapter 5). In addition, to improve the ASSR detection in terms of efficiency and robustness, multisensor data fusion (MSDF) technique is used to provide combined data outputs (Chapter 5).

- To develop an objective ASSR evaluator by implementing a linear regression technique to model the background noise, thus could further improve the ASSR detection rate (Chapter 6). Moreover, to further enhance the accuracy of the objective ASSR evaluator when dealing with possible outliers, robust regression technique is used to model the background noise (Chapter 6).

1.6 Thesis Outline and Contributions

The remainder of the thesis is arranged in the following manner:

Chapter 2 introduces the theoretical concepts of the ASSR in terms of its history, physiological model, stimulus parameters, recording and analysis approaches. The chapter also briefly describes other existing ASSR detection algorithms.

Chapter 3 develops an alternate ASSR detection approach using Luenberger observer (continuous state estimation approach) for its merit in simplicity for single-channel ASSR recording. This state estimation approach is based upon the idea of estimating or filtering the ASSR signal from the background noise. Two ASSR detection schemes (via amplitude-based or power-based evaluation) are introduced as part of the observer-based method. Several simulation platforms were developed to evaluate the performances of the proposed algorithms with synthetic data. Besides the simulation studies, experimental data recorded from the BIOPAC data acquisition system were used for the preliminary studies on the ASSR. The experimental data were also used in testing and evaluation of the proposed observer method.

Chapter 4 develops a discrete version of the state estimation approach which operates adaptively. An on-line adaptive ASSR detection scheme based on the AKF is proposed. It has the advantages in estimating the ASSR with unknown AEP's SNR and noise statistics. The idea is to estimate the noise statistics adaptively and thus extracting the ASSR from recorded AEP in real-time with suitable gain parameters. As for the decision making in detection rate, a thresholding method is proposed by using an empirical pre-defined level to determine the existence or non-existence of the ASSR. Simulation studies with synthetic data were used to evaluate the performances of the proposed ASSR detector in terms of accuracy and speed of convergence in the detector. BIOPAC recorded data with single and multiple ASSRs were also used to test the

practicality of algorithms towards real-world data. In order to further reduce the test duration, an approach consisting of ASSR's multiple harmonics (includes not only its fundamental frequency component) is used in detection.

Chapter 5 considers the problem of the robustness of the ASSR detection against extreme values or artefacts in measurement. Although the AEP measurement is assumed to be pre-bandpass filtered to avoid highly non-Gaussian and noise interfered regions, artefacts (e.g. muscle movement, eye blinking and etc.) or sometimes known as extreme values or outliers may still occur by chance in AEP. The proposed ASSR detector in Chapter 4 is not robust against artefacts contaminated measurements, even one extreme value would have the detection biased. As a result, to improve the robustness of the ASSR detector against unprecedented artefacts, a more robust approach is integrated into the detection. However, sample mean (non-robust) and sample median (robust) both have their advantages depending on the normality or non-normality (e.g. skewness, kurtosis and asymmetrical) of the data sampled (measurement). In general, sample mean operates better (higher output efficiency) if the sample data is normal and symmetric, whereas the sample median performs better if the data is skewed (existence of significant value of outlier within the data distribution). Since no *a priori* knowledge is available regarding if any of the measurement is to be corrupted with artefacts or not, combining these two approaches would in theory produce an output which has best of both statistical operations. The MSDF strategy is used to fuse the estimates from multiple AKFs (one with sample mean operator and the other with median operator) in order to produce a better ultimate ASSR detector.

Chapter 6 presents an objective ASSR decision making approach through a comparison between the estimated ASSR and its background noise estimated. Regression modelling is used to predict the expected noise component that has same frequency to the ASSR based on the neighbouring noise estimates. The ASSR detection rate via the thresholding method (proposed in Chapter 4) is based on time domain, whereas the noise estimation via regression modelling is based on frequency domain but able to be converted into the time domain through an evaluation module. In addition, the thresholding approach can be seen as a 'semi-objective' decision making approach because its threshold level needs to be empirically pre-defined, whereas the regression based approach is completely automatic in determination of ASSR existence. In order to improve the robustness of estimating the background noise, robust regression approach

is used instead of linear regression modelling. The ordinary least square method is commonly used in the linear regression but it is not robust against outlier contaminated data. On the other hand, there are several methods available for robust regression, the interactive reweighted least-squares technique (with Tukey's Bisquare weight) is chosen because of its reliable outlier-robustness performance and computation moderate.

Chapter 7 comprises a general conclusion of the research and with an overview of future research directions.

1.7 Author's Publication List

The following is a list of publication that have been accepted and submitted during his PhD candidacy:

- Cheah, L. A., and Hou, M. (2010), "Real-time Detection of Auditory Steady-State Responses", *32nd International Conference of the IEEE Engineering in Medicine and Biology Society*, August 31—September 4, Buenos Aires, Argentina, Accepted for presentation.
- Cheah, L. A., and Hou, M. (2010), "Detection of Auditory Steady-State Responses via Dual-Channel Observers", *IEEE Transactions on Biomedical Engineering*, Submitted for publication.

1.7.1 Publications in Preparation

The following is a list of publications currently under preparation for submission:

- Cheah, L. A., and Hou, M. "Improving the Robustness of Auditory Steady-State Responses Detection against Artefacts via Fusing Multiple Adaptive Kalman Filters", *To be submitted to the IEEE Transactions on Biomedical Engineering*.
- Cheah, L. A., and Hou, M. "Automatic Detection of Auditory Steady-State Responses by using Adaptive Thresholding", *To be submitted to the IEEE Transactions on Biomedical Engineering*.

2 . An Overview on Auditory Steady-State Responses

2.1 Introduction

This chapter describes the fundamentals of auditory steady-state responses (ASSRs) and gives an overview of the existing detection techniques. The aim of Section 2.2 is to cover the theoretical aspects of the ASSR, which includes its history, terminology, stimulus methodology, recording and processing methods. A brief description of the current commercially available ASSR detection system is also presented in Section 2.2. An overview of its clinical applications is provided in Section 2.3. Concluding remarks for the Chapter made in Section 2.4.

2.2 Theoretical Overview of ASSR

2.2.1 History and Terminology

An ASSR is an evoked potential ‘whose constituent discrete frequency components remain constant in amplitude and phase over infinity long time period’ (Regan, 1989). The ASSR is a type of the auditory evoked potential (AEP) and recorded when stimuli are presented periodically. The resulting response often resembles a sinusoidal waveform whose fundamental frequency is the same as the stimulation rate. In other words, the stimulus drives the human brain’s auditory response. Human steady-state

evoked potentials are not new, in fact first recorded in 1960 from the scalp of a human in response to visual stimuli (Regan, 1966). The averaging method was developed and used to extract these steady-state responses from the background electroencephalogram (EEG) (Geisler, 1960).

However, the main trigger for the extensive research into human ASSR came with the publication by Galambos *et al.*(1981) concerning that the response is very predominant at stimulus rates near 40 hertz (Hz) or known to be *40-Hz ASSR*. It was also found that the response was smaller (decrease) when the subject was drowsy or asleep (Galambos *et al.*, 1981; Linden *et al.*, 1985; Cohen *et al.*, 1991) and very difficult to record in infants (Suzuki and Kobayashi, 1984; Stapells *et al.*, 1988; Rance *et al.*, 1995). Studies investigating the neural sources of 40 Hz response have concluded that the response is a combination of both brainstem and cortical generators (Herdman *et al.*, 2002). According to the study by Rickards and Clark (1984), the ASSR can be recorded in different stimulus rates, and the amplitude of the responses decreases with increasing stimulus rate. In addition, stimulus rates greater than 70 Hz were not affected by sleep (Cohen *et al.*, 1991). To date, there has been relatively little study and discussion of the nature and origins of 70—100 Hz or simply known as *80-Hz ASSR*. Many studies investigating the neural sources of *80-Hz ASSR* for both humans and animals indicate they originate primary from brainstem structures (Herdman *et al.*, 2002; Kuwada *et al.*, 2002). Although no final conclusion was made, researchers believe that *80-Hz ASSR* corresponds to the actually auditory brainstem response (ABR) wave V, to rapidly presented stimuli. This is also known as brainstem ASSR. An extensive overview of the historical development of ASSR can be found in (Picton *et al.*, 2003 and 2006).

2.2.2 Physiological Model

Pre-defining how the cochlear transducer works is essential for the understanding of the underlying principle of ASSR. A physiological model for ASSR can be described as compressive rectification of the signal waveform (Lins and Picton, 1995; Lins *et al.*, 1996). Sinusoidal amplitude modulated tone (stimulus) has no acoustic energy at the modulation frequency, while containing energy at the carrier frequency and at two sidebands separated from the carrier by the modulation frequency (as shown in left hand side of Figure 2.1). This means that the stimulus only activates limited or specific part of the cochlear, centred at the carrier frequency. A process of rectification occurs when

the stimulus (sound) is captured by the ear and a transduction occurs in the cochlear to which is further discharged (depolarized) in the auditory nerve fibres. Only depolarization causes the auditory nerve fibres to transmit action potentials. The rectified signal now contains energy both at the frequency of the original signal and at the modulation frequency (as shown on the right hand side of Figure 2.1). The neurons in the brainstem then synchronize either to the carrier frequency to generate a frequency-following response (FFR) or to the modulation frequency to produce the envelope-following response or known to be ASSR. In other words, FFR is a steady-state response to the carrier frequency, whereas the ASSR is a response to the modulation frequency (or envelope) of the modulated tone. The disadvantage of using FFR is that it cannot be easily recorded at low intensity or at frequencies higher than 1000 Hz, whereas the envelope-evoked ASSR can be recorded for all carrier frequencies and at intensities near to hearing thresholds.

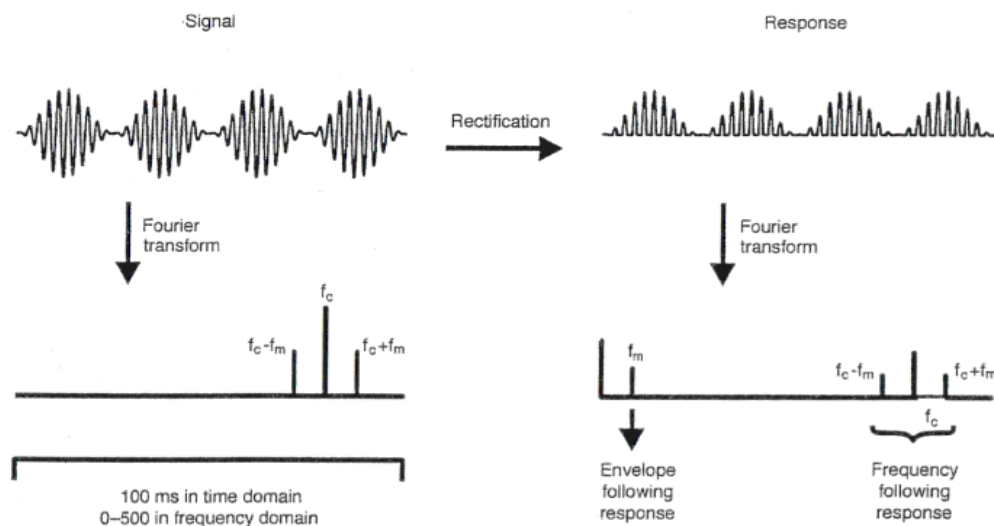


Figure 2.1: A simple model for comprehensive rectification (Picton, 2006).

2.2.3 Stimulus Paradigms

Although the ASSR can be evoked by various stimulus types such as clicks, tone burst or sinusoidal amplitude or/and frequency modulated tones, modulated tones stand out with their frequency specific characteristics (Picton *et al.*, 2003a). Several aspects on selection or presentation of stimulus are to be discussed as follows.

Carrier frequency

The carrier frequency determines the activation area of the basilar membrane in the cochlear. Although octave frequencies from 125—8000 Hz are commonly assessed in audiometric tests, only the frequencies between 500—4000 Hz that are particularly important for human speech understanding are assessed with the audiogram (Petitot *et al.*, 2005; Tlumak *et al.*, 2007). A typical example of an audiogram is shown in Figure 1.5, with the x-axis representing the range of carrier frequencies to be used and the y-axis representing the intensity at a particular frequency.

Modulation frequency

The modulation rate of the presented stimulus defines the characteristic of the ASSR response. As the ASSR is embedded in the EEG, the amplitude of the ASSR is measured as the amplitude at the modulation rate, which is the sum of the signal amplitude and the residual EEG noise. Typically, the ASSR amplitude decreases with an increasing modulation rate (see Figure 2.2). However, in certain regions, there is an enhancement of the response above the general decline, especially at 40 Hz and 90 Hz. In other words, the detection rate of the ASSR relies on the characteristics of the EEG (main component of the background noise). The EEG consists of several simultaneous oscillations, which are subdivided into frequency bands such as delta (1—3 Hz), theta (4—8 Hz), alpha (8—12 Hz), beta (about 14—30 Hz) and gamma (around 40 Hz). When a response is recorded from the brain, the EEG itself is intermixed with other electrical activities from the scalp muscles, eyes, skin and tongue. However, the EEG activity decreases with increasing in frequency, where its activity is most prominent at frequencies below 25 Hz. Although, the response amplitude reduces at higher modulation rates, in fact the SNR is increasing (Picton *et al.*, 2003a). As mentioned above, the 40-Hz ASSR response is influenced by both sleep and sedation, and it is much more difficult to measure from young children, because of the effect of the overlapping of the short latency responses from the brainstem and the middle latency responses from the primary auditory cortex. In this context *latency* is a measure of the time taken for the auditory system to respond after a stimulus has been presented.

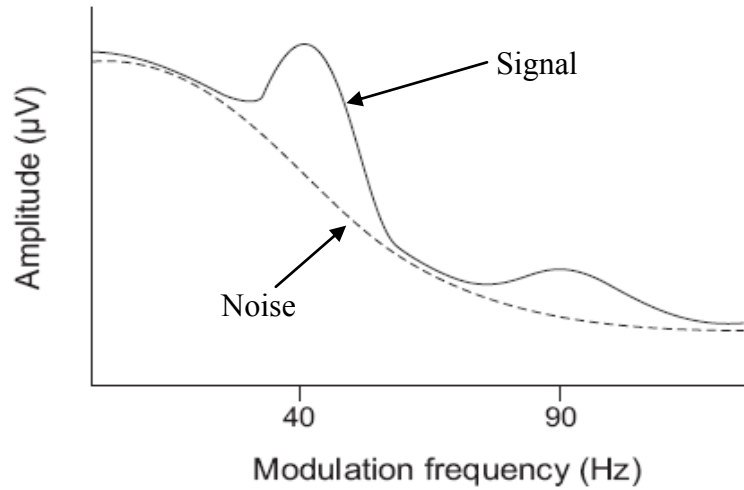


Figure 2.2: Example of measurement of signal and noise at different ASSR frequencies (adapted from Picton *et al.*, 2003a).

Intensity

The intensity of the stimulus has significant effects on the recording of individual response with regard to the presentation of single or multiple stimuli. Generally, as the intensity of the stimulus increases, the amplitude of the response increases and the latency decreases (Galambos *et al.*, 1981; Stapells *et al.*, 1984; Picton *et al.*, 2003).

Types of Modulation

The commonly utilized stimuli to evoked ASSR are sinusoidal amplitude modulated (SAM) tones, simply known as amplitude modulation (AM). These stimuli have a simple spectrum, containing spectral energy at the carrier frequency and in two sidebands on each side of the carrier frequency. The formula that represents AM is:

$$s_{AM} = A[1 + m_a \sin(2\pi f_m t)] \sin(2\pi f_c t) \quad (2-1)$$

where A is the amplitude of the stimulus, t is the time, f_m is the modulation frequency of AM, f_c is the carrier frequency, and m_a is the depth of AM (ratio of the difference between the maximum and minimum amplitudes of the signal to the sum of the maximum and minimum amplitudes). As m_a increases, the spectral energy at the carrier frequency decreases and the energy at the sidebands increases. A modified AM tone can be achieved by replacing the normal amplitude modulation envelope by an exponential envelope. This is known as exponential modulation (AM^m) (John *et al.*, 2002) and can be represented mathematically as:

$$s_{AM^m} = A \left[1 + 2m_a \left(\frac{[1+m_a \sin(2\pi f_m t)]^m}{2} - 0.5 \right) \right] \sin(2\pi f_c t) \quad (2-2)$$

where all the variables in Eqn. (2-2) are similar to Eqn. (2-1) except that in this case the variable m is the required exponent, ranging from 2 and above. If $m=1$, Eqn. (2-2) will then be the same as Eqn. (2-1), i.e. representing now the standard AM, rather than AM^m . Exponential modulation causes both amplitude and latency of the auditory steady-state response to increase significantly with increasing index m .

Frequency modulation (FM) tones can also be used to evoke ASSR, which involves changing of the frequency rather than the amplitude of the carrier in AM (Maiste and Picton, 1989). The FM depth is defined as the difference between the maximum and minimum frequencies divided by the carrier frequency. By increasing the depth of modulation, the amplitude of the frequency modulated tones is also increased. However, the specific frequency of the FM will decrease with increasing depth modulation, making it less attractive in ASSR stimulus selection. A combination of both AM and FM generates approximately 30% larger ASSR responses than conventional AM or FM tones (Cohen *et al.*, 1991; John *et al.*, 2001b), and this is referred to as mixed modulation (MM). MM involves the simultaneous modulation of both the amplitude and frequency of the stimulus, and it can be represented as:

$$\varphi = \left[\frac{m_f f_c}{2f_m} \right] \sin(2\pi f_m t + \phi) \quad (2-3)$$

$$s_{MM} = A[1 + m_a \sin(2\pi f_m t)] \sin(2\pi f_c t + \varphi) \quad (2-4)$$

where f_m is the modulation frequency (both amplitude and frequency), f_c the frequency of the carrier, m_f is the depth of frequency modulation, m_a is the depth of amplitude modulation, A is the amplitude of the stimulus, t is the time, and phase delay ϕ is set to -90° ($\pi/2$ radians) for maximum correlation between stimulus amplitude and its frequency (John and Picton, 2000a).

Several types of stimuli (presenting in both time and frequency domains) have been used to evoke an ASSR. Typical stimuli are shown in Figure 2.3. Usually, the AM tone is used as the stimulus to evoke the ASSR while other more sophisticated tones (e.g. FM, MM, AM^m and etc.) can stimulate larger ASSR responses than achieved by the standard AM by approximately 30% (Maiste and Picton, 1989; Cohen *et al.*, 1991; Picton *et al.*, 2003a). However, the AM tone is widely accepted as a standard stimulus and implemented in the commercial equipment (e.g. MASTER)

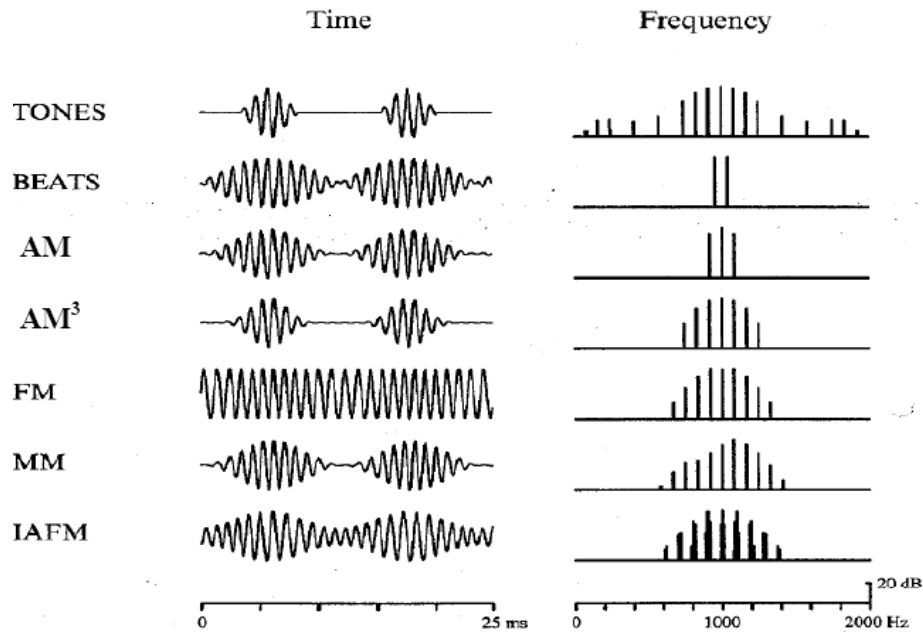


Figure 2.3: Examples of stimuli used in evoking ASSR (Picton *et al.*, 2003a).

Single/ Multiple ASSRs

A unique feature of the ASSR is that its stimuli can be presented in either single or multiple (simultaneously) forms (Lins and Picton, 1995; John and Picton, 2000a; John *et al.*, 2001b; Stapells *et al.*, 2004). Figure 2.4 shows an example of combining four individual single ASSR stimuli (i.e. AM tone) into multiple ASSRs stimuli (multiple AM tones).

The advantage that the multiple ASSR has over the single stimulus scheme is that it facilitates the evaluation of several frequencies for both ears simultaneously. This leads to a further reduction in the hearing test time by a factor of two or three times (Lins and Picton, 1995). There are however some limitations when using the multiple stimulus technique, as follows:

- Loss of ASSR amplitude because of the interaction of the combined stimuli in the auditory nerve (Picton *et al.*, 2003a) or overlap on the basilar membrane (Lins and Picton, 1995).
- These effects deteriorate when the stimulus intensities used are above 75dB sound pressure level (SPL) (Lins and Picton, 1995; Lins *et al.*, 1996).
- Similar effects will occur if the modulation frequencies used are less than 1.3 Hz apart. i.e if the carrier frequencies used are less than one octave apart (John and Picton, 2000a).

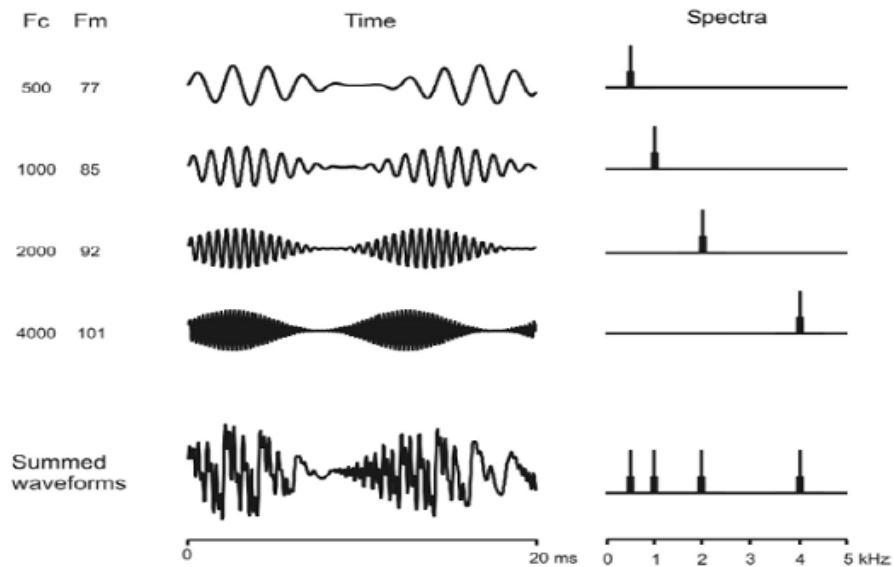


Figure 2.4: Time and frequency spectra of multiple ASSR stimuli (Stapells *et al.*, 2004).

2.2.4 Recording and Analysis Techniques

The greatest drawback of the ASSR technique is the lengthy recording time needed for reliable hearing threshold estimation. In general, approximately 45 minutes to an hour is needed to record the measurements required for the hearing threshold diagnosis (Luts and Wouters, 2004; Van Dun *et al.*, 2009). Due to its lengthy test time, the acceptance of the ASSR technique (by the audiology community) as a hearing screening tool is poor and impractical even considering its advantages compared to other screening methods, e.g. the OAE and ABR. The general detection methodology of ASSR can be divided into *two* main parts. Firstly, a stimulus or a set of stimuli generated by an auditory stimulator is used to evoke the ASSR response that is to be picked up by the surface electrodes on the scalp. Secondly, the response is recorded and then amplified and further processed by a series of signal processing techniques before finally being sent for display (Mason, 1993).

Although, there are several types of modulation that can be used as a stimulus (see Section 2.2.3), the AM stimulus is more commonly used to evoke ASSR response. In order to shorten the recording time, the multiple stimuli approach can be an advantage over the single stimulus approach (John *et al.*, 2001b; Luts and Wouters, 2004). In order to record the evoked potentials, surface electrodes are placed on the scalp. There are however two approaches, single-channel (also including dual-channel) (Lins *et al.*,

1996; van der Reijden *et al.*, 2005) and the multichannel ASSR recording (Malmivuo and Plonsey, 1995). Although the multichannel recording approach does have some advantages in terms of analysis, the measurements collected by the single-channel recording approach are still comparable (with no significant differences) to those obtained by the multichannel approach with optimal electrode placements, but with less complex recording system (Picton *et al.*, 2003a). Thus, the electrode placements implemented within all the experimental study in this thesis are based on the single-channel recording approach. For standard single-channel ASSR recording, the non-inverting electrode is mostly placed at the vertex (Cz) or high forehead (not recommended for adults). The inverting electrode is placed at the *ipsilateral mastoid* in the case of monotic stimulus presentation or at the neck for the case of dichotic stimulus presentation. The positioning of the reference electrode can be more flexible, this can be placed on the contralateral mastoid, i.e. the neck position inion (Oz) or the clavicle (Pz). As shown in Figure 2.5. where the electrode placement position mentioned can be seen from a typical 10-20 standard of electrode placement.

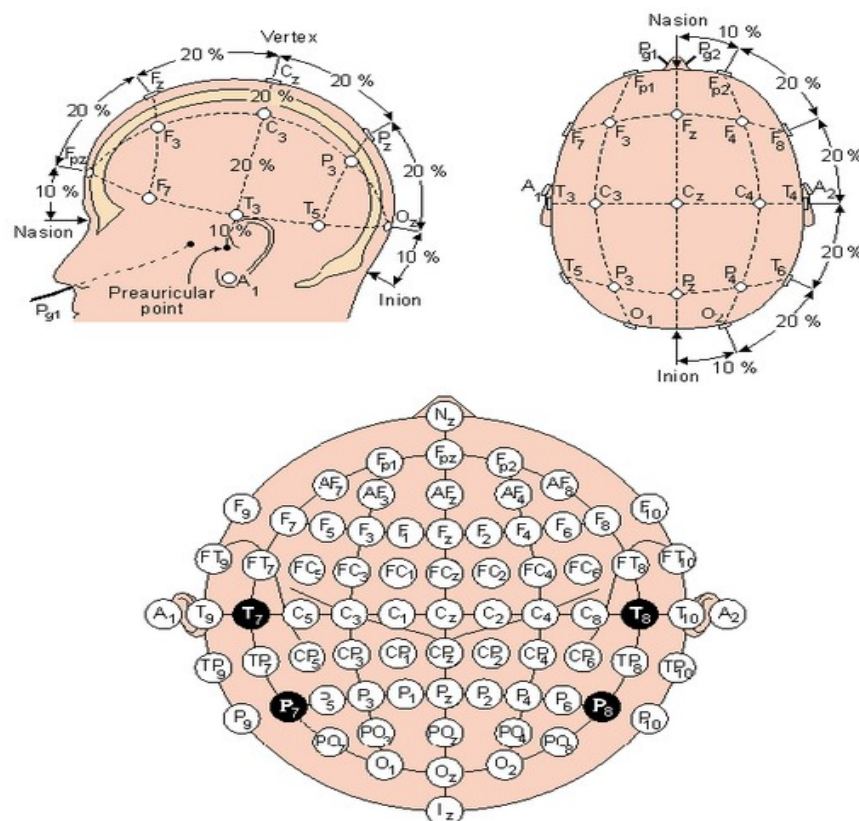


Figure 2.5: International 10-20 standard of electrode placement (Sharbroug *et al.*, 1991).

ASSRs are faint electrical signals embedded within the much stronger EEG signals. The EEG itself typically has a signal magnitude in the range 10 μ V to 100 μ V, whilst the

ASSR level lies typically in the much smaller range of 10 nV to several μ Vs. Thus an amplification gain of at least 10k is needed before further detection procedure can be utilised. As the ASSR is recorded in conjunction with EEG activity (referred to as 'background noise'), the SNR becomes a very important aspect of the signal abstraction/detection process. The low SNR can be improved by pre-filtering together with artefact rejection and time-domain averaging. Typically, a low-pass or band-pass filter will be placed just after the amplification stage, only to bypass the required frequencies. Artefacts originating from the external source, e.g. electromagnetic interference (Picton and John, 2004) or from the patient, such as potentials related to patient movement (e.g. muscle movement and eye-blinking) that are not part of the ASSR response (Hall, 1992). These artefacts can be removed from the previously filtered input if the signal exceeds a chosen preset voltage threshold, and this is known as "artefact rejection" (John and Picton, 2000a). On-line artefact rejection will discard epochs or sweeps that have been contaminated with artefacts to ensure the processing reliability, where these extreme artefact values could easily bias the detection. In addition, to ensure the effective artefact rejection (optimal rejection by individual subject tailored), the procedure is to be conducted offline with no artefacts rejected on the pre-recorded AEP (Luts and Wounter, 2005; Van Dun *et al.*, 2009).

After lowpass/bandpass filtering and artefact rejection of the recorded signal, waveforms are averaged in the time domain repeatedly to reduce the noise level in the recording. The averaged data can now be transformed from the time domain to the frequency domain by fast Fourier transform (FFT) (see example in Figure 2.6), thus information of the amplitude and phase of each frequency is then provided by FFT and then followed by statistical analysis to reveal the existence of ASSR. By its nature, the method of combined averaging and FFT cannot operate in real-time. Moreover, this technique is effective only with the availability of long strings of recorded data to ensure reasonable output resolution. This gives rise to a very lengthy procedure that is particularly troublesome in hearing tests for infants, because during the tests babies need to be in sleep or otherwise sedated. Consequently, if the subject is not relaxed, this would cause an increase in artefact activity, which could further delay the ASSR detection because some measurements may have to be discarded as part of the artefact rejection. Before the popularity in the use of FFT processing in this application field, the Fourier Analyzer was the key option (Regan, 1989). This method operates by multiplying the recorded signal by the sine and cosine of the stimulus frequency and

filters the resultant products to obtain the real and imaginary components of the responses (Stapells *et al.*, 1984). However, this method is limited in analysing a single response at a time, whereas the FFT approach provides a spectrum that includes the responses and the background noise.

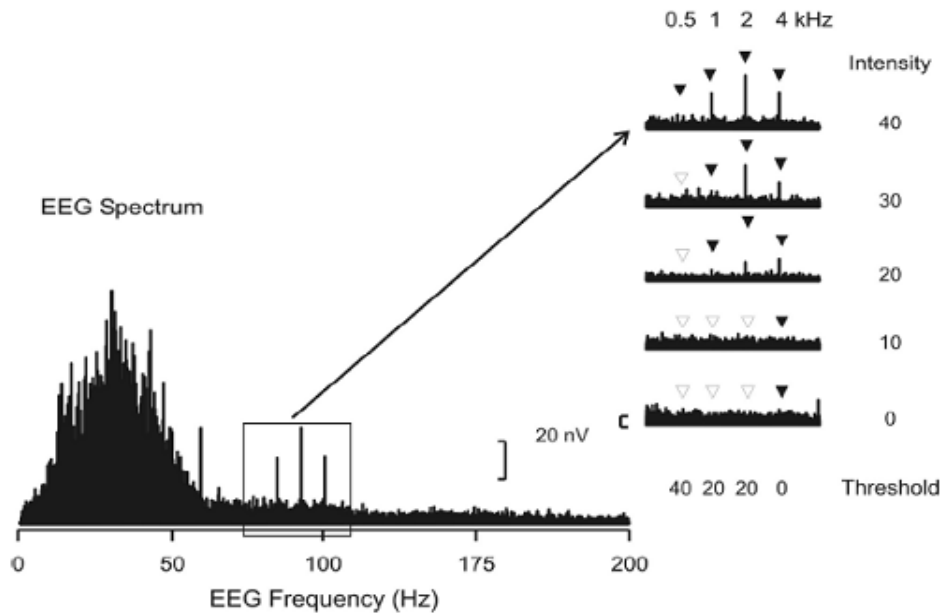


Figure 2.6: Example of multiple ASSRs recorded corresponding to multiple stimuli (Staples *et al.*, 2004).

According to Regan (1989), both the amplitude and phase of a steady-state response are constant and could be used to determine the availability of the response (to determine the existence of ASSR signal). The most two common statistical analyses utilized are the phase coherence and the F-test. The phase coherence method assesses similarity in phase across replications, a response is considered present if its phase remains stable over time rather than varying randomly (Stapells *et al.*, 1987; Rance *et al.*, 1995; John and Picton, 2000b). On the other hand, the F-test evaluates the difference between the amplitude and phase of the response at the stimulus frequency with those of the noise at the adjacent frequencies (Lins *et al.*, 1996).

At present, there are some commercially audiometric instruments available which operate on the basis of the detection principles outlined above. Among them, MASTER (Multiple Auditory STEady-state Responses) is a popular research audiometric instrument developed by Rotman Research Institute at Toronto University (John and Picton, 2000a). MASTER was first introduced eleven years ago. Several advanced

processing techniques based on single-channels recording were developed following the introduction of the use of averaging technique (Geisler, 1960). Examples include, weighted averaging (John *et al.*, 2001a), averaging with phase-locking (Parker and Matsebula, 1992; Picton *et al.*, 2001) and nonlinear signal processing (McNamara and Ziarani, 2004). These methods are used to improve the SNR. As for the methods developed using multichannel recording, Independent Component Analysis (Van Dun *et al.*, 2007a) and the Wiener Filter (Van Dun *et al.*, 2007b) were proposed. Although the technology of ASSR has improved since first introduced, the ASSR test might still require 45—60 minutes to obtain a four-frequency audiogram for both ears (Van Maanen and Stapells, 2005) using the existing instruments. Hence, the ASSR testing remains a challenge with the length procedure as the main technical obstacle in its widespread adoption for clinical use. This is particularly the case when used as a screening tool where fast detection is highly desirable.

2.3 Clinical Applications

In general, the use of ASSR could be in several clinical areas, such as in audiometric (e.g. hearing screening test and hearing thresholds diagnosis), anaesthesia and neurologic applications. Health care for adults and particularly infants having hearing impairment will benefit from the developments of ASSR usage in clinical practice and from the research conducted in recent years (Lins *et al.*, 1996; Heardman and Stapells, 2001 and 2003; Perez-Abalo *et al.*, 2001; Drimitrijevic *et al.*, 2002; Cone-Wesson *et al.*, 2002b; Picton *et al.*, 2003a and 2005; van der Reijden *et al.*, 2006). Potential applications of ASSR in the anaesthetics community are to search for effective monitoring of surgical unconsciousness depth, and 40-Hz ASSR could be the answer (Plourde and Picton, 1990; Plourde *et al.*, 1998; Picton *et al.*, 2003b). The use of the ASSR has not been extensively evaluated in patients with neurologic disorders. However, in recent years there are signs of an increase in research interest in this area and it is hoped that this interest will further develop (Brown, 2005).

2.4 Concluding Remarks

This chapter has briefly described the important features of the ASSR technique, its applications and gives an overview of the current ASSR detection methods. There are several ways to reduce the test time, in terms of stimulus, recording and signal processing methods. Instead of the normal AM signal as stimulus, other types of

modulation can be used, for instance MM or AM^m, which would evoke larger responses by a third, hence indirectly improve the ASSR detection. Besides, the multiple stimulus approach can improve the time efficiency by a factor of two to three compared to the single stimulus approach. For the purpose of objective assessment of hearing threshold, modulation rates around the region of 90 Hz are preferred. This is because the ASSR at lower frequencies is not reliably recordable particularly for infants since at these frequencies the detection is influenced by sleep and sedation. All the detection methods presented are based on single-channel recording. Among them, the most widely cited techniques, are averaging and weighted averaging with statistical analysis (e.g. F-test). Although both single-channel and multichannel recording approaches are comparable, the latter approach does provide some useful information that could lead to further diagnostic test time reduction. However, the characteristic of multi-channel methods will not be discussed further in this thesis. The focus of this thesis is thus on the ASSR detection approach, based on the single-channel recording strategy.

3 . Preliminary Study of ASSR using Observer Approach via BIOPAC

3.1 Introduction

As stated in Section 2.2.4, the most popularly used auditory steady-state response (ASSR) detection method does not operate in real-time in principle. It is also complicated with a series of processing methods (e.g. artefact rejection, averaging, fast Fourier transform (FFT) and statistical test). As a result, this makes the hearing screening or diagnostic tests lengthy especially when conducting the tests on infants. An alternative technique, known as state estimation, which is believed to have better performances (e.g. reduced test duration, moderate complexity and real-time implementation) in detecting ASSR from the overwhelm background noise, is to be proposed in this Chapter.

In general, the state estimation can be provided by Luenberger observer or Kalman filter (KF). In system theory, Luenberger observers are designed for deterministic systems whereas KF for stochastic system. They work as mechanisms in reconstructing the state variables of a dynamic system based on an analytical model of the system and measurements of partial or limited combination of the variables. Both observer and

filter can operate in real-time and have the same structure, similar synthesis and compatible performances, but different interpretations of the designs. Commonly, the Luenberger observer operates in the continuous time, while the KF operates in the discrete time.

Section 3.2 introduces the theory of Luenberger observer and its design as a sinusoidal detector, and also describes the practical issues concerning its implementation as an ASSR detection scheme. Two ASSR detection schemes (via amplitude-based or power-based evaluation) are introduced as part of the observer-based method. Initial simulation evaluations on the developed detection scheme are presented in Section 3.3. In Section 3.4, ASSR validation studies are carried out with the detection scheme applied to real ASSR measurement recorded from a BIOPAC system. The BIOPAC system is a data acquisition unit developed by BIOPAC Company. This is a data acquisition system that made specially specializes for medical use. A short description of the BIOPAC system and its experimental setup also are presented in Section 3.4. Concluding remarks of the chapter are provided in Section 3.5.

3.2 Observer-based Sinusoid Detector

The ASSR detection problem can be viewed as tracking a sinusoidal signal corrupted by noise based on the assumptions that an ASSR signal is a sinewave like waveform with oscillating frequency the same as the stimulus applied and is embedded within noise elements. The proposed sinusoid detector can be divided into two stages, the processing stage (i.e. sinusoid extraction) and the decision stage (i.e. variables estimation and thresholding) as shown in Figure 3.1. In the processing stage, the desired sinusoid-like ASSR signal for estimation is extracted from auditory evoked potential (AEP) by using an observer with the known stimulus frequency. Whereas the decision stage is responsible for evaluating the amplitude or power of the extracted sinusoid, in order to make a decision on the existence of the ASSR based on a pre-defined threshold.

The proposed sinusoid detector is based on the use of a state observer (or Luenberger observer). An observer can be seen as an auxiliary system which provides estimation of the variables describing dynamics of a plant by using the knowledge of the plant's model together with measurement information about the plant (Luenberger, 1971). An ASSR can be considered as an output of a dynamic system described by a second-order

differential equation. The proposed method uses observers to estimate the sinewave and its amplitude or power to identify the existence of the ASSR, and is motivated by the estimation method proposed by Hou (2005). The study here has further extended the approach and tailored it towards amplitude/power estimation of noisy sinusoidal signals in extreme low signal-to-noise ratio (SNR) environment with known inputs frequencies (mimicking ASSR application).

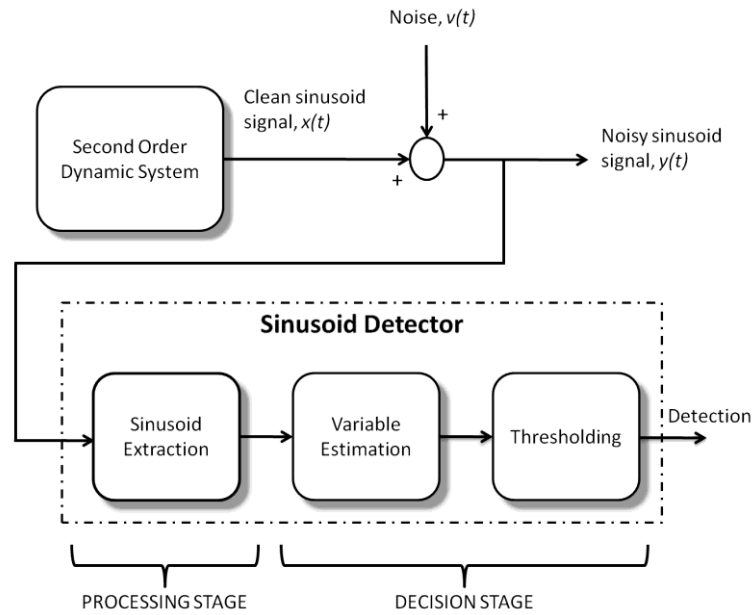


Figure 3.1: Architectural block diagram of the sinusoid detector.

3.2.1 Sinusoid Extraction

The rationale behind the proposed approach is to consider the ASSR as a signal generated by a second order dynamic system with a known natural frequency ω , as shown in Figure 3.1. Since the state observer reconstructs the sinusoid, it is necessary to determine the intensity of the wave. A natural way of doing it is to estimate the amplitude of the sinusoid. An adaptive observer is derived for this purpose.

Suppose the measured signal $y(t)$ in Figure 3.1 is described by

$$y(t) = x(t) + v(t) \quad (3-1)$$

The sinusoid $x(t) = A \sin(\omega t + \phi)$ is the output of the second-order system because $x(t)$ satisfies the differential equation:

$$\ddot{x}(t) = -\omega^2 A \sin(\omega t + \phi) = -\omega^2 x(t) \quad (3-2)$$

where $\ddot{x}(t)$ stands for the second order derivative of $x(t)$. This means that the second-order system can be described by the transfer function of $1/(s^2 + \omega^2)$. It can be assumed that this sinusoid is the ASSR with the known angular frequency ω and unknown amplitude A and phase ϕ . In real applications, A and ϕ are assumed to be constants or slowly varying variables. Whereas $v(t)$ is a random variable representing the system and measurement noise. The objective is to extract the sinusoid $x(t)$ from $y(t)$ and then estimate the sinusoidal amplitude.

Define $x_1(t) = x(t)$ and $x_2(t) = \dot{x}(t)$. A state observer for estimating $x_1(t)$ and $x_2(t)$ is described by:

$$\dot{\hat{x}}_1(t) = \hat{x}_2(t) + l_1[y(t) - \hat{x}_1(t)] \quad (3-3)$$

$$\dot{\hat{x}}_2(t) = -\omega^2 \hat{x}_1(t) + l_2[y(t) - \hat{x}_1(t)] \quad (3-4)$$

where $\hat{x}_1(t)$ is the estimate of $x(t)$, and $\hat{x}_2(t)$ of $\dot{x}(t)$ with the *a priori* known ω . l_1 and l_2 are the observer gains. It can be easily verified that in the absence of noise, with suitable positive gains l_1 and l_2 , $\hat{x}_1(t)$ and $\hat{x}_2(t)$ converge asymptotically to $x_1(t)$ and $x_2(t)$ respectively. Although the observer is designed according to the state observer method applied in a deterministic systems framework. The Luenberger observer has the same structure as the Kalman filter (Anderson and Moore, 1979), however the latter is more appropriate for stochastic systems that include random noise signals. For example when Eqn. (3-1) includes a random noise signal $v(t)$, the gain matrices in Eqns. (3-3) and (3-4) need to be determined as the Kalman filter gain that generates minimum variance estimates of $x_1(t)$ and $x_2(t)$. Since the statistical properties of the noise signals are assumed unknown, the optimal filter gain cannot be determined and a sub-optimal gain must be used. As a result, the observer gains l_1 and l_2 , will be adjusted from simulation studies.

According to the Eqns. (3-1) and (3-2), the continuous-time system model, yields

$$A_c = \begin{bmatrix} 0 & 1 \\ -\omega^2 & 0 \end{bmatrix}, \quad C_c = [1 \quad 0] \quad (3-5)$$

and the system is observable with

$$rank = \underbrace{\begin{bmatrix} C_c \\ C_c A_c \end{bmatrix}}_{\text{observability matrix}} = 2 \quad (3-6)$$

With the observability matrix being of full rank, stable eigenvalues of $A_C - LC_C$ can be assigned by $L = \begin{bmatrix} l_1 \\ l_2 \end{bmatrix}$ to the left hand side of the s -plane with $l_2 \leq l_1$. These constraints are to ensure the stability of the eigenvalues remained via selection of positive gains l_1 and l_2 for the detector. This can be justified through Eqns. (3-7)—(3-9), by denoting the characteristic polynomial:

$$\lambda I - (A_C - LC_C) = \begin{bmatrix} \lambda + l_1 & -1 \\ -\omega^2 - l_2 & \lambda \end{bmatrix} \quad (3-7)$$

The characteristic equation of this system is determined as:

$$\det[\lambda I - (A_C - LC_C)] = \lambda^2 + l_1\lambda + (l_2 + \omega^2) = 0 \quad (3-8)$$

Hence the characteristic equation roots {the eigenvalues of $(A_C - LC_C)$ } are:

$$\lambda = \frac{-l_1 \pm \sqrt{l_1^2 - 4(l_2 + \omega^2)}}{2} \quad (3-9)$$

For instance, if $l_1 = 0.3$ and $l_2 = 0.3$ (commonly used gains in Chapter 3), a stable pair of eigenvalues are obtained as $-0.15 \pm 62.8341i$ in the case $\omega = 20\pi$. This verifies the concept of gain selection for the observer-based detector.

3.2.2 Variable Estimation

Two observer-based evaluation approaches (via amplitude-based or power-based) are to be introduced in following as part of the proposed ASSR detection scheme. It is essential to obtain an estimate of amplitude or power, which will be presented in this section.

Amplitude Estimation

The sinusoid $\hat{x}_1(t)$ is obtained from the observer (Eqns. ((3-3) and ((3-4)), and its amplitude A needs to be estimated. Following a the similar treatment in Hou (2005), define a variable as

$$z = x\dot{x}(t) \quad (3-10)$$

and its time derivative is

$$\begin{aligned} \dot{z} &= \dot{x}^2(t) + x\ddot{x}(t) \\ &= \omega^2 A^2 [\cos^2(\omega t + \phi) - \sin^2(\omega t + \phi)] \\ &= \omega^2 A^2 [1 - 2\sin^2(\omega t + \phi)] \\ &= \omega^2 A^2 - 2\omega^2 x^2(t) \end{aligned} \quad (3-11)$$

Rewriting \dot{z} equation as

$$\dot{z} = \theta - 2\omega^2 x^2(t) \quad (3-12)$$

where $\theta = A^2\omega^2$ is the unknown parameter to be estimated. If $x\dot{x}(t)$ is available, a standard adaptive observer for z and θ is given by

$$\dot{\hat{z}} = \hat{\theta} - 2\omega^2 x^2(t) + \alpha[x\dot{x}(t) - \hat{z}(t)] \quad (3-13)$$

$$\dot{\hat{\theta}} = \gamma[x\dot{x}(t) - \hat{z}(t)] \quad (3-14)$$

where α and γ are positive numbers. In order to eliminate the term $x\dot{x}(t)$ in Eqns. (3-13) and (3-14), a change of variables is defined according to Hou (2005) as

$$\hat{z} = \xi + \alpha x^2(t)/2 \quad (3-15)$$

$$\hat{\theta} = \eta + \gamma x^2(t)/2 \quad (3-16)$$

It is straight forward to verify that ξ and η are governed by

$$\dot{\xi} = \eta - 2\omega^2 x^2(t) - \alpha\xi + (\gamma - \alpha^2)x^2(t)/2 \quad (3-17)$$

$$\dot{\eta} = -\gamma(\xi + \alpha x^2(t)/2) \quad (3-18)$$

If γ in Eqn. (3-17) is chosen to be equal to α^2 , a simplified version of Eqns. (3-17) and (3-18) is obtained as

$$\dot{\xi} = \eta - 2\omega^2 x^2(t) - \alpha\xi \quad (3-19)$$

$$\dot{\eta} = -\alpha^2(\xi + \alpha x^2(t)/2) \quad (3-20)$$

Hence, Eqn. (3-16) is rewritten as

$$\hat{\theta} = \eta + \alpha^2 x^2(t)/2 \quad (3-21)$$

The estimation of \hat{A} can be calculated from $\hat{\theta}$ as

$$\hat{A} = \sqrt{\hat{\theta}}/\omega \quad (3-22)$$

To apply the adaptive observer of Eqns. (3-19)—(3-22) to the amplitude estimation, x in Eqns. (3-19)—(3-21) needs to be replaced by its estimate $\hat{x}_1(t)$ obtained from Eqn. (3-3).

Power Evaluation

As an alternative to amplitude estimation, the power of $\hat{x}_1(t)$ from the observer Eqns. (3-3) and (3-4) can be defined as

$$p(t) = \frac{1}{t+\varepsilon} \int_0^t \hat{x}_1^2(\tau) d\tau \quad (3-23)$$

where $p(t)$ can be seen as the average power over time t and to avoid numerical error when $t = 0$, ε is set to be a small positive constant (i.e. 1×10^{-6}). Denote $p_{no}(t)$ as the power of $\hat{x}_1(t)$ when $x(t)$ is absent and $p_x(t)$ otherwise. It is expected that $p_x(t) > p_{no}(t)$ for all $t > 0$.

3.2.3 Thresholding

This section describes the proposed evaluation approaches, via amplitude and power estimation.

Amplitude Thresholding

Denote A_x as the amplitude of $\hat{x}(t)$ when $x(t)$ is present and A_{no} otherwise. It is expected that $A_x > A_{no}$. Define detection rate as the percentage difference between the estimated amplitude in the presence and absence of the ASSR, as

$$A_d(\%) = \frac{[A_x - A_{no}]}{A_{no}} \times 100\% \quad (3-24)$$

Since A_x and A_{no} are respectively amplitude estimates of ASSR and the background noise at the modulation frequency, $A_d(\%)$ is actually a time-varying variable. $A_d(\%)$ can be used as an indicator of the degree of existence of $x(t)$ with a pre-defined threshold to determine the existence or non-existence of the sinusoid.

Power Thresholding

Denote $p_{no}(t)$ as the power of $\hat{x}(t)$ when $x(t)$ is absent and $p_x(t)$ otherwise. Again, it is expected that $p_x(t) > p_{no}(t)$ for all $t > 0$. To indicate the percentage difference between the estimated power in the presence and absence of the ASSR, the detection rate defined as:

$$p_d(\%) = \frac{[p_x(t) - p_{no}(t)]}{p_{no}(t)} \times 100\% \quad (3-25)$$

is issued in a similar way as $A_d(\%)$ to identify the existence of $x(t)$. This implies that when an ASSR is present $p_d(\%)$ should be distinctively greater than that when the ASSR is absent.

3.2.4 ASSR Detection Scheme

The sinusoid detector illustrated in Figure 3.2 is presented schematically with the two evaluation methods. In practice only a single detection method is used at any one time, either using the amplitude-based or the power-based detection. The proposed detection scheme employs dual channels of identical observers. One observer has a noisy sinusoid as input and a sinusoid estimate as output. The other observer's input is the noisy sinusoid subtracted by the estimate offered by the upper observer. The output of the lower observer may be interpreted as the background noise filtered by the observer. Both estimated outputs from the observers are then used to estimate their amplitudes or powers. The degree of (i.e. amplitude or power) difference between both channels indicates the existence or non-existence of the sinusoid according to the pre-defined threshold. To clarify the scheme, only case of single sinusoid detection is explained. The method can be readily extended to detect multiple sinusoidal signals by duplicating the dual-channel detector as many as the number of sinusoidal signals. Use of the multiple dual-channel type of detector is preferred over a higher order observer for estimating multiple sinusoidal signals. In principle, duplicated dual-channel observers produce similar results as compared to the dual-channel higher order observers, but the design and structure of the dual-channel observers are simpler than those of higher-order observers.

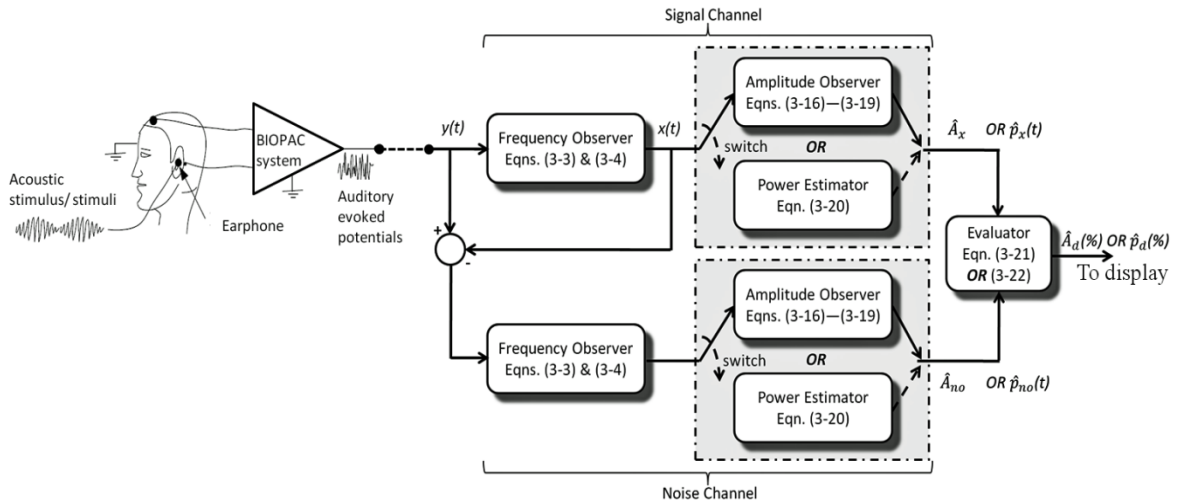


Figure 3.2: On-line ASSR detection scheme acquiring AEP via BIOPAC system.

To evaluate the proposed detection scheme, Matlab/SIMULINK simulations have been carried out for three cases as Figure 3.3. In the simulations, all the integral initial conditions were set to be zero. In the first simulation, a ‘noise-free’ signal $y(t) = \sin(20\pi t)$ is applied to the detection scheme (as shown in a noisy sinusoidal signal

$y(t) = \sin(20\pi t) + v(t)$, with $v(t)$ considered as a white noise signal with mean $\mu = 0$ and standard deviation $\sigma = 0.5$, is now applied (SNR= 6dB). The observer gains are held constant with $\alpha = 1$. Lastly, the same detection is applied to the noise $y(t) = v(t)$ with the same statistical properties as the one before. The Gain α was reduced to 1 in the last two scenarios for the purpose of having smoother convergence, thus indirectly improving the detection rate but with slower convergence. In other words, as the SNR decreases so does the gain α to counter the inaccuracy caused by the noisy AEP. The amplitude responses of the all three cases stated above are shown in Figure 3.3.

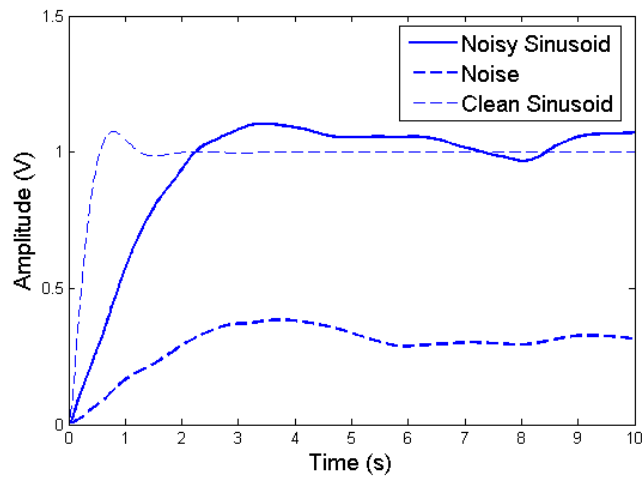


Figure 3.3: Simulation results of (i) clean sinusoid (ii) noisy sinusoid (iii) noise.

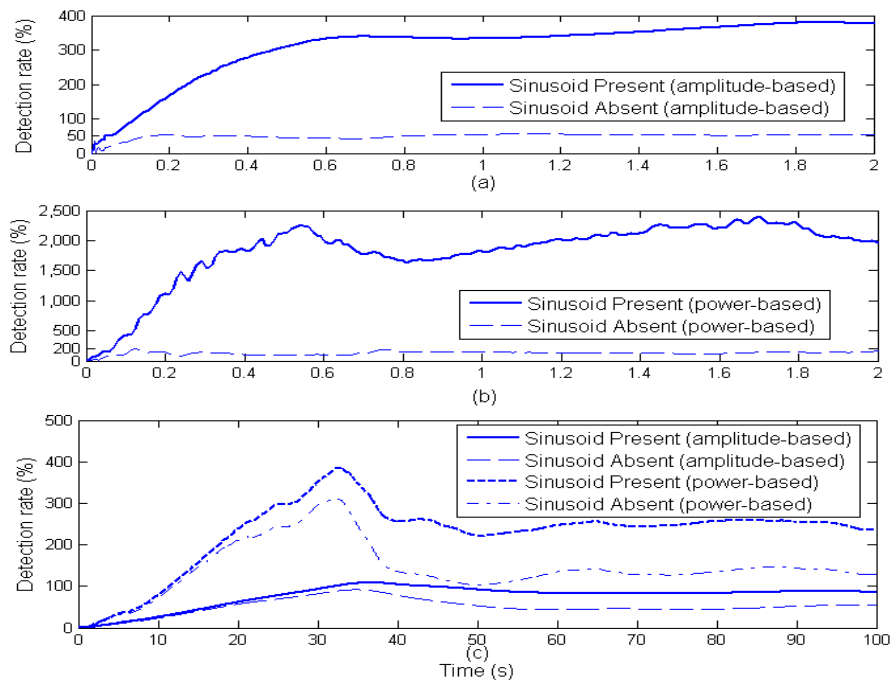


Figure 3.4: The detection rate in identifying the presence of sinusoid via amplitude and power-based approaches (a) and (b) SNR ≈ 6dB (c) SNR ≈ -30dB.

As illustrated in Figure 3.3, the amplitude estimate converged to the actual amplitude of 1 volt in less than one second for the ‘noise-free’ sinusoid and about 2s for the noisy sinusoidal signal. As for the noise only signal, the estimated amplitude (at the specified frequency) is far below the actual sinusoid amplitude. This is expected and meets the idea that any noise estimate should be significantly lower (depended on the SNR) than the sinusoid estimate. Figure 3.4a and Figure 3.4b illustrate the detection rates in terms of either amplitude or power percentage differences. The responses are distinctively higher if the sinusoid is present. A threshold of 50% is defined empirically which is used as a way to identify the existence or non-existence of sinusoid, whereas a threshold of 200% is chosen for power-based detection to determine the detection rate of the sinusoid using Eqns. (3-24) and (3-25). Both thresholds were determined based on the average responses obtained through 50 simulation trials in conditions where SNR is -30 dB and noise generated with random seeding in each trial. Although the power-based response is generally larger than the amplitude-based response, their detection rates are comparable at approximately at 0.1s, as illustrated in Figure 3.4a and Figure 3.4b. To further clarify the detection rate similarity, Figure 3.4c is used to illustrate that both their responses are significantly reduced to the level just above the pre-determined threshold as the SNR decreased significantly. As shown in Figure 3.4, the detection rate achieved even though the estimation has not yet converged to the expected true amplitude (as shown in Figure 3.3). In general, the detection rate response is more appropriate than the amplitude response as it provides a facility for objective decision making in terms of on-line sinusoid identification.

3.3 Simulation Study

Due to the difficulties in specifying the ASSR from its noisy environment in practice, synthetic data were generated with Matlab/SIMULINK and applied to the ASSR detector within simulation environment for preliminary validation of the performances (e.g. noise corrupted signal and gain tuning) of the proposed algorithms.

3.3.1 Gain Tuning

Both amplitude-based and power-based approaches performed satisfactorily and their detection rates are comparable as shown in Figure 3.4. The amplitude-based approach shows slight advantageous due to the availability of a tuneable parameter α that permits

design flexibility, according to the expected SNR. This parameter can be tuned; a larger α gives rise to a faster convergence for the case of a high SNR scenario. Alternatively, a smaller lower value of α has the effect of smoothing the convergence to get better accuracy, particularly for the low SNR scenario. Furthermore, the inclusion of ε in Eqn. (3-23) is used to prevent initial numerical error which may still cause initial overshoot in the response. As a result, the amplitude-based detection scheme will be the focus for the remaining sections of the thesis. The flexibility of the amplitude-based detector with the extra gain parameter is compared with the power-based detector is illustrated in Figure 3.5. This illustrates the effect of the selection of the observer gains ($l_1; l_2; \alpha$) on the performances of the noisy sinusoid detection of $y(t) = \sin(20\pi t) + v(t)$ (a) $\text{SNR} \approx 6\text{dB}$ and (b) $\text{SNR} \approx -15\text{dB}$. As shown in Figure 3.5a, a faster convergence rate can be achieved by tuning the l_1, l_2 and by selecting a larger tuning parameter α . On the other hand, if the SNR is poor, smaller values of l_1, l_2 and α are preferable to ensure smoother convergence and improve the immunity to noise and in turn improving the accuracy, as shown in Figure 3.5b.

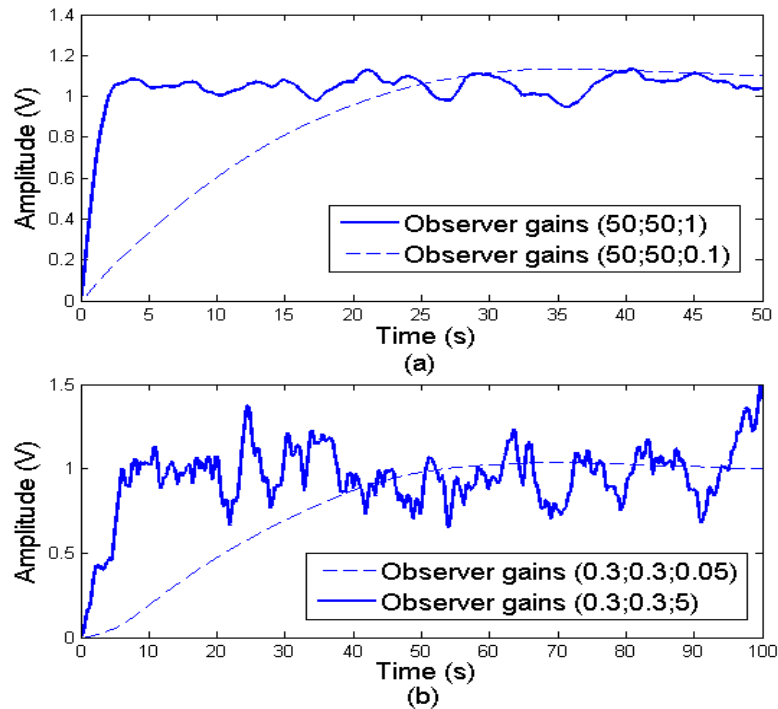


Figure 3.5: Tuneable gain parameters to improve the sinusoid responses (a) $\text{SNR} \approx 6\text{ dB}$ (b) $\text{SNR} \approx -15\text{dB}$.

3.3.2 Noisy Sinusoidal Signal (Low SNR)

Several simulations were conducted to test the responses of the proposed algorithms

with respect to noisy sinusoids with different SNRs, and their results are illustrated in Figure 3.6. According to Figure 3.6, the time duration needed to achieve 50% threshold increases as the SNR worsens. In other words, the SNR is inversely proportional to the duration required to achieve a suitable detection rate for cases where sinusoids are present. Moreover, the gain parameters in Eqns. (3-3) and (3-4) are to be reduced if the SNR is poor. Typically during the simulation trials l_1 and l_2 are chosen to be less than 1 if the SNR is less than 0 dB to ensure better sinusoid extraction from the background noise. As discussed in Section 3.3.1 the positive gain constant α affects the speed and smoothness of the amplitude estimation. The smaller the gain the more insensitive the estimation is to noise corruption (smoother amplitude estimation), albeit with a slower convergence. The proposed algorithms encountered difficulties when processing and identifying sinusoids at SNR levels smaller than -35dB ; their responses are either marginally floating around 40%—50% or worse.

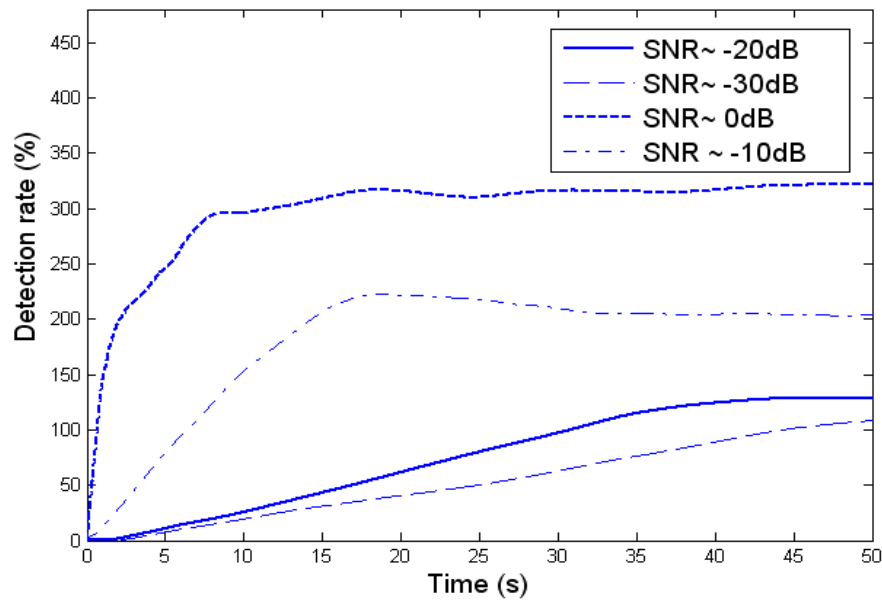


Figure 3.6: Detection rates of the different SNR scenarios.

3.4 Experimental Validation Study

In order to verify the simulation results conducted and the practical detection performances (e.g. reliability in detection, detection time required, correct indication of threshold evaluation and etc.), experimental studies are needed with the recording of real data from subjects. Several test scenarios were conducted, and they are as follows:

- Relationship between ASSR (fundamental frequency) and its harmonics
- Response to different intensity levels

- Response to different modulating frequencies
- Response to the effects of sedation and non-sedation
- Response to various types of modulation
- Response to multiple ASSR stimuli

The experimental test platform for recording ASSR, stimulus and recording parameters used are described this section. This test set-up remains basically the same for all studies described in Chapters 4 to 6 of this thesis.

3.4.1 Experimental Setup

The ASSR experiments were conducted in an ‘non-controlled environment’ (at the Medical Engineering Laboratory at Hull University) with background noise level between 20—30 dB(A) sound pressure level (SPL). A common practice of ASSR recording is to conduct the test in a soundproof room ~~with a Faraday cage~~ since lower background noise is preferable, typically at 12 dB(A) SPL. A schematic diagram showing the apparatus setup for ASSR recording is given in Figure 3.2. The data acquisition unit used presently in this research is from BIOPAC, a company that specializes in electronic data acquisition equipment for medical use. The instrument enables more flexibility and customisation of experimental parameters.

As mentioned in Chapter 2, the electrode placement approach is based on single channel method with non-inverting electrode positioned on the vertex of the scalp, the inverting electrode at the ipsilateral mastoid (where auditory stimulus applied), and the reference electrode at contralateral mastoid which acts as a ground. The electrodes were placed on the subject’s scalp after the skin was abraded with abrasive skin prepping to reduce the resistive. Electrode gel and additional bandage support were used to keep the electrodes in place and to avoid impedances exceed 5 K Ω (no more than 10 K Ω). Only if the impedance is within acceptable range, were the tests undertaken. The gain of the amplifier for the recording channel was set to 10k. The analogue-to-digital conversion rate of 10 kHz was used for AEP recording via BIOPAC system.

All the stimulus used throughout the experiments were generated using Matlab/SIMULINK with sampling rate of 20 kHz, pre-recorded and then played via standard PC sound card to a headphone for subject stimulation. All stimuli created were first measured using a Sound Level Meter 222A and typically stimulated between

39—64 dB SPL (32—57 HL) and having mean of 58.77 dB SPL (51.77 HL). Several types of modulated tones with various modulating frequencies were produced at the intensity range stated, with detailed descriptions of the stimulus used to be discussed in the following sections. The BIOPAC recorded data (bandpass filtered between 60—200Hz) with SNR range between -25dB and -33dB were then down-sampled to 1k via zero order-hold and post-processed in Matlab/SIMULINK since the proposed detection algorithms operates in the continuous time. The parameters were selected to be $l_1 = l_2 = 0.3$ and $\alpha = 0.05$ when carried out detection on experimental recorded data in the remaining Section 3.4.

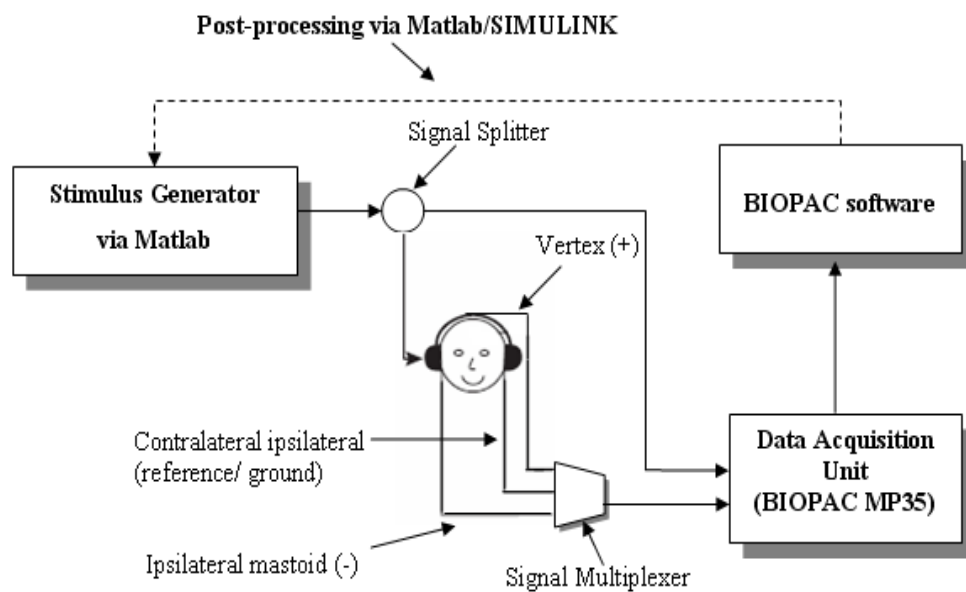


Figure 3.7: Schematic of the experiment setup for ASSR experiment (adapted from Luts, 2005).

3.4.2 Fundamental Frequency and its Harmonics

As discussed by Picton *et. al* (2003a), ASSR often consists of more than one harmonic responses but highly significantly at the stimulus frequency. However, so far majority of the ASSR detection are based upon detecting at the stimulus frequency and not its harmonics. Besides it is more significant at its fundamental frequency (stimulus frequency), higher computations are required if its harmonics are to be taken into the consideration of the detection. The calculation of harmonics might not be efficient though it is believed that the detection rate performance would be improved by combination of these harmonics and its fundamental frequency.

3.4.3 Intensity

The purpose in carrying out detection for different intensity stimuli, low intensity of 39—42 dB SPL and high intensity of 50—64dB SPL, evoked responses is to investigate the capability of the proposed detection scheme dealing with smaller evoked responses. This could be incorporating into the detection scheme in estimating hearing threshold where broad ranges of intensity level are required in the audiogram (see Figure 1.5). Figure 3.8 illustrates the non-sedated (subject) responses evoked by stimuli with modulating frequency at 40 Hz and 90 Hz, and carrier frequency of 1 kHz. In principle, the evoked responses of lower intensity stimuli produced smaller responses compared to the responses evoked from higher intensity stimuli, which is agreed with the studies by Picton *et al.* (2003a).

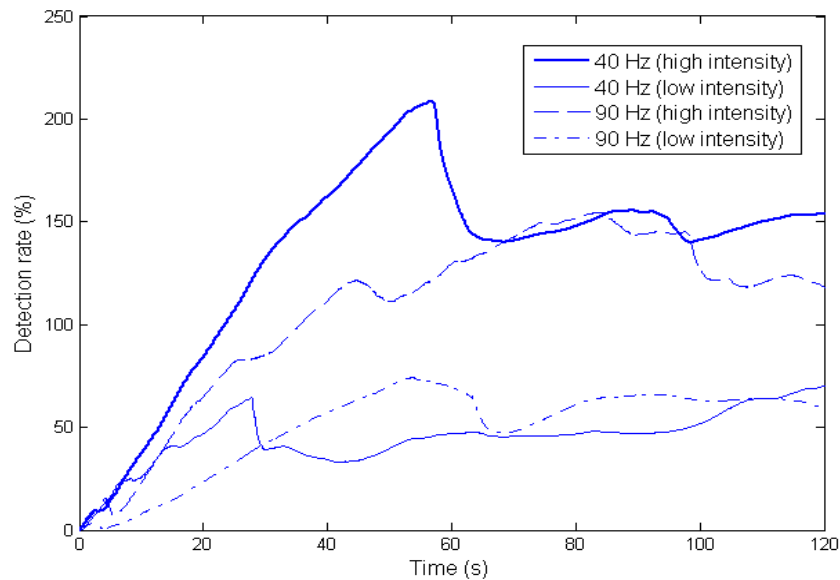


Figure 3.8: Responses to various intensity stimuli.

3.4.4 Modulating Frequency

The purpose of the test is to investigate how the ASSR responses to different modulating frequencies and the effectiveness of the proposed detection model in detecting them with subject sedated (relaxed position and eye-closed) and non-sedated (be alert and eye-open). AM modulated stimuli were used with modulating frequencies of 40 Hz and 90 Hz, but having the same carrier frequency at 1 kHz. All four responses to 40 Hz and 90 Hz illustrated clear indication when ASSR are present (see Figure 3.9) when compared to a zero stimulus evoked (ASSR absent) cases, as shown in Figure 3.10.

In order to verify the reliability of the results by the proposed detector, scenarios where no stimulus is generated is being used as a control scenario against the cases of ASSR existing. As illustrated in Figure 3.9 and Figure 3.10, the proposed ASSR detector successfully indicated a distinct difference in responses to the existence of ASSR, by using the thresholding. In general, the detection rate from these data displayed satisfactory accuracy (able to identify existence or non-existence of ASSR) within sensible time duration (less than 20s). In general, the responses evoked by stimulus with modulating frequency 40 Hz achieved higher and faster responses than the 90 Hz modulating frequency (Picton *et al.*, 2003a; Stapells *et al.*, 2004; Petitot *et al.*, 2005).

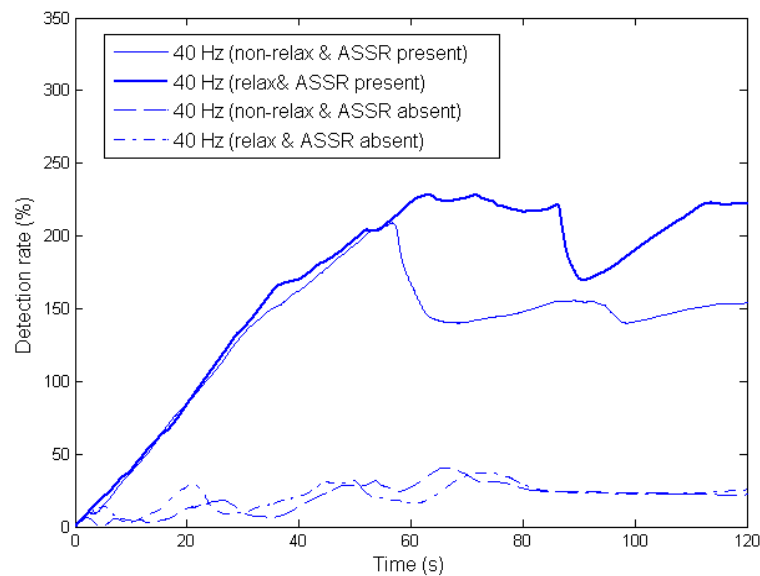


Figure 3.9: Responses to 40Hz ASSR in relaxing and non-relaxing conditions.

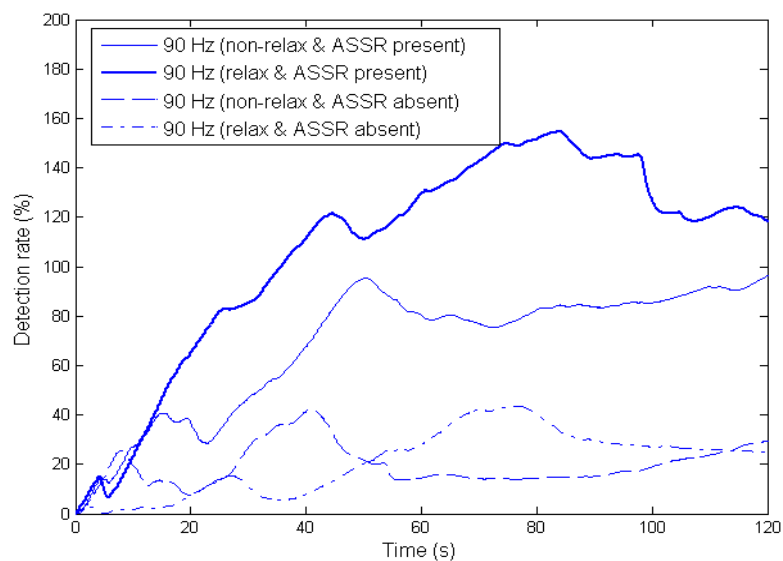


Figure 3.10: Responses to 90Hz ASSR in relaxing and non-relaxing conditions.

3.4.5 Relax and Non-relax

By maintaining the same modulating frequencies and carrier frequency as in previous test (Section 3.4.2), this test is designed to study the ASSR responses in both relaxed and non-relaxed cases. Under the non-relax condition, the subject was in an alert state with eyes open, whereas the subject is in more relaxing mood and resting with eyes closed under the relaxed condition. According to the responses in Figure 3.9 and Figure 3.10, it is clear that relaxation improves the ASSR responses in terms of reduction in background noise (better SNR) for both 40 Hz and 90 Hz modulating frequencies, as also indicated in Linden *et al.* (1985), Cohen *et al.* (1991) and Picton *et al.* (2003a).

3.4.6 Types of Modulation Tones

According to the results shown in Figure 3.9 and Figure 3.10, it can be said that although subject's relaxing or non-relaxing states affect the SNR of ASSRs, they were not interfering or affecting the operation of the proposed detection method. Hence, the following tests (including the tests in Chapters 4 to 6) were conducted without sedation, aiming to test the proposed detection scheme exposed to poor SNR responses. But to evoke responses with various non-conventional (more advanced) types of modulation stimuli, which some researchers believe to be 'better' stimuli (Picton *et al.*, 2003a; John *et al.*; 2002 and 2004) compared to pure AM modulated tones, the case with modulating frequency at 90 Hz and carrier frequency at 1 kHz are simulated and the results are illustrated in Figure 3.11. The idea to carry out this particular test is to show the effectiveness of various types of modulation that used throughout the literature besides the most commonly known amplitude modulation (AM).

According to John *et al.* (2004), AM² (exponential modulation, $m = 2$) and MM (mixed modulation) tones should evoke larger responses than normal AM tones. However, based on results shown in Figure 3.11, their responses were slightly lower compared to the AM tone response. In principle, AM^m and MM would evoke larger responses than normal AM. Hence, a combination of both AM^m and MM in principle would evoke much larger response. A stimulus, known as exponential-frequency modulation (EFM) is introduced here by combining equations Eqns. (2-2) to (2-4) as

$$s_{EFM}^m = A \left(1 + 2m_a \left[\left(\frac{[1+m_a \sin(2\pi f_m t)]}{2} \right)^m - 0.5 \right] \right) \sin(2\pi f_c t + \varphi) \quad (3-26)$$

where f_m is the frequency modulation (both amplitude and frequency), f_c the frequency of the carrier, m_f is the depth of frequency modulation, m_a is the depth of amplitude modulation, A is the amplitude of the stimulus, t is the time, and φ which governed by phase delay $\theta = -90^\circ$ ($\pi/2$ radians) (see Eqn. (2-3)) for maximum correlation between stimulus amplitude and its frequency, the characteristic of the stimulus is a combined character of both MM and AM^m . MM, EM^4 and EFM^4 have faster evoked responses in exceeding 50% threshold (empirically pre-defined threshold level) compared to normal AM modulated tone to be detected by the detector. In summary, different types of modulations may evoke larger responses and the proposed ASSR detection method is capable of detecting all of them, which not only beneficial to ease the detection in low SNR environment but also improves the time required to achieve the 50% threshold for reliable analysis.

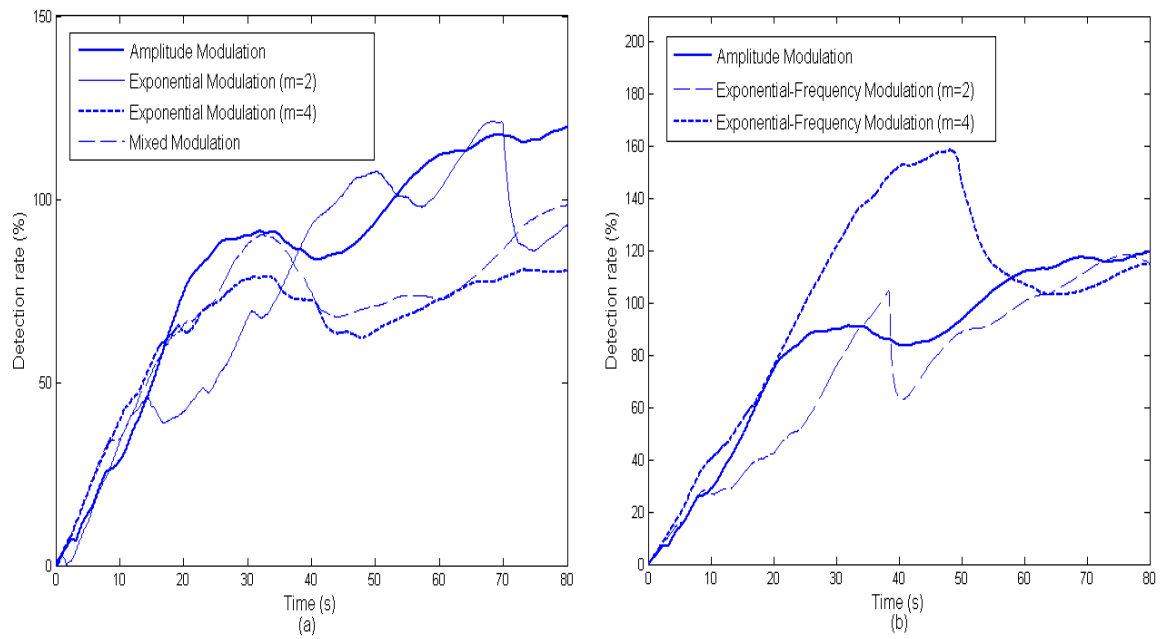


Figure 3.11: ASSR responses to various types of modulation at 90 Hz modulated.

3.4.7 Comparison between ASSR Detection Methods

Multiple (simultaneous) stimuli evoked ASSR responses (raw AEP data) corresponding to pre-recorded data provided by MASTER (software developed by Rotman Research Institute). Table 3.1 illustrates the detailed selection of the multiple stimuli used for multiple ASSRs detection. The terminology behind the ASSR detection is to estimate the ASSR (sinusoidal-like signal) that oscillates at a specify frequency stimulated by the modulating frequency of the stimulus input.

No. Stimuli	Carrier Frequency (Hz)	Modulating Frequency (Hz)
1 (Left ear)	750	80.078
2 (Left ear)	1500	84.961
3 (Left ear)	3000	89.844
4 (Left ear)	6000	94.727
5 (Right ear)	500	78.125
6 (Right ear)	1000	83.008
7 (Right ear)	2000	86.914
8 (Right ear)	4000	91.797

Table 3.1: Multiple stimuli parameters.

A comparison of the detection time required for multiple ASSRs stimuli recording approach between normal averaging, weighted averaging and the proposed observer-based detection scheme is shown in Table 3.2 (without artefact rejection) and Table 3.3 (with artefact rejection).

Stimulus (Hz)	MASTER Normal Averaging Time, (s)	MASTER Weighted Averaging Time, (s)	Observer-based Detection Time, (s)
<u>Data set 1</u>			
78.125	180.244	147.456	143.0
80.078	65.536	81.92	30.0
83.008	65.536	32.768	28.5
84.961	16.384	16.384	19.2
86.914	16.384	16.384	14.5
89.844	16.384	16.384	12.1
91.797	65.536	65.536	60.0
94.727	32.768	32.768	22.8
<u>Data set 2</u>			
78.125	16.384	65.536	15.9
80.078	49.152	98.304	44.2
83.008	16.384	16.384	23.5
84.961	32.768	32.768	16.4
86.914	16.384	16.384	19.5
89.844	32.768	32.768	23.6
91.797	49.152	49.152	23.1
94.727	114.688	131.072	90.0
<u>Data set 3</u>			
78.125	196.608	196.608	100.2
80.078	163.384	131.072	128.4
83.008	16.384	16.384	26.1
84.961	32.768	32.768	18.0
86.914	16.384	16.384	12.0
89.844	16.384	16.384	17.3
91.797	16.384	16.384	14.2
94.727	49.152	32.768	23.3

Table 3.2: Comparison between various detection methods for multiple ASSRs stimuli (without artefact rejection).

Stimulus (Hz)	MASTER Normal Averaging Time, (s)	MASTER Weighted Averaging Time, (s)	Observer-based Detection Time, (s)
		<u>Data set 1</u>	
78.125	180.244	147.456	143.0
80.078	65.536	32.768	30.0
83.008	49.152	32.768	28.5
84.961	16.384	16.384	19.2
86.914	16.384	16.384	14.5
89.844	16.384	16.384	12.1
91.797	49.152	65.536	60.0
94.727	32.768	32.768	22.8
		<u>Data set 2</u>	
78.125	131.072	131.072	15.9
80.078	49.152	98.304	44.2
83.008	16.384	16.384	23.5
84.961	32.768	32.768	16.4
86.914	16.384	16.384	19.5
89.844	32.768	32.768	23.6
91.797	49.152	49.152	23.1
94.727	114.688	147.456	90.0
		<u>Data set 3</u>	
78.125	65.536	65.536	100.2
80.078	163.384	131.072	128.4
83.008	16.384	16.384	26.1
84.961	32.768	32.768	18.0
86.914	16.384	16.384	12.0
89.844	16.384	16.384	17.3
91.797	16.384	16.384	14.2
94.727	49.152	32.768	23.3

Table 3.3: Comparison between various detection methods for multiple ASSRs stimuli (with artefact rejection at $80\mu\text{V}$).

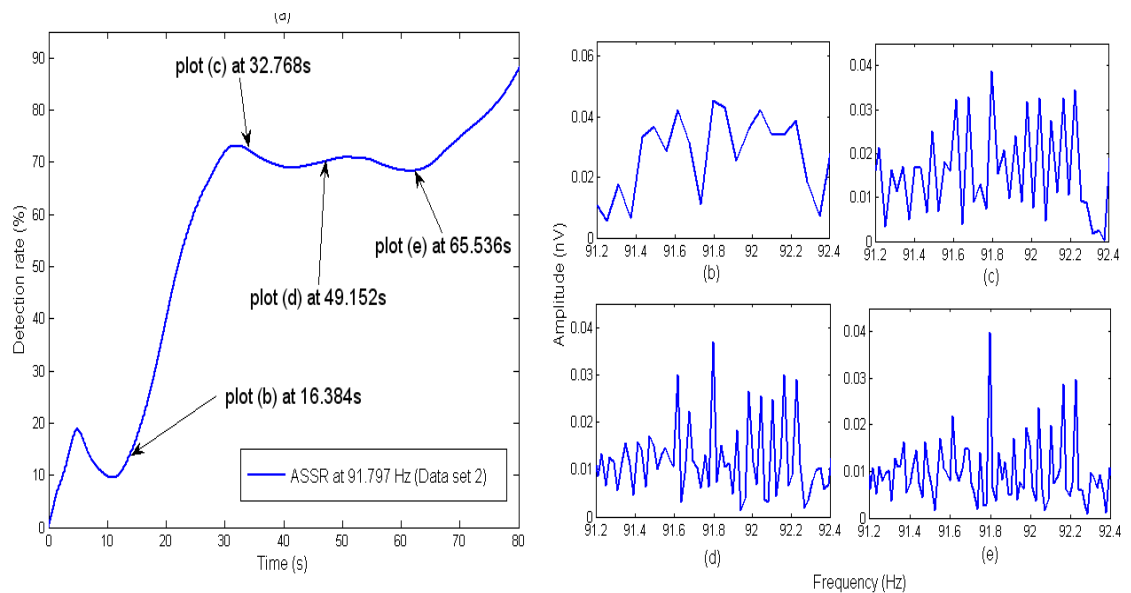


Figure 3.12: ASSR detection rate (a) using observer-based thresholding approach, (b)–(e) normal averaging plus FFT.

Figure 3.12 illustrates the ASSR detection rate response with respect to stimulus at 91.797 Hz using the proposed method as compared to the normal averaging. As the

detection achieved at 23.1s using observer-based method, a clear decision is only confirmed at 49.152s using normal averaging as shown in Figure 3.12c. As the number of ‘sweeps’ (data sample with length of 16.384s) used in averaging increased, the distinctive peak voltage of the ASSR appears in FFT spectrum, as shown in Figure 3.12b—3.12e.

It appears that the proposed detection scheme offers improved or at least comparable overall performance compared with the most widely used ASSR detection methods. The proposed method has the advantage not only of having a fast detection rate (shorter test duration) but and also the ability to perform the detection on-line by updating available data instantaneously without the need of pre-storing the data. Moreover, the proposed detection scheme needs neither sophisticated processing protocols nor complicated designs in terms of the hardware and data acquisition unit required. Typically, the selection of the small observer gains as stated before performs well for low SNR scenarios. The gains used here were designed empirically via earlier simulation trials to produced ‘fine tuned’ gains that have a good balance between the two influential factors of fast detection rate and noise rejection, which is guided by the observer theory (Kwakernaak and Sivan, 1972).

3.5 Concluding Remarks

An alternate method for ASSR detection in real-time is introduced in this Chapter. The method is based upon the state estimation technique, known as Luenberger observer method. The proposed method views the ASSR detection from a different angle, the idea is to treat the ASSR problem as a classical filtering or signal estimation issue. This is because according to the literature, the ASSR is a faint sinusoidal like signal oscillating at a constant frequency and embedded within the noisy AEP (low SNR). In general, the Luenberger observer performs well both with synthetic data (via simulations) and BIOPAC recorded data (via experiments).

This Chapter introduced two different types of detection, one based on amplitude-based and the second on power-based approaches. As presented in the proposed ASSR detector, the decision making in the detection rate of either $A_d(\%)$ or $p_d(\%)$ is based on an empirically pre-defined threshold to determine the existence or non-existence of ASSR within the recorded AEP. If the response exceeds the threshold, it means that the

ASSR is present or otherwise. As mentioned in Section 3.3.1, the amplitude-based detection is preferred because of its flexibility of the algorithm. Although the ASSR detection scheme performed well so far with observer gains being constant (chosen through empirical studies), this could lead to problems if the SNR assumptions are not reliable. Therefore, a better approach based on adaptive principles is to be presented in Chapter 4.

To date there have been no other studies reported about research on ASSRs which are recorded using the BIOPAC data acquisition system. The results from the preliminary studies presented in this Chapter have confirmed capability of recording ASSRs from BIOPAC and matched with the research carried out on ASSRs using MASTER. This also clarifies the performance of the proposed ASSR detection approach and the suitability of the BIOPAC system for recording of ASSR. Moreover, BIOPAC provides a basis for the development of an adaptive ASSR detection approach which is presented in Chapter 4.

4 . On-line Detection of ASSR via Adaptive Kalman Filter

4.1 Introduction

Although the observer-based detection scheme described in Section 3.2 operated efficiently under simulated conditions (as shown in Sections 3.3 and 3.4), it does have drawbacks when applied to the real ASSR data. The main disadvantage of the observer-based detection approach is the need for gain parameter tuning when the signal-to-noise ratio (SNR) condition is unknown and varying. In order to have satisfactory detection under various SNR scenarios, the gain needs to be manually tuned via trial-and-error or by a series of empirical studies. Manual gain tuning could be time consuming and may not be applicable to real world applications, this is particularly crucial in the ASSR based hearing test if the subjects are newborn and children. In general, this can be overcome by implementing the Kalman filter (KF) as this provides the optimal state estimate, provided all *a priori* model and statistical information are available. The standard KF theory is summarised in Section 4.2 and a comparison with the observer-based ASSR detector (described in Chapter 3) is outlined.

Typically, an optimal Kalman filter can be implemented but only if all *a priori* information are available. For this particular application, limited *a priori* information is known or not available at all. As a result, the automatic gain parameters tuning facility is needed to provide reliable detection under the conditions of unknown and probably varying SNR. An alternative KF method which operates adaptively is known as an adaptive Kalman filter (AKF). An overview of AKF and the mathematical formulation of the AKF-based detection scheme are presented in Section 4.3, which also included its preliminary simulation results. Experimental validation of the adaptive detection approaches is described in Section 4.4. Chapter concluding remarks are provided in Section 4.5.

4.2 Kalman Filtering

The KF is a special type of observer that accounts for the presence of process and measurement noise, and its gain is determined by using statistical information on the system (Kalman, 1960; Kalman and Bucy, 1960). Therefore, it can be seen as an optimal state observer or sometime referred as a stochastic state estimator. The KF was initially used in the 1960s for aerospace applications. Widespread success of the KF in aerospace applications has led to attempts to apply it to more common industrial applications.

The KF not only works well in practice, but also is theoretically attractive because, of all possible filters, it is the one that minimizes the variance of the estimation error under certain conditions. KFs are often implemented in embedded control systems because in order to control a process, good estimation of the process variables is essential (Gelb, 1974; Anderson and Moore, 1979; Maybeck, 1979). The standard linear KF has two versions, one is for discrete time systems and the other for continuous time systems. However in practice, the first version is preferable because the discrete-time version best illustrates the recursive concept and is useful for digital implementation. A general insight into the structure of a standard KF (discrete time-varying) will be presented briefly. The process of a KF can be described as a recursive estimation process utilizing a form of information feedback, for instance, the filter estimates the process state at some time and then obtains updated information in the form of (noisy) measurement.

To illustrate the implementation of discrete Kalman filtering in extracting sinusoidal signals from noise, consider a noisy sinusoid $y(k)$ that is similar to Eqn. (3-1) but with time index written as k (i.e. $k = T_s, 2T_s \dots nT_s$, $n = \text{integer}$). This can be viewed as a discrete-time output $y(k)$ of a second order dynamic system, with the output equation

$$y(k) = x(k) + v(k) \quad (4-1)$$

To develop a discrete model of the noisy sinusoid $y(k)$, define a state vector as:

$$x(k-1) = \begin{bmatrix} A \sin(\omega k T_s + \phi) \\ A \cos(\omega k T_s + \phi) \end{bmatrix} \quad (4-2)$$

where the amplitude A , the angular frequency ω , sampling period T_s , phase ϕ are constants and $v(k)$ is assumed to be a white noise signal satisfying a Gaussian distribution. Thus the $(k+1)$ th sample will be:

$$x(k) = \begin{bmatrix} A \sin(\omega(k+1)T_s + \phi) \\ A \cos(\omega(k+1)T_s + \phi) \end{bmatrix} \quad (4-3)$$

which is written according to the trigonometry expansions as:

$$\begin{aligned} \sin(a+b) &= \sin a \cos b + \cos a \sin b \\ \cos(a+b) &= \cos a \cos b - \sin a \sin b \end{aligned} \quad (4-4)$$

Eqn. (4-3) is now re-written as:

$$x(k) = A_D x(k-1) \quad (4-5)$$

where the transition matrix A_D is

$$A_D = \begin{bmatrix} \cos(\omega T_s) & \sin(\omega T_s) \\ -\sin(\omega T_s) & \cos(\omega T_s) \end{bmatrix} \quad (4-6)$$

So far, Eqns. (3-1) or (4-1) describes the sinusoid-like ASSR corrupted with $v(k)$ from the measurement is obtained. There is however, a second way of describing how the signal can be modelled, which is believed to be more realistic to human physiology. The reason for introducing the process noise $w(k)$ into the signal model $x(k)$ of Eqn. (4-3) is that $x(k)$ is assumed to be corrupted by additional noise $w(k)$ *a priori* to $v(k)$ while in the process of generating $x(k)$ in responses to stimulus. Hence, adding a noise term to Eqn. (4-5) gives

$$x(k) = A_D x(k-1) + w(k-1) \quad (4-7)$$

where the process noise $w(k-1)$ is

$$w(k-1) = \begin{bmatrix} w_1(k-1) \\ w_2(k-1) \end{bmatrix} \quad (4-8)$$

where $w_1(k)$ and $w_2(k)$ are uncorrelated to each other, whereas the output equation in Eqn. (4-1) is now written as

$$y(k) = C_D x(k) + v(k) \quad (4-9)$$

with output matrix C_D as

$$C_D = [1 \quad 0] \quad (4-10)$$

According to Eqns. (4-7) and (4-9), the system can be viewed as linear time-invariant (LTI) system. The system is observable with observable matrix (C_D, A_D) having full rank of 2. The random variables (Gaussian white) $w(k)$ and $v(k)$ represent the process and measurement noise (both noise statistics are uncorrelated), and with their means and covariances as:

$$\begin{aligned} E[w(k)] &= 0, & E[w(k)w(i)^T] &= Q(k)\delta(ki) \\ E[v(k)] &= 0, & E[v(k)v(i)^T] &= R(k)\delta(ki) \\ E[w(k)v(i)^T] &= 0 \end{aligned} \quad (4-11)$$

where $E[\cdot]$ denote the expectation and $\delta(ki)$ denotes the Kronecker delta function, with $\delta(kk) = 1$, else $\delta(ki) = 0$ for $k \neq i$. Moreover, the initial state $x(0)$ is jointly independent to all individual elements of $W(k)$ and $V(k)$ over time k , where $W(k) = [w(0), w(1), \dots, w(k)]$ and $V(k) = [v(0), v(1), \dots, v(k)]$.

A recursive cycle (between time update and measurement update equations) of the KF can be described by the following set of equations with initialisation parameters. With the following notations

$\hat{x}^-(k)$: *a priori* state estimate

$P^-(k)$: *a priori* covariance

$\hat{x}^+(k)$: a posteriori state estimate

$P^+(k)$: a posteriori covariance

$Q(k)$: covariance of process noise, $w(k)$

$R(k)$: covariance of measurement noise, $v(k)$

and the equations of Kalman filtering are given as follows:

Initialisation:

$$\hat{x}^+(0) = E[x(0)] \quad (4-12)$$

$$P^+(0) = E \left[(x(0) - \hat{x}^+(0))(x(0) - \hat{x}^+(0))^T \right] \quad (4-13)$$

Time update:

$$\hat{x}^-(k) = A_D \hat{x}^+(k-1) \quad (4-14)$$

$$P^-(k) = A_D P^+(k-1) A_D^T + Q(k-1) \quad (4-15)$$

Measurement update

$$K(k) = P^-(k) C_D^T [C_D P^-(k) C_D^T + R(k)]^{-1} \quad (4-16)$$

$$\hat{x}^+(k) = \hat{x}^-(k) + K(k) [y(k) - C_D \hat{x}^-(k)] \quad (4-17)$$

$$P^+(k) = [I - K(k) C_D] P^-(k) \quad (4-18)$$

The algorithms of the KF are separated into time update equations and measurement update equations. The time update equations are responsible for projecting forward (in time) the current state and error covariance estimate to obtain the *a priori* estimate for the next time step. Meanwhile, the measurement update equation is responsible for the feedback correction. To ease the implementation of the algorithms into Matlab/SIMULINK, the KF is expressed using *one-step a priori KF equations* (via combining *a priori* and *a posteriori* terms into a single equation) rather than the standard derivation as in Eqns. (4-14)—(4-18) (Simon, 2006).

Denote *a priori* state estimate expression from Eqn. (4-14) with time index increased by one and *a posteriori* expression from Eqn. (4-17) is substituted into Eqn. (4-14) to obtain

$$\hat{x}^-(k+1) = A_D \underbrace{\left\{ \hat{x}^-(k) + K(k) [y(k) - C_D \hat{x}^-(k)] \right\}}_{\hat{x}^+(k)} \quad (4-19)$$

This illustrates that the *a priori* state estimate can be computed directly without acquiring the *a posteriori* state in between. The same applies to the *a priori* covariance expression from Eqn. (4-15) with time index increase by one and a *a posteriori* expression from Eqn. (4-18) is substituted into the above equation to obtain

$$P^-(k+1) = A_D [P^-(k) - K(k) C_D P^-(k)] A_D^T + Q(k) \quad (4-20)$$

then gain expression from Eqn. (4-19) is substituted into Eqn. (4-20) to yield

$$P^-(k+1) = A_D P^-(k) A_D^T - A_D \underbrace{\left\{ P^-(k) C_D [C_D P^-(k) C_D^T + R(k)]^{-1} \right\}}_{K(k)} C_D P^-(k) A_D^T + Q(k) \quad (4-21)$$

The amplitude of the ASSR can be estimated by

$$\hat{A}(k) = \sqrt{\hat{x}_1^2(k) + \hat{x}_2^2(k)} \quad (4-22)$$

where $\hat{x}_1^2(k)$ and $\hat{x}_2^2(k)$ are posterior $\hat{x}^+(k)$ obtained using Eqns. (4-19) and (4-21). The estimated amplitude can be coherently averaged over short time interval to produce smoother and more accurate estimation

$$\bar{A}(j) = \frac{1}{2M} \left[\sum_{k=0}^M \hat{A}(k) + \sum_{k=0}^M \hat{A}(k-1) \right] \quad (4-23)$$

This is particularly vital for the evaluation module to indicate the existence of any ASSR signal within an AEP (low SNR) and to reduce the chances of false alarm which typically causes sudden artefact appearance. The length of the coherent averager is determined by M , in which sampled at j time step. In other word, $\bar{A}(j)$ is updated every time step j , while remained the same within time step interval.

Denote detection rate $\bar{A}_x(j)$ as the expected batch amplitude of $\hat{x}^+(k)$ when $x(k)$ is present and detection rate $\bar{A}_{no}(j)$ otherwise. It is expected that $\bar{A}_x(j) > \bar{A}_{no}(j)$ for all $j > 0$. The evaluation module is design similar to Eqn. (3-24) as

$$\bar{A}_d(\%) = \frac{[\bar{A}_x(j) - \bar{A}_{no}(j)]}{\bar{A}_{no}(j)} \times 100\% \quad (4-24)$$

where $\bar{A}_d(\%)$ can be used as an indicator to evaluate the degree of existence of $x(k)$, thus a threshold can be pre-defined to determine its existence. This implies that when a sinusoid is present $\bar{A}_d(\%)$ should be distinctively greater than that when it is absent. The pre-defined threshold is chosen from empirical trials and determined to be 200%. The level of threshold defined was based on the average response from 50 simulation trials with random seeding in the noise generated for each trial.

From the theories described, both Luenberger observer and the KF share a lot in common, for instance both can operate in real-time, have a similar structure, and are compatible in performances. Typically the Luenberger observer is applied to deterministic cases, whereas the KF applies in stochastic environment. Due to the property of the minimum variance of estimation, the KF can perform optimally while tracking a sinusoid corrupted by noise. To compare the responses of the optimal KF and proposed observer-based algorithms from Chapter 3, a noisy sinusoidal signal $y(k) = 0.015 \sin(20\pi k) + v(k)$ at sampling rate of 1k, process and measurement noise

standard deviations of $\sigma_Q = 1 \times 10^{-7}$ and $\sigma_R = 0.15$, and mean $\mu_{mean} = 0$ (SNR= -20dB) is applied to the observer-based algorithms with series of gain parameters chosen as $(l_1; l_2; \alpha)$ (as shown in Figure 4.1) and to KF with the parameters setting as follows:

KF	
Term	Value
$\hat{x}^+(0)$	$\begin{bmatrix} 0 \\ 0 \end{bmatrix}$
$P^+(0)$	$\begin{bmatrix} 0.1 & 0 \\ 0 & 0.1 \end{bmatrix}$
Q	$\begin{bmatrix} \sigma_Q^2 & 0 \\ 0 & \sigma_Q^2 \end{bmatrix}$
R	σ_R^2
M	1000

Observer-based detection	
Term	Value
$\hat{x}(0)$	$\begin{bmatrix} 0 \\ 0 \end{bmatrix}$

Table 4.1: Parameters setting for KF and observer-based detectors.

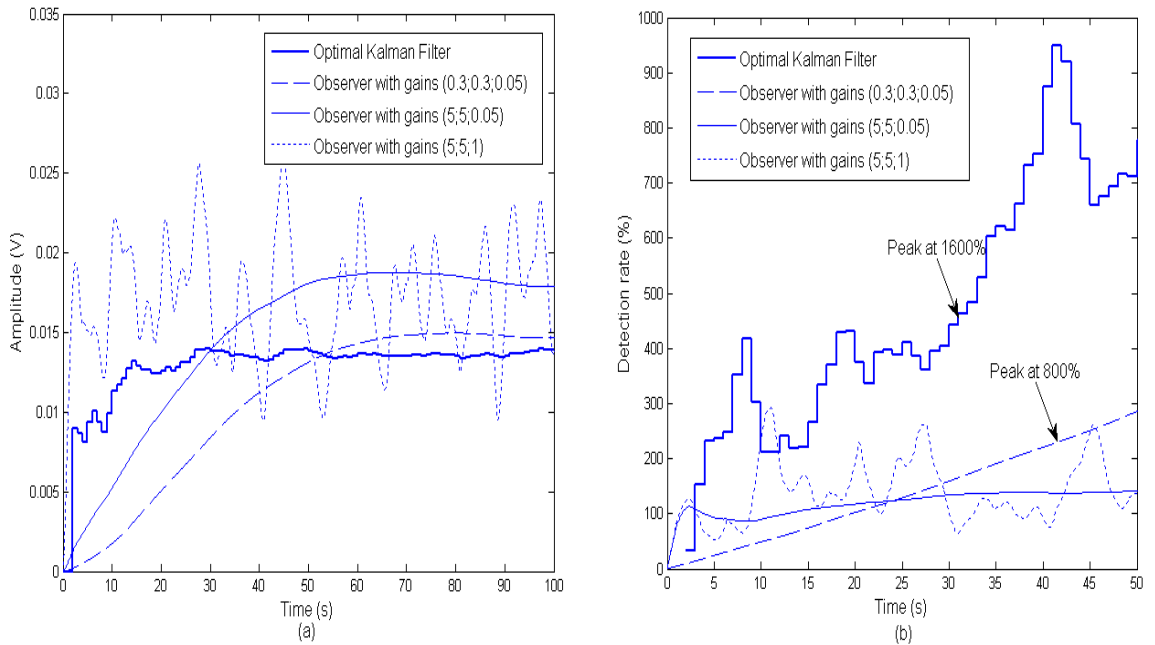


Figure 4.1: Comparative between KF and observer-based detectors via (a) amplitude response and (b) detection rate.

If the observer gains are tuned carefully, its detection rate is comparable to the optimal KF or better (via higher gains) as shown by final two examples (dotted and solid line responses) in Figure 4.1b. However, higher gains cost the smoothness of the amplitude convergence and more sensitive to noise interference, as illustrated by the last example (dotted line response) in Figure 4.1a. On the other hand, smaller gains improve the

smoothness of the convergence and more resilience to noise, but may result in slower detection rate if knowledge of SNR is unavailable (which is unknown in ASSR detection), as illustrated by the second example (dash line response) in Figure 4.1a and Figure 4.1b. This is due to, if the observer gain L (l_1 and l_2) is chosen so that $A_C - LC_C$ has stable eigenvalues, the observer may no longer provide a good estimate under different noise situations.

On the other hand, manual gain tuning is not required in the KF because it operates with the given *a priori* parameters information (e.g. variables in Table 4.1) and provides optimal estimation. Empirical gain tuning is time consuming, thus KF is preferable since optimal gain can be computed and suitable to implement in stochastic case study. In fact, the observer and KF are relatively similar if the observer gain L is chosen according to Algebraic Riccati equation, the observer then becomes a steady-state KF with known variances Q and R .

4.3 Adaptive Kalman Filtering

4.3.1 Background

An KF is a recursive algorithm developed to solve the state estimation problem of a known system based on the complete *a priori* knowledge about the system's mathematical model, input signal and noise statistics. However in practice, the exact *a priori* information required are seldom available, thus implementing KF may no longer be straight forward. The use of wrong *a priori* parameters or erroneous noise statistics in the design may yield poor results and even divergence of estimation errors. Therefore, the utilization of adaptive Kalman filter (AKF) is needed to reduce or at least bound these errors caused by ill known *a priori* information in the design. There are a number of different approaches in designing an AKF. Since in the targeted ASSR application study, the main source of uncertainty is due to unknown noise statistics, thus it is utmost important to identify or estimate the noise statistics.

Several AKFs have been proposed for the identification of noise covariance matrices since 1960s and majority of the algorithms were originated in the 70—80s. The existing approaches so far can be briefly divided into four categories: Bayesian approach (Magill, 1965; Hilborn Jr and Lainiotis, 1969; Sage and Husa, 1969; Alspach and Abiri,

1974), Maximum likelihood estimation (Kashyap, 1970), covariance-matching techniques (Meyers and Tapley, 1976; Morein and Kalata, 1990; Hsu *et al.*, 1991) and correlation methods (Mehra, 1970a, 1971 and 1972; Scharf and Alspach, 1972; Carrew and Bellanger, 1973; Sinha, 1973; Belanger, 1974; Sinha and Tom, 1977; Dee *et al.*, 1985; Oussalah and De Schutter, 2000). Generally, the Bayesian and the Maximum likelihood methods demand more computations and mainly based on the assumption that the noise statistics are stationary. Covariance-matching techniques are mainly based on detection scheme to ensure that the filter residuals are consistent with their theoretical covariances, but this method may sometimes be restrictive. However, the correlation methods are the most fruitful ones among the four. The idea is to establish a set of equations relating the system parameters (noise statistics specifically) to the autocorrelation of the measurement or residual sequence. The resultant equations are then solved simultaneously for the unknown parameters. Besides the four types of the noise identification approaches, other methods in resulting AKF can be found in (Friedland, 1982, 1990; Moghaddamjoo, 1986; Niedwiecki, 1988, 1990). As mentioned earlier, the unknown noise statistics make it difficult to utilise the standard KF for the ASSR application. Thus, identification of the noise statistics is crucial. As a result, the correlation method is to be emphasised in the AKF-based ASSR detector because of its practically proven records, simplified structurally and lower computation requirement.

The correlation methods have been deployed for noise estimation in time domain analysis for quite a long time. The correlation methods are mainly divided into, output correlation method (based on measurement $y(k)$) and innovation correlation method (based on residual $y(k) - C_D \hat{x}^-(k)$). Many of these methods were originated from Mehra (1972). The fundamental idea of the correlation method is to correlate the output of the system directly or after a known linear operation. A set of equations are established to relate the system parameters to the measured autocorrelation function and then solved simultaneously for the unknown parameters. These methods are commonly applicable to LTI system. Mathematical formulation of the proposed AKF-based detection scheme will be discussed in the following section.

4.3.2 Development of On-line Adaptive ASSR Detector

As presented on the system's parameters in section 4.2, the standard KF may not provide optimal estimation if the correct information is unavailable and an AKF is

needed. The challenge of this topic of study is to determine the existence or non-existence of the ASSR signal that embedded within an overwhelm background noise ($\text{SNR} \approx -30\text{dB}$), but with noise parameters varying between subjects and hearing test environments. The measurement noise $v(k)$ in Eqn. (4-9) is represents the main source of background noise, which mediates via human physiological fluctuations (e.g. EEG and electromyography (EMG)), equipment and power line interferences, but with predominates mainly by human EEG.

Both $v(k)$ and $w(k)$ are assumed to be stationary and with slow varying statistics within the LTI model. Therefore, two tiers of sampling time intervals were introduced, where T_s is the standard as sampling rate at time step k and T_{ad} is referred as adaptation rate at time step j ($T_{ad} = T_s \times N$) with $T_{ad} \gg T_s$. In other words, N number data points of noise statistics $Q(k)$ and $R(k)$ within a batch and assumed to vary between T_{ad} instead of T_s . The advantages are to decrease the computation load and producing much accurate expectation of the covariances $R(j)$ and $Q(j)$, but still enable the filtering process to track the measurement noise statistics by producing a time-varying Kalman gain $K(k)$. The following approach is considered as output correlation method because the input used for correlation is based on the measurement $y(k)$.

Estimation of noise covariance $R(j)$ is much straight forward, according to the output correlation method by Mehra (1972). Denote $\Gamma(i)$ to be the i th lag autocorrelation of the output measurement (row vector) $[y(k) \ y(k-1) \dots y(k-N+1)] = Y(j)$, which is a vector containing N numbers of data samples of $y(k)$ in batch.

$$\Gamma(i) = E[Y(j)Y(j-i)^T] \quad (4-25)$$

Assuming $Y(j)$ is stationary so that the autocorrelation is only a function of lag. The expression for $\Gamma(i)$ can be derived from a generalised case of Eqns. (4-7) and (4-9) (Mehra, 1972), thus

$$\Gamma(i) = \begin{cases} C_D S(j) C_D^T + R, & i = 0 \\ C_D A_D^i S(j) C_D^T, & i > 0 \end{cases} \quad (4-26)$$

where $S(j) = E[x(j)x^T(j)]$ is the state covariance. Rewriting Eqn. (4-26) explicitly for $i = 1, 2$

$$\begin{bmatrix} \Gamma(1) \\ \Gamma(2) \end{bmatrix} = D S(j) C_D^T \quad (4-27)$$

where number of i is chosen based on the system order (i.e. 2nd order system) in order to balance both sides of equation. Whereas

$$D = \begin{bmatrix} C_D A_D \\ C_D A_D^2 \end{bmatrix} \quad (4-28)$$

is a square matrix since C_D is a row vector. D is also a non-singular matrix because it is the product of the observability matrix and the non-singular transition matrix. Thus Eqn. (4-27) is then rewritten as

$$S(j)C_D^T = D^{-1} \begin{bmatrix} \Gamma(1) \\ \Gamma(2) \end{bmatrix} \quad (4-29)$$

Hence, estimate of covariance $\hat{R}(j)$ can now be computed using Eqn. (4-26) ($i = 0$) as

$$\hat{R}(j) = \Gamma(0) - C_D[S(j)C_D^T] \quad (4-30)$$

If the sinusoid-like ASSR is described as a sinusoid corrupted with measurement noise $v(k)$ as stated in Eqn. (4-1), only measurement noise covariance $\hat{R}(j)$ from Eqn. (4-30) is needed for the implementation of AKF. On the other hand, if the second idea is adopted where sinusoid-like ASSR is contaminated by two levels of noise, process noise $w(k)$ and measurement $v(k)$, thus both process noise covariance $Q(j)$ and measurement noise covariance $R(j)$ are required. With measurement noise covariance matrix obtained from Eqn. (4-30), only process noise covariance $Q(j)$ remains, which can be viewed as a ‘waste basket’ for unknown modelling errors. However, direct estimation of covariance $Q(j)$ is not possible because of the immeasurable state vector $x(k)$ from the system or in this case from the human subject. Moreover, the optimal estimation of Q_{opt} (unique solution) is a very difficult task with specific conditions (e.g. system must be controllable and observable) to be satisfied and lengthy period may be required to achieve optimum steady state (Mehra, 1970 and 1972; Moghaddamjoo, 1986). However, these conditions may be impossible or impractical in real applications, thus in practice the process noise covariance is usually made through empirical study, trial-and-error or simply a guess. In general, there is no universal solution to this problem.

In order to estimate the process noise covariance $Q(j)$, the state covariance of the signal model $S(k) = E[x(k)x^T(k)]$ needed to satisfy the steady-state Algebraic Riccati Equation

$$S = A_D S A_D^T + Q \quad (4-31)$$

A numerical iterative gradient search technique (e.g. steepest descent method) is therefore been developed for solving state covariance S , which will lead to the computation of Q (Mehra, 1970b). Firstly, initialised the $S(0)$, $\Lambda(0)$ and $\bar{Q}(0)$. Then,

$$S(j+1) = A_D S(j) A_D^T + \bar{Q}(j) \bar{Q}^T(j) \quad (4-32)$$

where $\bar{Q} \bar{Q}^T = Q$ (through built-in Cholesky Factorization in Matlab and Q is non-singular), which does not lose generality of the notation. With updated $S(j+1)$ now being substituted into together with $\Lambda(0)$ into Eqn. (4-32), hence

$$\Lambda(j+1) = A_D \Lambda(j) A_D^T + G C_D + C_D^T G^T - S(j) C_D^T C_D + C_D^T C_D S(j) \quad (4-33)$$

New updated $\bar{Q}(j+1)$ can now be obtained through

$$\bar{Q}(j+1) = \bar{Q}(j) + 2\alpha \Lambda(j) \bar{Q}(j) \quad (4-34)$$

The iterative cycle of Eqns. (4-32) to (4-34) with obtained via a user defined (typically small) step size of α .

In order obtained $Q(j) = \bar{Q}(j) \bar{Q}^T(j)$ that satisfy Eqn. (4-31), assumption were made in Eqn. (4-11) where $x(0)$, $W(k) = [w(0), w(1), \dots, w(k)]$ and $V(k) = [v(0), v(1), \dots, v(k)]$ are all jointly Gaussian and independent (uncorrelated). With the assumption made, denote $E[x(k)x^T(k)]$ as

$$\begin{aligned} E[x(k)x^T(k)] &= E[\{A_D x(k-1) + w(k-1)\} \{A_D x(k-1) + w(k-1)\}^T] \\ &= E[A_D x(k-1)x(k-1)^T A_D + w(k-1)w(k-1)^T \\ &\quad + A_D x(k-1)w(k-1)^T + A_D x(k-1)w(k-1)] \end{aligned} \quad (4-35)$$

where $x(k)$ from Eqn. (4-7). The $E[A_D x(k-1)w(k-1)^T]$ and $E[A_D x(k-1)w(k-1)]$ in Eqn. (4-35) are determine to be zero because of the $E[x(k-1)w(k-1)^T]$ and $E[x(k-1)w(k-1)]$ are assumed uncorrelated for entire time step k . Thus Eqn. (4-35) is now

$$E[x(k)x^T(k)] = E[A_D x(k-1)x(k-1)^T A_D] + E[w(k-1)w(k-1)^T] \quad (4-36)$$

If the state covariance denoted as $S = E[x(k)x^T(k)]$, Eqn.(4-36) can be re-written as

$$S(k) = A_D S(k-1) A_D + Q(k-1) \quad (4-37)$$

In order for Eqn. (4-37) to achieve steady-state state covariance $S = A_D S A_D^T + Q$ of Eqn. (4-31), the process noise variance $Q(k-1)$ is required to be stationary and the transition matrix A_D must be stable. As mentioned above, the process noise Q is assumed to be constant but with a pair marginal stable eigenvalues of the transition

matrix A_D are obtained as $0.8443 \pm 0.5358i$ (absolute value of 1) in the case of $\omega = 180\pi$ and $T_s = 0.001$. These eigenvalues do not change for different values of ω or T_s . This is due to the natural characteristic of a sinewave (continuous time) where only the imaginary part exists and when this is converted into discrete form the discrete-time equivalent eigenvalue is located on the unit circle, leading to marginal stability. This does not satisfies the condition of a steady-state state covariance $S = A_D S A_D^T + Q$, and the approach of solving Q is not suitable in this case. Hence, the implementation of the AKF is not complete without the information of $Q(j)$. Since the optimum computation of $Q(j)$ is not possible, the $Q(j)$ is to be obtained empirically via simulations.

Alternatively, a type of innovation correlation method which involves direct computation of the Kalman gain $\hat{K}(j)$ uses only the residual information sequence $h(k) = y(k) - C_D \hat{x}^-(k)$ without the need to solve solve for $Q(j)$ (Mehra, 1970: 1972) is implemented. Denote $\Gamma(i)$ as the i th lag autocorrelation of the innovation (residual) $H(j) = [h(k) \ h(k-1) \dots h(k-N+1)]$, is a vector containing N data samples of $y(k)$ in the batch:

$$\Gamma(i) = E[H(j)H(j-i)^T] \quad (4-38)$$

Assuming $Z(j)$ is stationary so that the autocorrelation is only a function of lag. Where

$$\Gamma(i) = \begin{cases} C_D P(j) C_D^T + R, & i = 0 \\ C_D [A_D (I - K(j) C_D)]^{i-1} A_D [P(j) C_D^T + K(j) \Gamma(0)], & i > 0 \end{cases} \quad (4-39)$$

Where $P(j)$ is the state estimation error covariance, I is the identity matrix and $K(j)$ is the gain matrix of the AKF. Rewriting Eqn.(4-39) explicitly for $i = 1, 2$:

$$\Gamma(1) = C_D A_D P(j) C_D^T - C_D A_D K(j) \Gamma(0) \quad (4-40)$$

$$\Gamma(2) = C_D A_D^2 P(j) C_D^T - C_D A_D K(j) \Gamma(1) - C_D A_D^2 K(j) \Gamma(0)$$

where the number i is chosen based on the system order (i.e. 2nd order system) in order to balance both sides of equation. Hence, $P(j) C_D^T$ can now be expressed as

$$P(j) C_D^T = K(j) \Gamma(0) + G^{-1}(j) \begin{bmatrix} \Gamma(1) \\ \Gamma(2) \end{bmatrix} \quad (4-41)$$

where

$$G(j) = \begin{bmatrix} C_D A_D \\ C_D A_D (I - K(j) C_D) A_D \end{bmatrix} \quad (4-42)$$

is a square matrix and is non-singular.

Therefore, the estimate of covariance $\hat{R}(j)$ of the innovation sequence can now be computed using Eqn. (4-39) ($i = 0$) as:

$$\hat{R}(j) = \Gamma(0) - C_D[P(j)C_D^T] \quad (4-43)$$

The advantage of using this particular method is that Kalman gain can be obtained without the need of process noise covariance $Q(j)$. The gain is computed via Eqn. (4-16) with time step of j .

$$\hat{K}(j) = P(j)C_D^T \left[\frac{CP(j)C_D^T + R}{\Gamma(0)} \right]^{-1} \quad (4-44)$$

where $CP(j)C_D^T + R = \Gamma(0)$, according to Eqn. (4-39) when $i = 0$. By substituting $P(j)C_D^T$ from Eqn. (4-41) into Eqn. (4-44), a recursive algorithm for the computation of the gain matrix with time step j is:

$$\hat{K}(j) = \hat{K}(j-1) + G^{-1}(j-1) \begin{bmatrix} \Gamma(1)/\Gamma(0) \\ \Gamma(2)/\Gamma(0) \end{bmatrix} \quad (4-45)$$

The gain matrix $\hat{K}(j)$ obtained is held constant within the time interval j , whilst updated for every adaptation step j .

To illustrate the performances between first and second AKF algorithms, simulations were conducted to validate their suitability in scenarios mimicking the ASSR (poor SNR). Figure 4.2a illustrate comparison between both AKF algorithms operating within a scenario where a noisy sinusoid $y(k) = 0.015 \sin(180\pi k) + v(k)$ at sampling rate of 1kHz with SNR of 20dB, and the filter parameters were set accordingly to Table 4.2. The covariance Q which is required by the first AKF algorithm (scheme 1) is defined as zero based on the first description of signal model where only measurement noise existed, detailed discussion on this will be presented in later section. According to the amplitude responses obtained via the two AKF algorithms in Figure 4.2a, both detectors performances are comparable either in cases with or without the present of a sinusoidal signal. To demonstrate the performances of these AKF algorithms in low SNR environment of -20 dB that regarded as a typical SNR for ASSR detection. However, according to Figure 4.2b, the second AKF algorithm (scheme 2) suffers from difficulties in identifying the sinusoid amplitude correctly in a scenario in which a sinusoid is present. This was correctly identified under higher SNR environment in Figure 4.2a. Moreover, the second method is not capable of distinguishing between cases with and

without sinusoids, as shown in Figure 4.2b. Hence based on the simulation conducted in two distinct SNR environments, it is fair to comment that both AKF algorithms are comparable in performances under a high SNR condition, but the second AKF algorithm (scheme 2) is ineffective for a low SNR condition which makes it unsuitable for ASSR detection where SNR could be much lower than the SNR used in the trial (SNR ≈ -30 dB).

Variable	$x(0)$	$P(0)$	N	M
Index	$\begin{bmatrix} 0 \\ 0 \end{bmatrix}$	$\begin{bmatrix} 0.1 & 0 \\ 0 & 0.1 \end{bmatrix}$	1000	1000

Table 4.2: Parameters setting of ASSR detector.

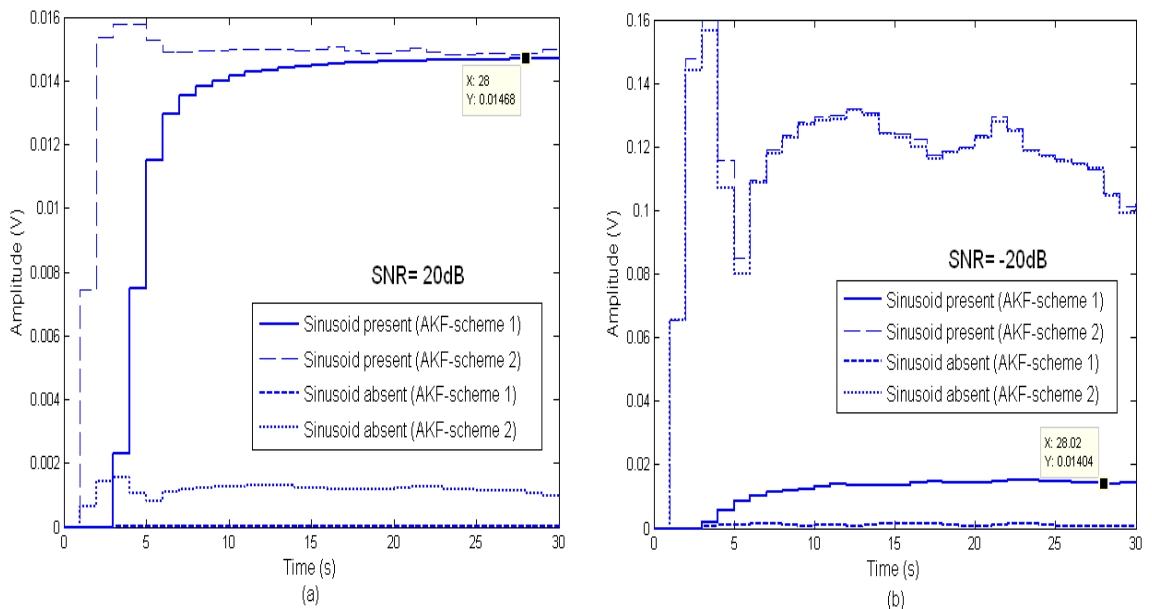


Figure 4.2: Amplitude responses between both AKF algorithms in (a) SNR= 20dB and (b) SNR= -20 dB.

As illustrated in Figure 4.2, the second AKF algorithm (scheme 2) performs well under a high SNR environment, but has difficulty in detecting sinusoids from low SNR signals. Before stating the reason for its poor performance in low SNR, it is essential to understand the key concept of the algorithm. The main advantage of the second AKF algorithm compared with the first is that it does not require information about the covariance $Q(j)$ in performing the detection, whereas it relies on the information about its residual in tuning its gain matrix. This gain tuning mechanism is based on the concept originated by Kailath (1968), where the Kalman gain can be tuned according to the level of randomness of its residual. The mechanism operates with the Kalman gain

to be tuned larger if the residual is correlated, whereas the tuning will be reduced once the residual is uncorrelated. However, if this AKF mechanism performs poorly in determining the randomness of its residual, the poor performance will be due to inappropriate tuning of the Kalman gains.

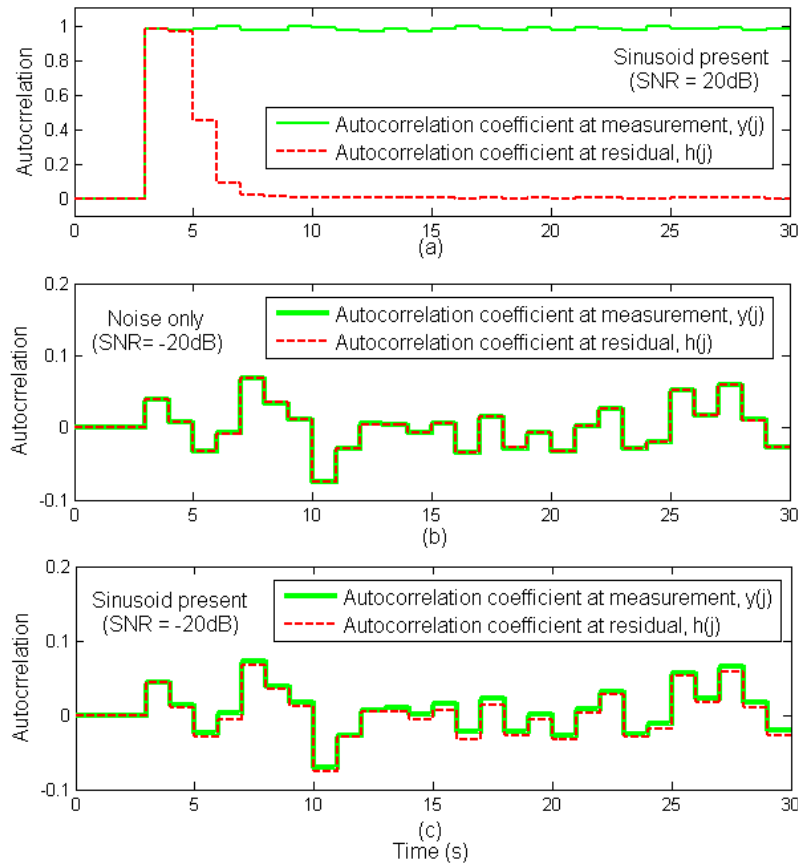


Figure 4.3: Autocorrelation plot for various test scenarios.

As an illustration, Figure 4.2 shows the autocorrelation plots for both the low and high level SNR scenarios corresponding to the use of the second AKF algorithm. The plots show the randomness between the residuals and measurements. The autocorrelation plot is a common tool (Hayter, 2002) based on both autocorrelation and cross-correlation to check the randomness of a data set, its response will be close to zero if the data are random and its response will be significantly non-zero (either close to 1 or -1). The autocorrelation coefficient that is used to define the degree of randomness in an autocorrelation plot is given as:

$$\rho(j) = \frac{\Gamma(i)}{\Gamma(0)}, \quad i > 0 \quad (4-46)$$

where $\Gamma(0)$ and $\Gamma(i)$ are autocorrelation and cross-correlation and obtained via Eqns. (4-25) and (4-38). In fact, the recursive Kalman gain matrix from Eqn. (4-45) uses the autocorrelation coefficients of Eqn. (4-46) where $i = 1$ and 2 , which can be written as

$$\hat{K}(j) = \hat{K}(j-1) + G^{-1}(j-1) \begin{bmatrix} \frac{\Gamma(1)/\Gamma(0)}{\rho(1)} \\ \frac{\Gamma(2)/\Gamma(0)}{\rho(2)} \end{bmatrix} \quad (4-47)$$

The noisy sinusoid shown in Figure 4.3a has SNR of 20dB and is initially highly correlated between its measurement and residual, but the residual later indicates a randomness or whiteness, indicating a success in extracting the sinusoid from the noisy data. The autocorrelation coefficient close to zero is significantly different from its highly correlated measurement data. However, the second scenario of a noisy sinusoid with SNR of -20dB, as shown in Figure 4.3c, displays a high correlation between its autocorrelation coefficient at its measurement and residual. These responses are similar to the case of testing with a noise only sample as shown in Figure 4.3b. From this there is hence no way of telling if a measurement is a sinusoid corrupted with noise or just a noise only measurement (without sinusoid) and the Kalman gain therefore cannot be tuned appropriately. Hence, the second AKF algorithm (scheme 2) is not suitable in this application, where the SNR is low.

Figure 4.4 illustrates the first AKF algorithm (scheme 1) or on-line adaptive ASSR detection scheme with the signal description assuming the existence of only the measurement noise.

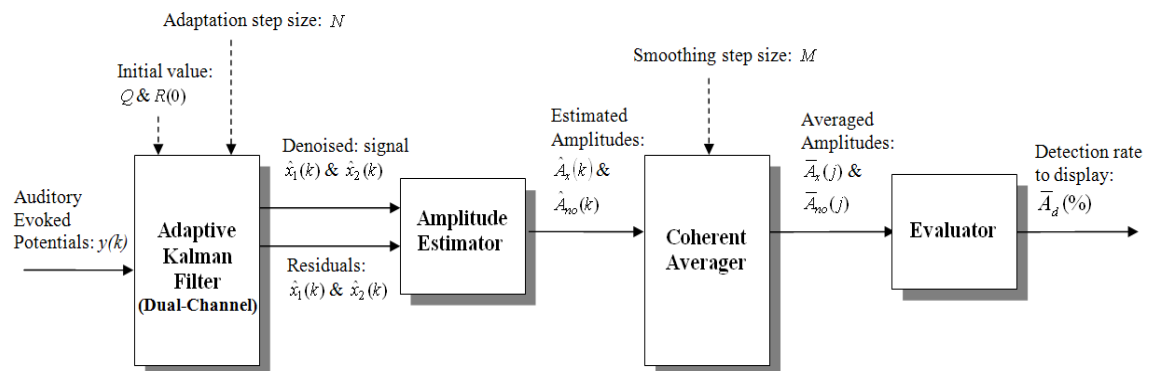


Figure 4.4: Schematic of the proposed on-line adaptive ASSR detection scheme.

4.3.3 Simulation Results

To demonstrate the performance of the proposed adaptive ASSR detector, synthetic data were initially used under simulation conditions. Trials conducted using experimental recorded data are presented in Section 4.4. In order to illustrate the capability of the ASSR detector in processing a noisy sinusoid signal $y(k) = 0.015 \sin(20\pi k) + v(k)$ with sampling rate of 1kHz, and with the parameters given in Table 4.2. The parameters given in Table 4.2 are used throughout all the simulation experiments described in this section unless otherwise stated.

Impact of process noise on the detection rate response

As mentioned earlier, finding the optimal Q_{opt} is difficult and could be impossible particularly for this application since the actual ASSR signal is not measurable and also no AEP model is available so far. However, two different assumptions of the ASSR model were made in the beginning of this chapter. If $Q(j)$ is non-zero, it corresponds to the concept of modelling the ASSR with process noise added to $x(k)$, whereas $x(k)$ is assumed to be noise-free if $Q(j)$ is set to be zero. To illustrate the performance of using different Q matrices (assumed stationary), several trials were conducted and their responses are presented in Figure 4.5. The process noise covariances are denote as:

$$Q_1 = \begin{bmatrix} 1 \times 10^{-12} & 0 \\ 0 & 1 \times 10^{-12} \end{bmatrix},$$

$$Q_2 = \begin{bmatrix} 1 \times 10^{-10} & 0 \\ 0 & 1 \times 10^{-10} \end{bmatrix},$$

$$Q_3 = \begin{bmatrix} 1 \times 10^{-8} & 0 \\ 0 & 1 \times 10^{-8} \end{bmatrix},$$

$$Q_4 = \begin{bmatrix} 0 & 0 \\ 0 & 0 \end{bmatrix}.$$

According to Figure 4.5a, various sets of Q will eventually produce satisfactory detection rate response with the larger the value of Q the faster the convergence rate to exceed the pre-defined threshold at 200% at SNR almost equal to 0 dB. However, for the case where the SNR is approximately equal to -30 dB, the performances of all the choices of Q are relatively close except Q_3 which tends to be less immune to large noise signals by having a poorer detection rate response. This is due to the fact that for larger values of Q (representing larger process noise levels) there is a trade-off of high sensitivity to noise interference (e.g. low SNR) as shown in Figure 4.5b. Hence, the idea is to balance between the factors of faster detection rate and higher noise immunity

particularly in the application where SNR is low, for instance in the ASSR detection problem. Having said that, it is still a challenge to select the Q , when the ASSR model is unavailable. Therefore, the first concept of describing the ASSR is to be endorsed with the assumption that $x(k)$ or $x(t)$ are noise-free sinusoidal signals by choosing $Q = \begin{bmatrix} 0 & 0 \\ 0 & 0 \end{bmatrix}$.

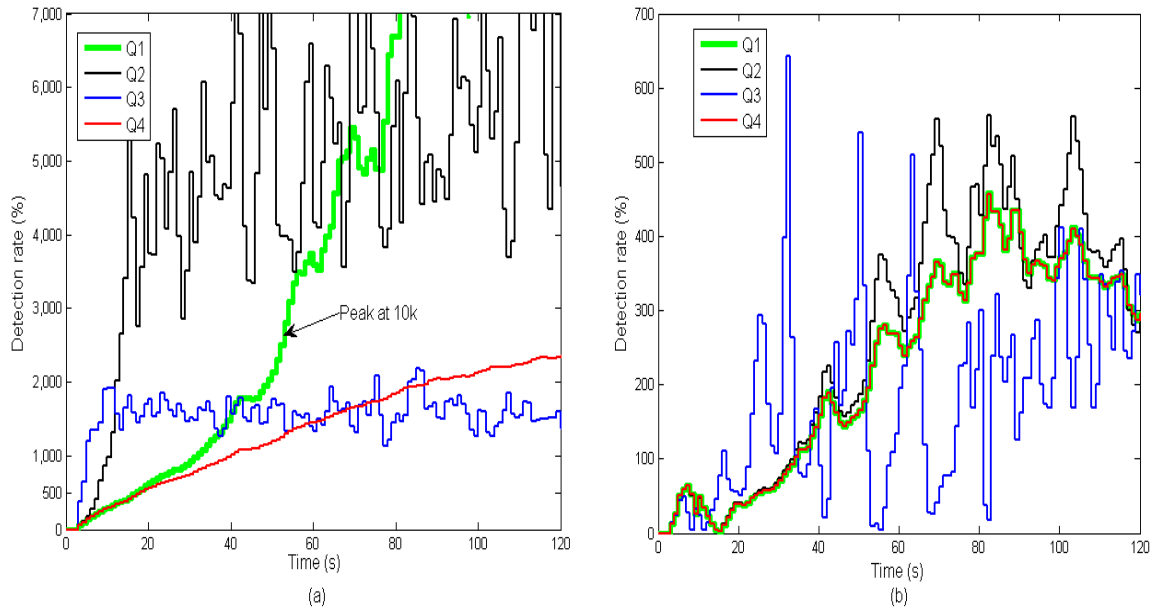


Figure 4.5: Output responses from process noise signals of (a) SNR 0dB and (b) SNR = -30dB.

Comparison between optimal KF and AKF

Since $Q = \begin{bmatrix} 0 & 0 \\ 0 & 0 \end{bmatrix}$ is assumed, the adaptable gain now depends on only the measurement noise $R(j)$. A comparison is made between the optimal KF and the AKF, in order to illustrate the performances in estimating a noisy sinusoid with a low SNR environment of -30dB, which is shown in Figure 4.6. The result presented in Figure 4.6 is a typical response from 10 simulation trials. The simulation parameters are the same as provided in Table 4.2. In general, their performances in terms of amplitude response and detection rate are relatively close, with MSE between optimal KF and AKF is shown in Figure 4.6b. Since the MSE between these methods are relatively small, it would be no surprise that their detection rate responses are quite similar, as in Figure 4.6c. Their close similarity in terms of their performances is because of the $Q_{opt} = \begin{bmatrix} 1 \times 10^{-10} & 0 \\ 0 & 1 \times 10^{-10} \end{bmatrix}$ used in optimal KF is relatively small as compared to the

$Q = \begin{bmatrix} 0 & 0 \\ 0 & 0 \end{bmatrix}$ assumed in the AKF. If the Q_{opt} chosen in optimal KF is far bigger, it is expected that the optimal KF will be better performed. Due to the typically low SNR condition of the particular application that concern (mimicking ASSR detection), only limited range of Q is suitable and also they output comparable detection rate responses (see Figure 4.5b). Although their performances are generally comparable, the optimal KF is not suitable due to the lack of a priori knowledge of the noise statistics and SNR conditions, whereas the AKF estimates these parameters on-line simultaneously within its filtering process.

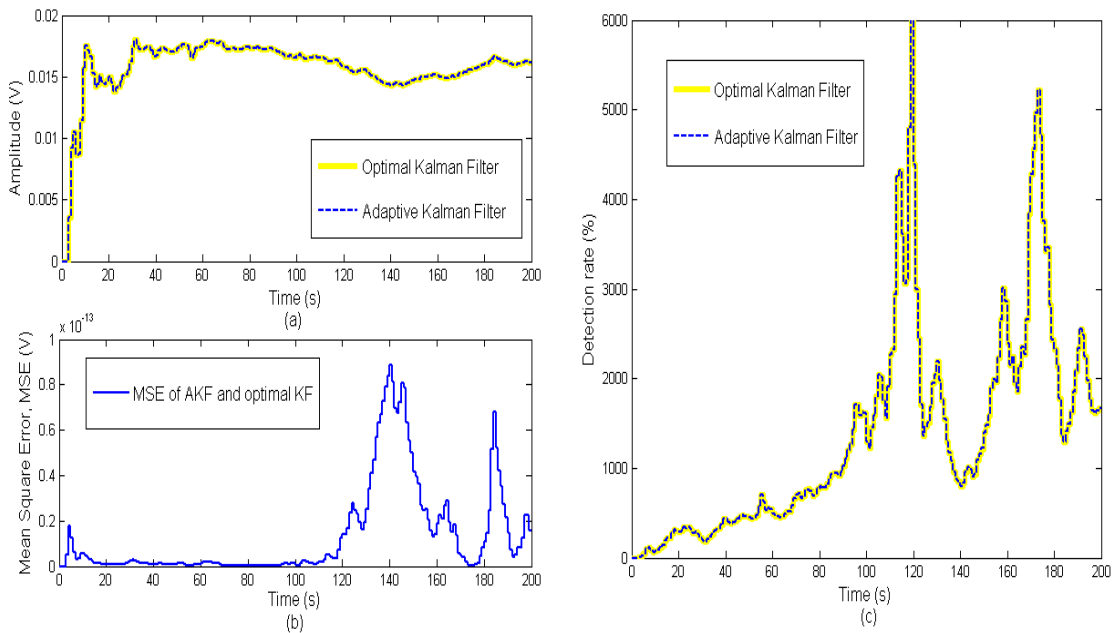


Figure 4.6: Comparative performance between optimal KF and AKF in detecting noisy sinusoid in $\text{SNR} \approx -30\text{dB}$.

Effectiveness of the AKF-based adaptive ASSR detector

As seen from the examples shown above, where the AKF with $Q = \begin{bmatrix} 0 & 0 \\ 0 & 0 \end{bmatrix}$ is comparable the performance of an optimal KF under the constraints of ASSR detection. In terms of decision making as to whether a sinusoid or ASSR is present or absent within a given detection, a thresholding is used in a similar manner to the observer-based detector in Chapter 3 where the decision making threshold is pre-defined as 50% in the detection rate plot. Therefore, a simulation trial was conducted to determine the benchmark threshold quantitatively. According to Figure 4.7a, the amplitude responses between detection of a sinusoid present and absent data are distinctively different and this result is applicable to all the trials tested. This verifies that the adaptive detector is

capable of estimating a particular sinusoid at a known frequency within a low SNR environment. For the detection rate plot in Figure 4.7b, the detection rate responses between existing and non-existing sinusoids are significantly different. The majority of the trials displayed close similarity to the detection rate responses as illustrated by the example 2 shown in Figure 4.7b. Thus, the pre-defined threshold is determined at 200% based on the simulations.

However, determining the threshold level for AKF may sometimes be tricky because some detection rate responses, for instance, case 1 (sinusoid present) in Figure 4.7b may occasionally peak above the 200% threshold benchmark even though its amplitude response can be well distinguished from the sinusoidal signal present in the response. Nonetheless, the responses obtained with these unexpected peaks are generally still significantly lower (general trend pattern lower than 200%) compared with cases where sinusoids are present, as similar to the example 1 in Figure 4.7b.

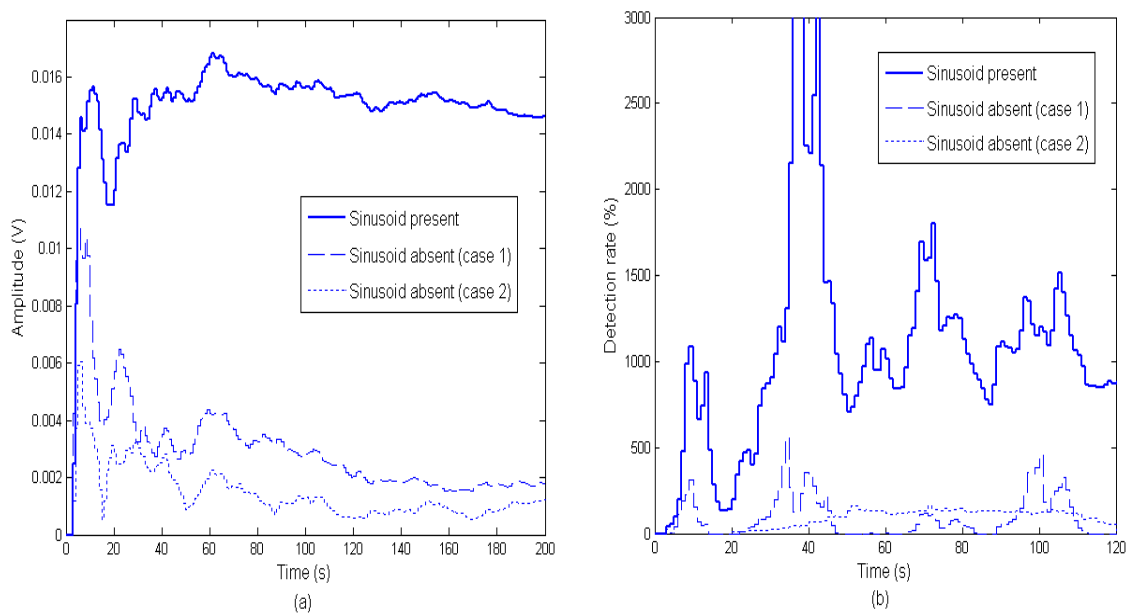


Figure 4.7: Identifying the existence and non-existence of a sinusoid in a low SNR environment ($\text{SNR} \approx -30\text{dB}$).

4.4 Experimental Results

So far the proposed adaptive detection scheme is evaluated using synthetic data, and the results are satisfactory. In order to verify it practically, experimental recorded data using BIOPAC acquisition system were used.

ASSR identification in practice

Figure 4.8a presents the estimated amplitudes of AEP with or without ASSR (oscillated at 90 Hz) at sampling rate of 1 kHz and with parameters settings as in Table 4.2, and a clear distinction between the responses where with existence or non-existence of ASSR.

Typically, the detection rate responses between the case when the ASSR is present and when it is absent are distinctive, as shown in both ‘case 1’ in Figure 4.8b. However, in some cases the ASSR identification may not be straight forward, for instances, the dash-line response of case 2 (ASSR present) displays a similar amplitude response as the case 1 (ASSR present) in Figure 4.8a. However in case 2 the pre-defined 200% threshold is not exceeded, although it is exceeded in case 1 (ASSR present). An explanation could be that the pre-defined threshold of 200% may not be adequate for each and every individual case, though it was determined based upon a series of empirical trials. In addition, case 2 (ASSR absent) in Figure 4.8b that peaked may complicate the empirical process of determining the threshold level. A bias in the process may have been artificially generated. Therefore, there are drawbacks of a thresholding approach that relies on the use of empirical trials. Hence, a more objective approach may be required to quantify the appropriate threshold levels adaptively for each individual case, without relying only on past trials. In general, both AKF-based and observer-based approaches to ASSR detection perform satisfactorily with thresholding, whilst the example in Figure 4.8 displays clearly the drawbacks of thresholding in AKF-based detection.

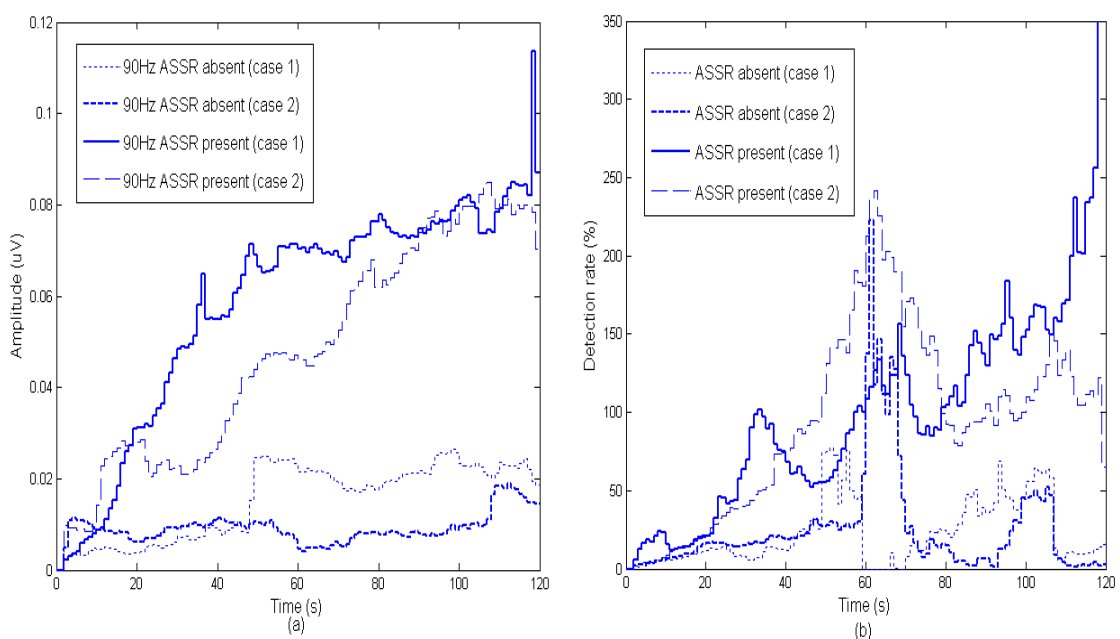


Figure 4.8: Determination of the existence and non-existence of ASSR.

Single vs Multiple Harmonics

To further reduce the detection time, a combination of the fundamental frequency of ASSR and its first harmonic is to be detected. Figure 4.9a illustrates the responses of ASSR detection for both its fundamental frequency at 90Hz and its first harmonic at 180Hz.

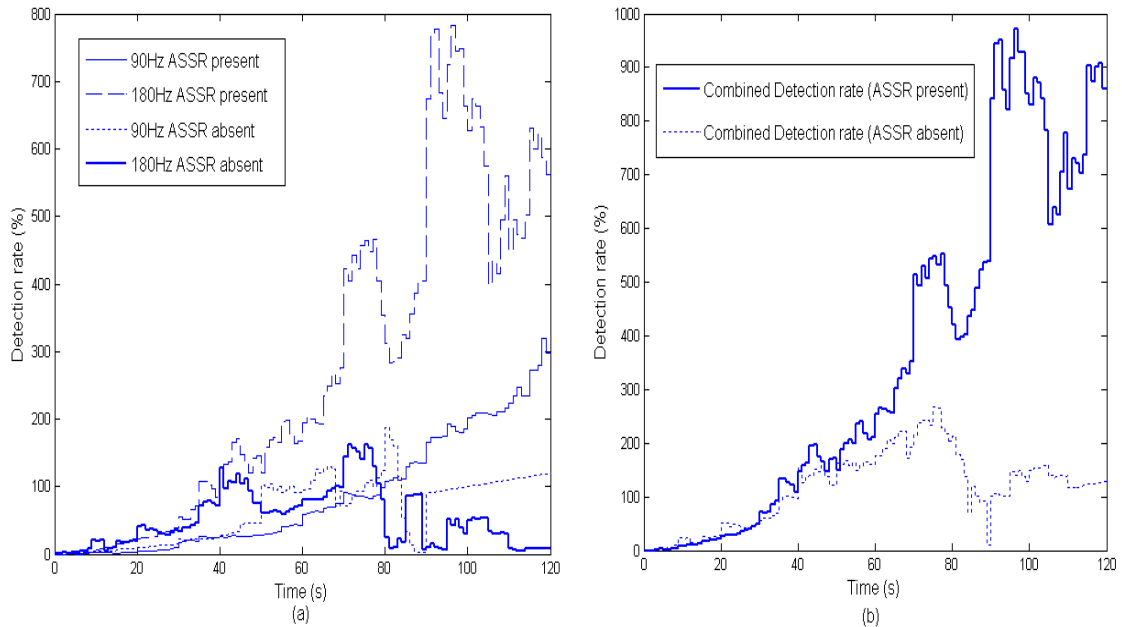


Figure 4.9: Comparison between standard the ASSR (single harmonic) and combined ASSR (multiple harmonics) detection rate responses.

According to Figure 4.9a, the responses to no existence of the ASSR are much smaller than when the ASSR is present. In addition, Figure 4.9b displays the combined responses (fundamental and harmonic frequencies) for both cases where the ASSR are present and vice versa. The original threshold is set to be 200% but with the combined responses, the threshold will now be 400%. Typically (according to the literature), in the standard ASSR detection, only a single harmonic (fundamental frequency) is considered because it is believed that the fundamental frequency response is significantly larger and distinctive to the surrounding background noise, so that neither the sole nor the combined ASSRs detection response will be significantly different (exceeding pre-defined threshold of 200%), as shown in Figure 4.9b. On the other hand, the combined detection approach would still be able to produce reliable and satisfactory results if the fundamental frequency response is poor without the user knowledge. However, this comes at a cost of more intensive computation because an additional ASSR detector is needed for estimating the same frequency. This could be non-practical

if large numbers of these detectors are needed, where issues like computational intensity and signal delay in processing will be involved.

Comparison between AKF-based and observer-based detections

So far, the proposed AKF-based detection scheme performs in a satisfactory manner. A comparison is made between the AKF-based and observer-based detectors, in order to study their relative performances. The parameter settings for these scenarios are give in Table 4.2 corresponding to observer gains of $l_1 = 0.3; l_2 = 0.3; \alpha = 0.05$.

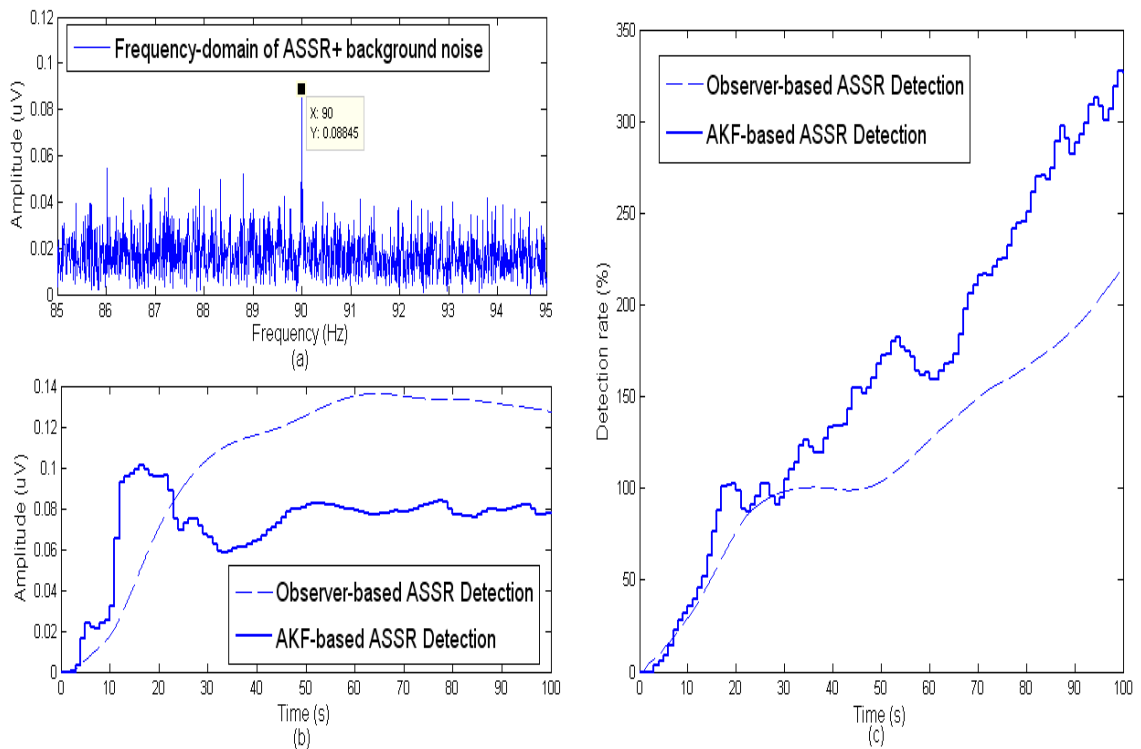


Figure 4.10: Comparison of performances between observer-based and AKF-based ASSR detectors.

The AKF-based detection in Figure 4.10b produced better amplitude estimation (approximately to $0.08\mu\text{V}$) as compared to the observer-based method (approximately to $0.12\mu\text{V}$). The comparison with the FFT response of $0.08845\mu\text{V}$ is shown in Figure 4.10a. The detection rate responses for both detection methods indicates the existence of the ASSR because of the pre-defined thresholds (50% for observer-based and 200% for AKF-based detection) were exceeded, as shown in Figure 4.10c.

4.5 Concluding Remarks

The key difference between this Chapter and Chapter 3 is the introduction of the adaptive ASSR detection scheme via Kalman filtering based approaches. In particular the AKF has been shown to have a near-optimal performance. In general, the Luenberger observer-based detection is structurally similar to KF. However, the former usually operates in the continuous time domain and the latter in the discrete-time. Generally, the KF is often seen as the optimal state estimator based upon the *a priori* information. However, if *a priori* information (e.g. system parameters and noise statistics) is unavailable, thus KF is no longer optimal. On the other hand, an AKF can be used to estimate the unknown parameters followed by the standard filtering process. As a result, the adaptive Kalman filtering is used to detect ASSR where the only information available is that the signal is a sinusoidal wave like with a known frequency. In order to determine the existence or non-existence of the ASSR signal, the detection rate is based on a thresholding where the level of threshold is pre-defined empirically. If the signal's response is higher than the pre-defined threshold, thus ASSR considered existing or otherwise.

Simulation studies were carried out to demonstrate the performances of the proposed on-line adaptive ASSR detectors with synthetic data. The studies are important to clarify the performances (e.g. detection rate, accuracy in signal extraction and detection rate) of the detector, since the 'true' amplitude of ASSR is unknown in practice. In general, the proposed detector performs well with experimental recorded data, thus justifying the assumptions (e.g. system parameters and model) made within the detection scheme. Although the thresholding may in some cases indicated clear ASSR detection rate response, the majority of the tests show that the thresholding is acceptable performance-wise. This drawback is accentuated by the fact that a large number of trials are impossible to make in some cases (e.g. varying level due to subjects and test environments). Hence, an objective way of quantifying the levels of threshold variation for each individual scenario is desired. A statistical-based method for achieving this is proposed in Chapter 6.

5 . Improving the Robustness of ASSR Detection via Multiple Filters Fusion

5.1 Introduction

The adaptive detection scheme based on the adaptive Kalman filter (AKF) presented in Chapter 4 is able to detect the existence or non-existence of auditory steady-state response (ASSR). However, it is assumed that the probability of the noise satisfies the normal distribution, and the measurements are without any artefacts. As mentioned earlier, the auditory evoked potential (AEP) recorded from the human scalp consists of an ASSR signal together with the electroencephalogram (EEG). The EEG is predominately the background noise, and other noise elements exist, for instance, electromyography (EMG), powerline interference and etc. Pre-filtering (i.e. bandpass filtering) is commonly used to filter out the lower frequency components which are considered highly non-Gaussian and to bypass a limited spectrum of the AEP signal where the ASSR's frequency is located, thus to improve the signal-to-noise ratio (SNR). Any unexpected artefacts within the recorded AEP (post-filtering) can be devastating to the ASSR detection and significantly bias the output results. Therefore, incorporating

robust functionality, in this case robustness towards artefacts is particularly crucial for the detection scheme proposed in Chapter 4. Since the reliability of the proposed detector is governed by having reliable estimation of the covariance $R(j)$ ($Q(j)$ assumed to be zero as described in Chapter 4) where it is assumed to represent all background noise, thus the idea is to improve the robustness in estimating the measurement covariance R . A brief description of possible artefacts within AEP and the statistical approaches (e.g. sample median operator) taken to improve the robustness of the noise covariance R are presented in Section 5.2.

In accordance to the estimated covariance $\hat{R}(j)$ of Eqn. (4-30) of the proposed ASSR detection algorithms, the correlation function obtained via Eqn. (4-25) played a key role in determining the sensitivity of the estimation of $\hat{R}(j)$. In general cases, the sample mean operator (similar to Eqn. (4-25)) which is seen as the non-robust method is more efficient in producing outputs with smaller deviations from artefact-free data, whereas the sample median operator that is a known robust method works better when the data are contaminated with artefacts. Due to no prior knowledge of whether or not any artefact exists during the recording, combining both methods could improve the accuracy of the detector in any scenarios. The way to combine both methods can be implemented via multisensor data fusion (MSDF), which is to be discussed in the second half of the chapter. An introductory of its historical background and applications of the approach are to be presented in Section 5.3. In addition, the section will also describe the existing class of techniques used in MSDF and the development of an ASSR detection scheme with enhanced robustness against artefacts using MSDF. To illustrate the advantages of having the newly developed detection scheme compared to the previous version without MSDF, simulation and experimental studies were conducted as described in Section 5.4. The concluding remarks of the Chapter are given in Section 5.5.

5.2 Artefact-Robust Detection

5.2.1 Background

An outlier (i.e. artefact) is generally defined as an observation that “lies outside some overall pattern of distribution” (Moore and McCabe, 1999) or similarly, Johnson (1992) stated that “an outlier as an observation in a dataset which appears to be inconsistent

with the remainder of that set of data". In this study, the occurrences of outliers are to be considered to arise within observation noise from unwanted artefacts or unanticipated disturbances. The artefacts in the AEP measurement are electric activities that are not part of the AEP response and that should not be included in the further processing of the recorded data. These artefacts can be electromagnetic (e.g. powerline interferences, electrode cable movement and etc.) or electrophysiology (muscle activity, eye blinks and etc.) from the subjects (Hall, 1992). The detection and analysis of the ASSR is very vulnerable to these unwanted artefacts, because they can significantly degrade the performance of the detector in terms of detection rate and time duration, especially when the ASSR is to be extracted from a low SNR recorded measurement. Although the AEP measurement is pre-filtered by a narrowband bandpass filter which is a standard practice in avoiding non-Gaussian noise regions especially at the lower frequency spectrum, an artefact-free AEP measurement is not guaranteed. So far, the proposed adaptive ASSR detection scheme operates well under artefact-free measurement, but the detection will be heavily influenced and biased with the artefacts infested data. Therefore, an artefact-robust facility was integrated into the adaptive ASSR detector from Chapter 4.

So far, one of the most effective existing techniques robust against the artefact proposed for ASSR detection is through removing of the recorded data (in batch) infested with artefacts before averaging via artefact rejection method. A set of pre-defined upper and lower bounds (thresholds) to reject any data batch that exceed the boundaries which kept fixed throughout the recording (John and Picton, 2000a). However, this approach has some drawbacks, and the greatest concern is towards the pre-fixed bounds for the artefacts rejection. If the boundaries are generously broad, the detection could be biased with infiltration of unwanted artefacts and thus increase in false alarm of the detection. On the other hand, if the boundaries are set to be too narrow, it could lead to an increase of batches of recorded AEPs to be discarded and thus further pro-long the already lengthy test duration. In addition, having same pre-fixed bound sizes for all subjects may not be appropriate, because the AEPs recorded are different between subjects, thus so should be the gap interval between the boundaries. Moreover, a real-time artefact rejection approach may not be feasible if the boundaries are to be tailored tuned individually to accommodate each subject (John *et al.*, 2001a).

The idea of removing or discounting the artefacts from the AEP data (measurement) is to be integrated into the readily developed AKF-based adaptive ASSR detector with minor modifications. Section 5.2.2 discusses briefly the background behind the statistical operators used to perform on-line outlier-robust detection.

5.2.2 Artefact-Robust Detection of ASSR via Statistical Operators

In the Chapter 4, the proposed adaptive ASSR detection is based on the AKF, but its performance degrades when the measurement (observation data) contains artefacts. This is due to the nature of adaptive filter (in real-time) without storing of past measurement data, hence the quality of the prediction will be less reliable if without the access to all pre-acquired measurements. Since no prior knowledge about noise statistics and AEP model available in ASSR detection, with only ASSR's frequency known, thus a simple and straight forward approach is taken to improve the robustness of the AKF-based ASSR detector via statistical operators. Since all possible artefacts are to occur only in AEP measurements, removing or discarding outliers from the measurement would be the intention of the robust mechanism.

The correlation in Eqn. (4-25) contributed to estimate of covariance R Eqn. (4-30) is based on sample mean operation. With output measurements defined in row vector notation as $[y(k) \ y(k-1) \ \dots \ y(k-N+1)] = Y(j)$, the autocorrelation is simply the summation of all the data points within a sample and divided by the number of data points, yielding:

$$\begin{aligned} \Gamma(i) &= E[Y(j)Y(j-i)^T] \\ &= \frac{1}{N} \sum_{k=1}^N y(k) \end{aligned} \tag{5-1}$$

where $y(k)$ is the representation of data points within a sample of N -dimensional vector (containing N number of data points).

In theory, if the probability density of the distribution is not exactly known, the true mean is impossible to obtain. This is particularly true of real-time applications because infinite long data need to be recorded. Therefore, sample mean is a commonly used statistical operator to produce an average or mean value from a given sequence of

sampled measurements (data population). However, as all the measurement values were treated equally (equal weights) by the sample mean operator, thus it is very sensitive to the existence of extreme values (artefacts) which could eventually distort its output accuracy. In ASSR detection, this would cause sudden rise in covariance R and leading to an unexpected drop in Kalman's gains. As a result, reduction in detection rate and increase of detection time are expected because of the unanticipated drop in convergence rates.

To overcome the problem, an alternate robust approach is to use the sample median operator. The sample median can be defined as the middle number of a sequence of measurements arranged in numerical order within a sample of length N . If the number of data points (measurement points) within the sequence is odd, the sample median can be found by picking the middle values within the sample as

$$\textit{selection of middle term} = \frac{N + 1}{2} \quad (5-2)$$

where N is number of counts of measurement points. If the number of measurement points containing within a sequence is even, then the sample median is the sum of the two middle values i.e. $f\left\{\frac{N}{2}\right\} + f\left\{\frac{N+1}{2}\right\}$ and divided by 2. Hence,

$$\textit{selection of middle term} = \frac{f\left\{\frac{N}{2}\right\} + f\left\{\frac{N + 1}{2}\right\}}{2} \quad (5-3)$$

The sample median operator is only computed from the middle values from the data samples, thus it is less affected by the artefact than sample mean operator which uses all available measurement points within a sampled sequence. Moreover, sample median operator is highly effective and robust against biased or skewed (non-symmetric) distributions within the sampled sequence of measurements than sample mean operator (Huber, 1981). To quantify the fact, the sample median can tolerate up to 50% of artefacts caused errors before it become arbitrarily large. For example, if a sampled sequence measurement with time interval of adaptation rate $T_{ad} = T_s \times N = 1s$ (where $N = 1000$ and each individual measurement points at time interval of sampling rate $T_s = 0.001s$), thus the breakdown point of a sample median operator would required artefacts to occur at least $N = 500$ or longer than the interval $T_{ad} = 0.5s$. On the other hand, the sample mean operator is not robust and a single significantly large outlier is enough to cause inaccuracy towards the computation of covariance $\hat{R}(j)$, because of its low breakdown points of 0%.

Instead of the sample mean operator used in the correlation of Eqn. (4-25) which led to estimate of covariance $\hat{R}(j)$ of Eqn. (4-30) of measurement noise, sample median operator is chosen for its robustness against outliers. The first step to find the median would be to extract the diagonal elements to create a vector, denote

$$YY(j) = \text{diagonal elements of } \{Y(j-i)^T Y(j)\} \quad (5-4)$$

$YY(j)$ is a N -dimensional vector created from extracting the diagonal components from $Y(j-i)^T Y(j)$ and sorting the values of the components in order to ease the middle term selection. Whereas $Y(j)$ is N -dimensional vector consisting batch of data points of $[y(k) \ y(k-1) \dots \ y(k-N+1)]$ with individual measurement point sampled at time-step k .

With $YY(j)$ obtained, the sample median can now be solve by locating the middle data point from vector $YY(j)$ and treat the value as

$$\Gamma(i) = \text{median } \{YY(j)\} \quad (5-5)$$

as mentioned in Chapter 4, the $\Gamma(i)$ is operating at time-step j , with $j \gg k$, hence with only one median is obtained for each time step j .

Under the assumption that the data samples are normal distributed and symmetrical, the samples mean and sample median operations should be equivalent. However, if the assumptions are violated, samples mean operator is no longer optimal and can perform poorly particularly in occurrence of extreme outliers (Hampel, 1971, 1974). With artefacts (outliers) infested data, sample median operator will have smaller deviation error than sample mean but higher error occurrence under normality distributed data (Huber, 1981; Staudte and Sheather, 1990; Wilcox, 2004). By modifying the sample mean operator in Eqn.(4-25) to Eqns. (5-4) and (5-5), this would improve the robustness of the measurement noise estimation as shown in Eqn. (4-30), thus making the proposed ASSR detector less affected by artefacts. As discussed above, both sample mean and median operators has their advantages and disadvantages relating to artefacts. In order to have the best of both operators, MSDF approach is used, which will be discussed in the following section.

5.3 Multisensor Data Fusion Strategy

5.3.1 Overview

MSDF is a process of combining sensory data or signal from multiple sensors (filters) in order to provide an estimation of the environment or process of interest (Llinas and Waltz, 1990; Chong *et al.*, 2000). It is more accurate and robust compared with the estimation using a single sensor. Unlike many subjects (e.g. automatic control, robotics and etc.), MSDF does not form an individual sub-discipline but not until recent years where it has been recognized as a separate branch of research. Historically, data fusion methods were developed primarily for military applications, for examples, automated target recognition, guidance for autonomous vehicles, battlefield surveillance and automated threat recognition systems (Hall and Linn, 1991; Harris *et al.*, 1998). However, in recent years these methods have been applied to civilian applications (e.g. remote sensing, robotics, finance, retail, automated manufacture and etc.), and there has been bidirectional technology transfer (Wright, 1980; Hall and Linn, 1991; Abidi and Gonzalez, 1992). The MSDF is being integrated into the monitoring system and operating together with detection or estimation techniques (e.g. KF and state observer) in order to reduce the effect of the uncertainty and obtain more complete knowledge of the state.

There are several methods that are commonly used to implement the MSDF approach, and they are mainly based on probabilistic methods which are generally referred to Bayes' rule for combining prior and sensory information. Commonly used methods in practice are, for instances KF Extended Kalman filter, sequential Monte Carlo method, Bayesian networks and Dempster-Shafer. Detailed overview of the existing MSDF methods can be found in (Dario, 1988; Goodman *et al.*, 1997; Hall and Llinas, 1997; Smith and Singh, 2006). Both linear and extended Kalman filtering techniques have established themselves well practically over a widespread of sensor fusion applications (Dunn *et al.*, 1976; Willsky *et al.*, 1982; Hashemipour *et al.*, 1988; Rao *et al.*, 1991; Gao and Harris, 2001).

5.3.2 Kalman Filter-based Fusion Method

The KF-based MSDF is among the most significant and the fusion method can be further divided into two sub-methods, they are the state-vector fusion and measurement

fusion (Roeckerand and McGillem 1988; Bar-Shalom and Li, 1995; Saha, 1996; Chang *et al.*, 1997; Saha and Chang, 1998). The state-vector fusion typically uses a bank of multiple KFs as sensor arrays to obtain measurements y_n (n is number of measurements) and produce state estimates \hat{x}_n (n is number of estimates) which are then fused to output a global improved joint state estimate \hat{x}_F , as shown in Figure 5.1. If state-vector fusion approach adopted decentralization architecture, it can be referred as Decentralized Kalman filter fusion.

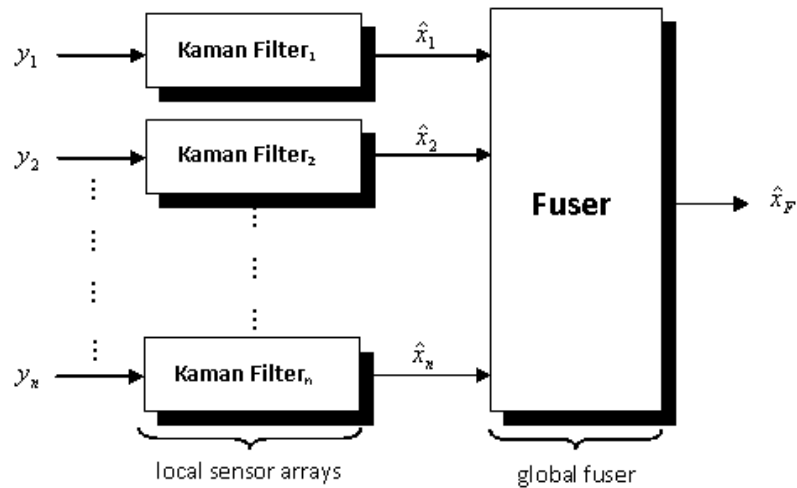


Figure 5.1: Decentralization fusion architecture: State-vector fusion.

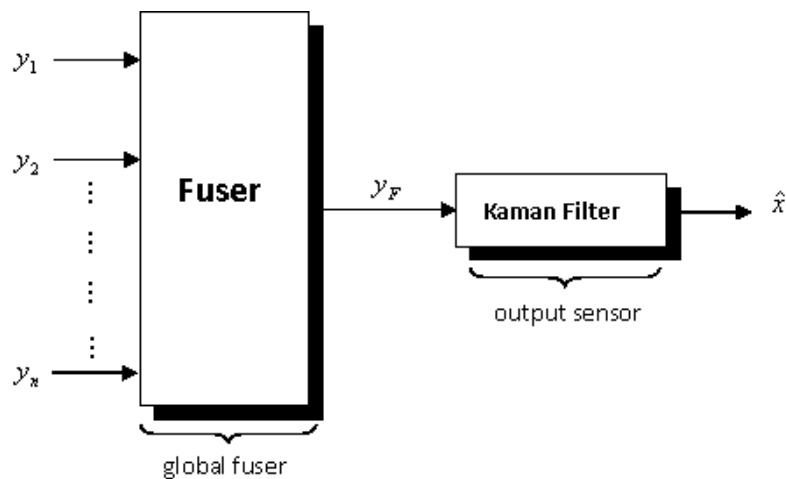


Figure 5.2: Centralization fusion architecture: Measurement fusion.

On the other hand, the measurement fusion method fuse the collected measurements y_n (n is number of measurements) to obtain a combined measurement y_F and the final state estimate \hat{x} is produced based upon the fused measurement via Kalman filtering, as shown in Figure 5.2. If measurements centralization architecture is adopted by the

measurement fusion approach, it can be known as Centralized Kalman filter fusion. In general, the measurement fusion method provides better overall estimation, but not without tradeoff. However, the state-vector fusion method is less computational intense and have the advantage of parallel implementation of local sensors (Qiang and Harris, 2001).

The development of state-vector-based decentralized fuser is the focus of the thesis (to be discussed in next section), because of its suitability to the ASSR problem by accommodating a bank of multiple adaptive Kalman filters (see schematic in Figure 4.4) with different statistical operators (e.g. sample mean and sample median operators) to ensure ‘optimum global estimate’ in either artefact-free or artefact infested AEP.

5.3.3 Development of Fusion-based ASSR Detector

As mentioned earlier, sample mean and sample median operators have their strength and weakness depending on whether the recorded AEP is artefact-free or artefact contaminated, and whether the probability distribution of the data symmetrical or skewed. However, since none of these information are known precisely (e.g. AEP measurement is assumed to be normal distribution and symmetrical), having two operators for estimation seem to be ideal. In order to have best of both worlds, the MSDF approach can be used to combine or fuse these state estimates through an implementation of multiple KFs (local sensor arrays) in order to obtain a refined and improved state estimate than using a single sensor alone. In this way optimum fused estimates that satisfy different scenarios are generated. Figure 5.3 illustrates a schematic diagram of the MSDF-based ASSR detection scheme. Instead of multiple measurements y_n as in Figure 5.1, only single measurement y_1 is used as the recorded AEP. This type of decentralization layout is also referred as *single measurement multiple sensors* (adaptive ASSR detectors in this case) as shown in Figure 5.3, where multiple estimations \hat{x}_A and \hat{x}_B are computed based on a single measurement y before producing a fused-estimate \hat{x}_{A+B} .

This MSDF-based adaptive ASSR detector is in principle operating similarly to the detection scheme proposed in Chapter 4 (see Figure 4.4), but with the replacing of single AKF (see schematic in Figure 4.4) with multiple AKF in arrays (see Figure 5.3). A bank of two local sensors (AKF-based ASSR Detector) with each having their own

estimations (both denoised and residual paths) of \hat{x}_A and \hat{x}_B of \hat{x} , associated respectively with the estimation error covariance P_A and P_B . All these local estimates are then passed to the global fuser. The state-vector fusion method is implemented as the global fuser to combine the local estimates and produce a better estimate (Qiang and Harris, 2001).

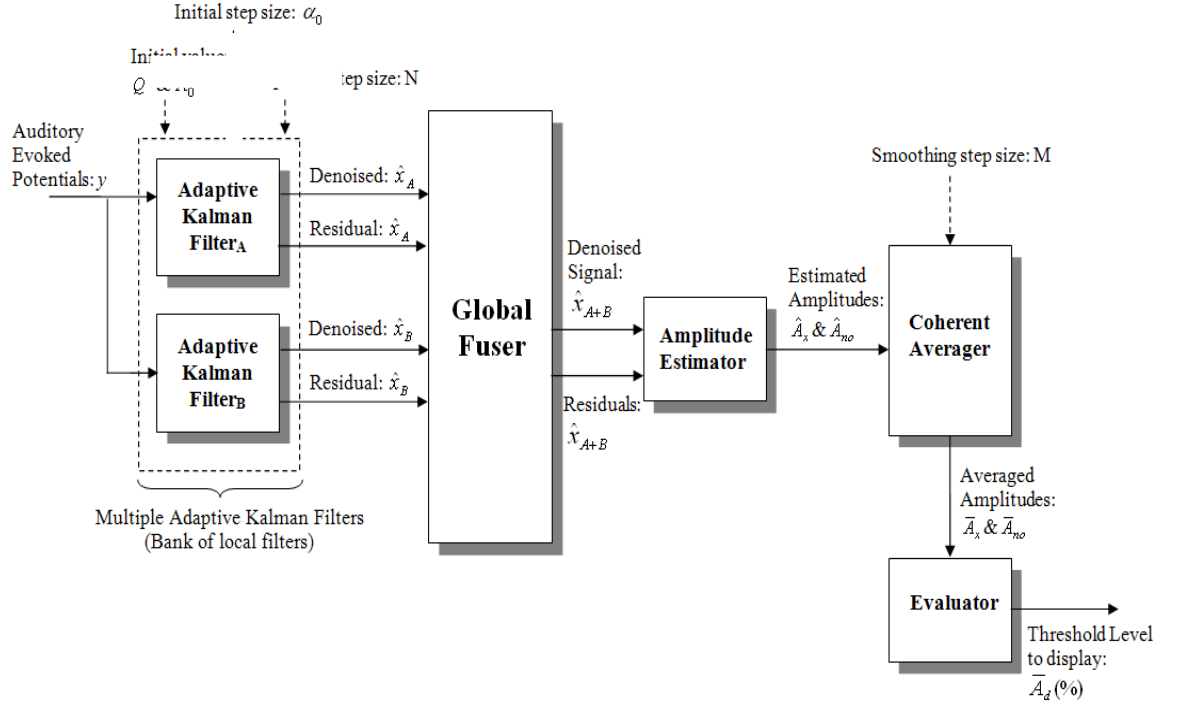


Figure 5.3: Schematic of the adaptive ASSR detection scheme via MSDF.

For simplicity the following expression will only concern about the denoised path, but identical explanations can be applied to the residual path. The fusion-based approach is inspired by Decentralized Kalman filter (Brown and Hwang, 1997; Drolet *et al.*, 2000). By using the weighted least square principle, the fusion of \hat{x}_A and \hat{x}_B is denote as

$$\hat{x}_{A+B} = P_{A+B}(P_A^{-1}\hat{x}_A + P_B^{-1}\hat{x}_B) \quad (5-6)$$

where \hat{x}_A and \hat{x}_B can be either denoised signal or noisy signal, and P_A and P_B are associated respectively with the estimation error covariance. This fused estimation has an error covariance of

$$P_{A+B} = (P_A^{-1} + P_B^{-1})^{-1} \quad (5-7)$$

Since each sensor (AKF-based ASSSR Detector) contributes to the global fuser in a way inversely proportional to its error covariance matrix as in Eqn. (5-6), thus the smaller error covariance of the estimate the larger its contribution to the global estimate. As a result, the fused estimate \hat{x}_{A+B} is expected to have combined characteristic

performances in producing reliable ASSR indication as compared to using single KF. The rest of the detection operate similarly to the proposed detector in Chapter 4, thus details will not be mentioned here (see Section 5.2.3). The purpose of incorporating MSDF approach into the adaptive detection scheme is to further improve the reliability of the detector in both artefact-infested samples and non-artefact infested samples as compared to the implementation of a single ASSR detector alone, since no prior knowledge about the probability of any artefact occurring. The sample mean operator is to provide the ‘expectation value’ from a given data sample, whereas median operator will act against any extreme artefacts that would occur.

5.3.4 Simulation Results

To illustrate the performances of the proposed artefact-robust ASSR detector, synthetic data were initially used for simulation, whereas evaluation based on real experimental recorded data will be presented in the next section. Outliers (mimicking artefacts) contaminated noisy sinusoid signal $y(k) = 0.015 \sin(20\pi k) + v(k)$ (see Figure 4.4), with sampling rate of 1kHz and with the simulation parameters used are the same as in Table 4.2 . Whereas, outliers contaminated noisy sinusoid is illustrated in Figure 5.4, and the parameters used for synthesizing these outliers are given as

Outlier	Occur at time (s)	Duration it occur (s)	Outlier’s variance
1	10	0.1	4
2	20	0.5	7
3	30	0.5	4
4	50	1	4
5	70	3	2

Table 5.1: Parameters setting of the synthesized outliers.

According to Table 5.1, five outliers were added to the noisy sinusoid with SNR approximately -30dB , as shown in Figure 5.4. The second and the third columns of the Table 5.1 indicate when a particular outlier occurred and the duration that specific outlier lasted for each individual outlier specified in the first column. The amplitude responses of these outliers were determined by the last column of the Table 5.1 through synthesizing with different variances.

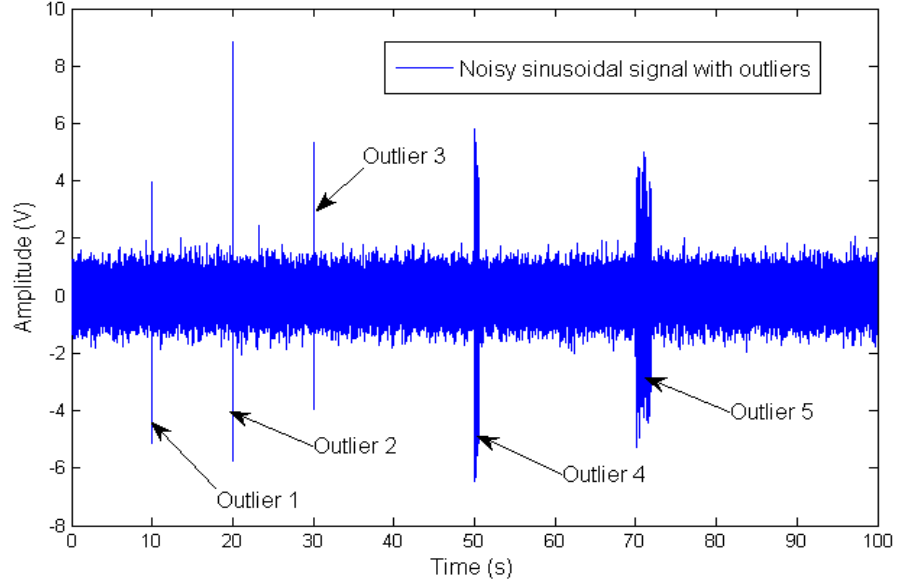


Figure 5.4: Synthesized noisy sinusoidal signal corrupted with outliers.

The noisy sinusoid with outliers (see Figure 5.4) is applied to four adaptive ASSR detectors with schematic illustrated as in Figure 4.4, with two detectors operated with sample mean operators (see Eqn. (4-25)) where one with $N = 1000$ and the other with $N = 4000$. Whereas, the remaining two adaptive ASSR detectors operated with sample median operators (see Eqn. (5-4)) where one with $N = 1000$ and the other with $N = 4000$. Figure 5.5 display the estimated variances of measurement noises obtained via Eqn. (4-30) of all four ASSR detectors between cases when outliers are present and absent, Table 5.2 quantifying the error (in percentage) between different scenarios as

$$e(\%) = \frac{[R(j)_{outlier\ present} - R(j)_{outlier\ absent}]}{R(j)_{outlier\ absent}} \times 100\% \quad (5-8)$$

where $R(j)_{outlier\ present}$ represents the estimated variances when outliers are present, and $R(j)_{outlier\ absent}$ is the estimated variance without outliers.

Adaptive ASSR detectors' operator	Outlier 1	Outlier 2	Outlier 3	Outlier 4	Outlier 5
	$e(\%)$	$e(\%)$	$e(\%)$	$e(\%)$	$e(\%)$
Sample Mean Operator 1 ($N = 1000$)	27	234	195	855	780
Sample Mean Operator 2 ($N = 4000$)	6.4	57	43	210	398
Sample Median Operator 1 ($N = 1000$)	2	13	14	206	773
Sample Median Operator 2 ($N = 4000$)	0.1	3	3.7	29	132

Table 5.2: Error e (%) between outliers present against outliers absent.

By comparing their error $e(\%)$ in Table 5.2 to the $R(j)$ in Figure 5.5, any error percentage that below 100% are visually indistinctive between cases when outliers present and absent. In terms of measurement noise estimation, the adaptive detector used so far is based on sample mean operator (with $N = 1000$) as proposed in Chapter 4. According to Figure 5.5a, this type of operator is highly sensitive to outliers, but performed well against *outlier 1* because of its small interfering duration of just 0.1s. In principle as mentioned earlier, the mean operator is not robust against any outlier since it has breakdown point of 0%. On the other hand, the sample median operator (with $N = 1000$) performed better than the sample mean operator with resistivity against the first three outliers (*outliers 1, 2 and 3*) but unable to deal with *outliers 4 and 5*, as shown in Figure 5.5c. This is because the interfering durations of the last two outliers are far bigger than its breakdown point of 0.5s. In order to compensate the drawback of having short data sample N , longer length of sampled interval is used to improve the resistivity against outliers in the same way improving the estimation of $\hat{R}(j)$. Once again, the result of using sample mean operator with $N = 4000$ show no sign of significant reduction against the outliers (see Figure 5.5b), but with some improvement against lower N (sample mean operator in Figure 5.5a) and comparable to the sample median operator ($N = 1000$) of Figure 5.5c, as shown in Table 5.1. According to Table 5.1, the sample median operator with $N = 4000$ displayed resistance to the highest error reduction and number of outliers except for *outlier 5* (see Figure 5.5d), again because of the interfering duration is larger than its breakdown point of 2s.

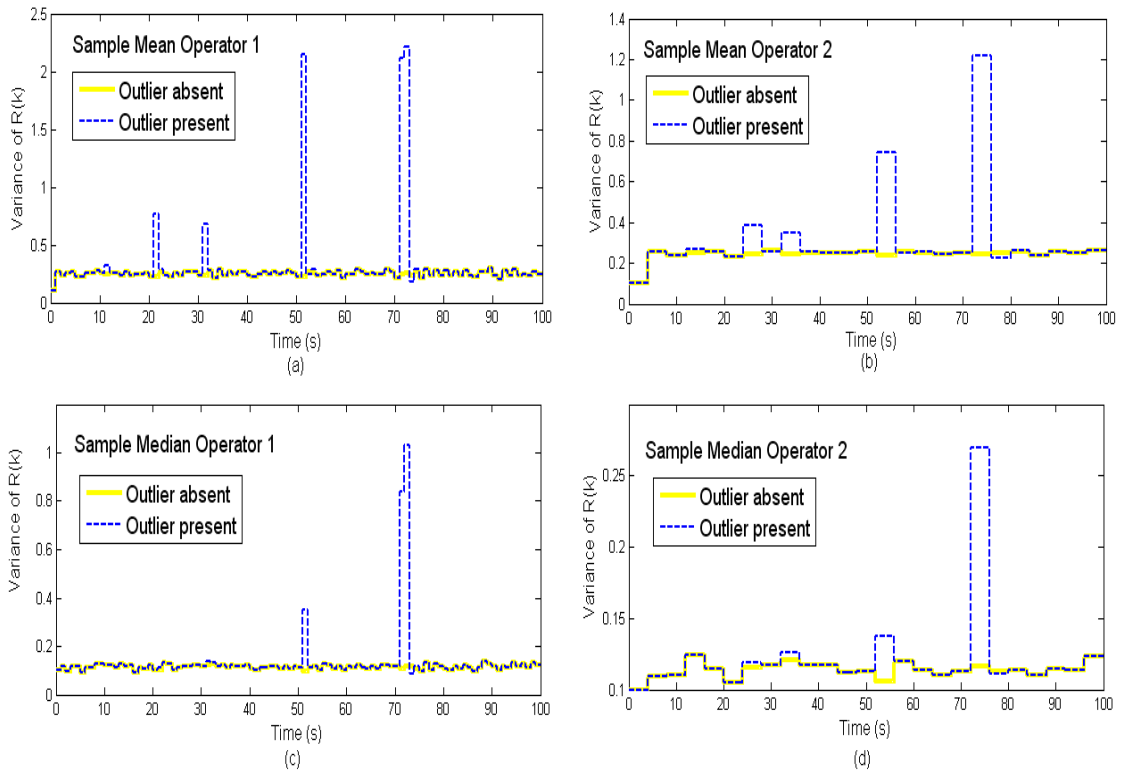


Figure 5.5: Variance of measurement noise of sample mean and sample median operators.

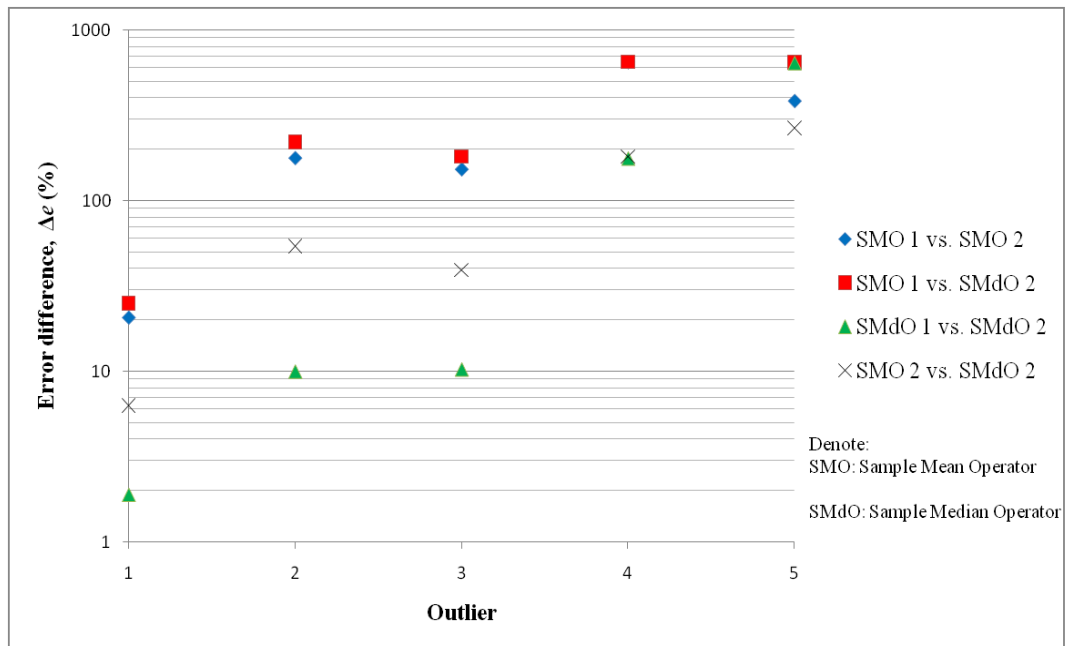


Figure 5.6: Error difference $\Delta e(\%)$ between different statistical operators.

Figure 5.6 illustrates a comparison between the use of different statistical operators in terms of their error rate $\Delta e(\%)$, when one type of operator is preferred over another when dealing with a particular outlier. In addition, the $\Delta e(\%)$ can also be seen as an improvement achieved of one over another choice of operator. And denote as the

absolute different between two operators with $e(\%)$ in Table 5.1. For instance, to compare the *outlier 1*, $\Delta e(\%)$ between sample mean operator 1 (SMO1) and sample mean operator 2 (SMO2) is denote as

$$\Delta e(\%) = |e(\%)_{SMO1} - e(\%)_{SMO2}| \quad (5-9)$$

Where $e(\%)_{SMO1}$ and $e(\%)_{SMO2}$ are the $e(\%)$ of sample mean operator 1 (SMO1) and sample mean operator 2 (SMO2).

According to Figure 5.6, larger N of either sample mean operator or sample median operator in general produced higher $\Delta e(\%)$ which can also be viewed as percentage of improvement achieved. The third and the fourth scenarios in Figure 5.6 illustrate minimal improvement rate, because of the comparison are based between operators with larger N and sample median operator. To summary, sample mean operators show less resistive against outliers than the sample median operators by producing ‘peaks’ in response to the presence of outliers (se Figure 5.5a) even when using longer length of data sample (four times longer) as shown in Figure 5.5b. Whereas the outcomes from the sample median operators are more outliers-resilience (se Figure 5.5c and Figure 5.5d) and with smaller error as compared to when without the present of outliers as presented in Table 5.1, in particular the one with longer length in sample.

Although the sample median operator with $N = 4000$ seems to be the better choice among the four, larger N operators as shown in Figure 5.7a produced slower convergence rate because of the longer data sample (measurements) required for computation, thus the tradeoff of encountering processing delay is inevitable with better outlier-robust performance. Since no *a priori* information is available regarding any possibility of the existence of outliers in practical ASSR detection, in order to have faster convergence rate and yet still be able to have satisfactory outlier-robust performance, MSDF approach is often seen as a method to combine the best of both worlds by fusing the performances of time-efficient sample mean operator ($N = 1000$) and the outlier-resistive sample median operator ($N = 4000$). Its response illustrated in Figure 5.7 indicates a fast convergence that close to those operators with $N = 1000$ and also achieved small mean-square error (MSE) which is less sensitive to outliers compared to other operators, as shown in Figure 5.7b in particular to the first two outliers. The MSE in Figure 5.7b present averaged error square between the estimated amplitudes in Figure 5.7a against its true amplitude of 0.015V over ten trials. In terms

of detection rate response as shown in Figure 5.8, the response by using MSDF showed combine properties between sample mean and median operators.

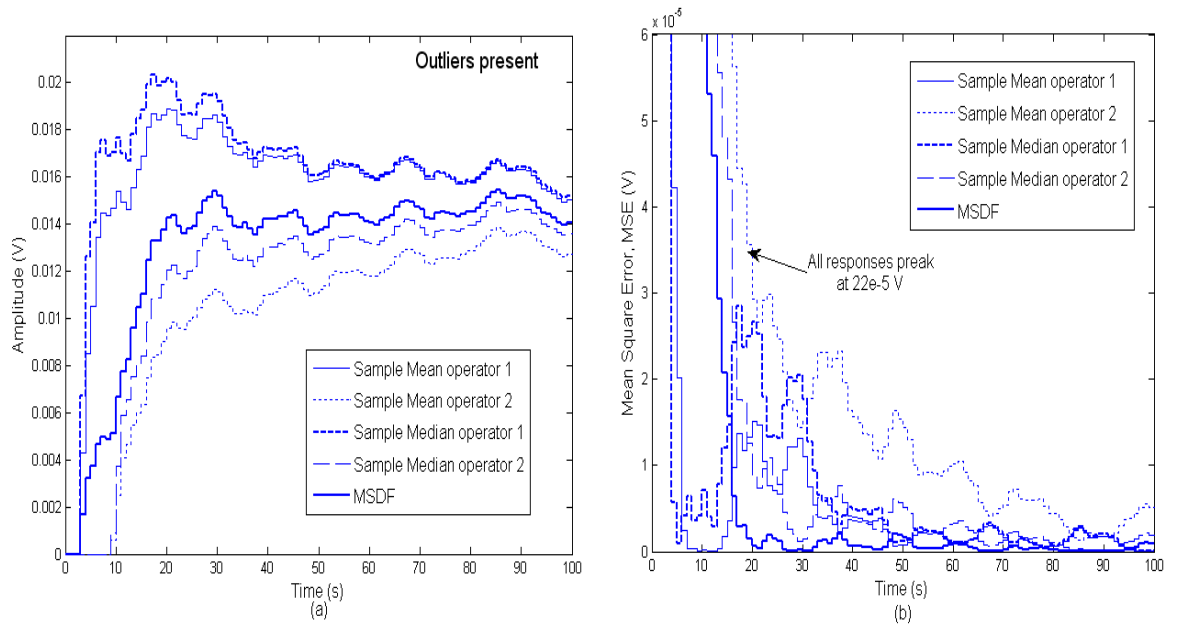


Figure 5.7: Comparative responses between detection using different operators via (a) amplitude response and (b) their mean square error.

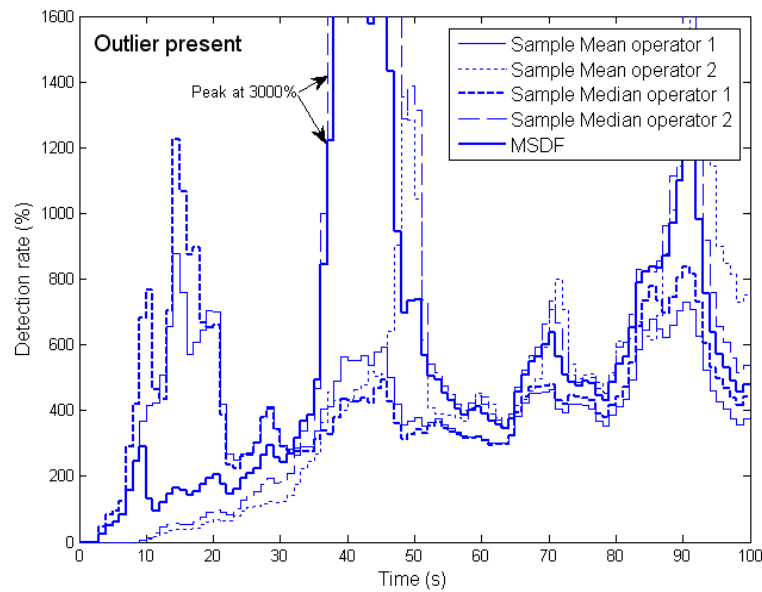


Figure 5.8: Detection rate response between different operators.

5.4 Experimental Results

To demonstrate the practical performances between the MSDF-based ASSR detector and previously proposed ASSR detector in Chapter 4, detection was conducted on the

experimental recorded AEPs. Figure 5.9 illustrates two sets of recorded AEPs, one with artefact contaminated (Figure 5.9a, c and d) and one artefact-free responses (Figure 5.9b, d and f).

The MSDF-based detection indicated minor improvement by having slightly larger amplitude responses against artefacts contaminated AEP as compared to the non-fused detector, as illustrated in Figure 5.9c. In the case where artefacts occurred at the beginning of the recording process, this would slow down the initial detection rate as can be seen in the synthesized scenario in simulation. Therefore, it is essential to have artefact-resistive mechanism to deal with these uncertain extreme outliers. In general, the MSDF-based detection displayed slight improvement in terms of higher response and detection rate. Although the improvement might be minor than expected in these cases (scenarios in Figure 5.9), adopting MSDF method into the detection can only enhance its performance in general than solely rely on non-fused detection.

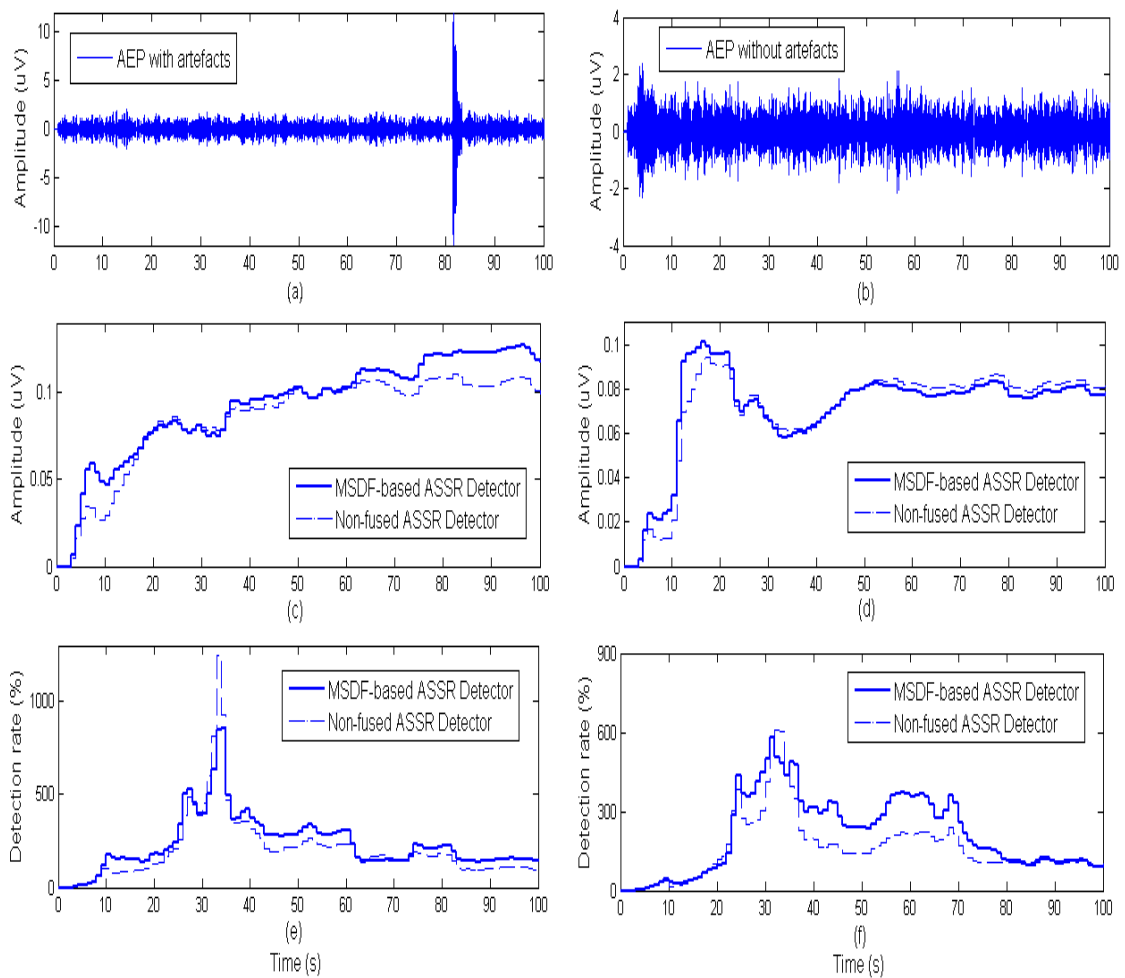


Figure 5.9: Comparative responses between fused and non-fused algorithms in ASSR detection.

5.5 Concluding Remarks

To improve the ASSR detection against possible artefacts in AEP, the real-time adaptive ASSR detector is modified to enhance its artefact-resistive capability. However, as mentioned in Section 5.4, the sample median operator is more robust but less efficient in terms producing outputs with smaller deviation error than the sample mean operator, which was used in the earlier version of the ASSR detector. In order to have the better out of these two operators, MSDF (specifically the state-vector fusion method with decentralization architecture) is used to combine the output responses from both detectors to provide better ASSR estimation. As demonstrated through simulation and experimentation, the MSDF-based approach performs better than the non-fused approach if the AEP is contaminated with artefact. Therefore regardless of the possible existence of artefacts within any recorded AEP, the MSDF-based detector operates in the same way as the proposed detection scheme in Chapter 4, but with the advantages of higher efficiency and more insensitivity to artefacts than the non-fused detector.

6 . Automatic ASSR Detection Scheme via Regression Modelling

6.1 Introduction

As presented in Chapter 4, the auditory steady-state response (ASSR) decision-making of the proposed detection is based on thresholding, where an ASSR threshold level is pre-determined based on empirical studies to indicate the existence or non-existence of ASSR signals. This thresholding is a partially automated approach with dependency of the pre-defined threshold via empirical trials, thus can be seen as a kind of qualitative approach. As shown in Chapter 4, the thresholding is so far effective and reliable in detecting the ASSR signals from the auditory evoked potential (AEP). However, there is one concern regarding the approach. If the signal-to-noise ratio (SNR) of a test is different from its expected value, it is unclear whether or not the pre-defined ASSR threshold would still be applicable. Due to the fact that, the pre-defined ASSR threshold is an expected value from empirical studies and remained constant for all tests. As a result, this could delay the identification of the presence of the ASSR when the actual SNR is higher than the expected threshold or could lead to an increase in false alarm in detection when the actual SNR is lower than expected threshold. Therefore, a statistical based decision-making approach is needed, which would quantify the outcome by

tailored specific to each individual test and be implemented as a fully automatic indicator as part of the ASSR detection scheme. Simple linear regression is used to model the unobserved background noise and to compare with the ASSR estimates in order to determine the existence of the ASSR objectively. Development of an automatic ASSR detection module using simple linear regression is presented in Section 6.2. However, linear regression normally associated with ordinary least-squares (OLS) is highly vulnerable to outliers. Therefore, this would result unreliability in detection rates or pro-long the ASSR detection time. A more advanced method known as robust regression (e.g. Interactive Reweighted Least-Squares (IRLS) with Tukey's Bisquare weight) is used because of its effectiveness against outliers is discussed in Section 6.3. Simulation studies of both methods against the proposed thresholding and their performances on the experimental data are to be shown in Section 6.4. The concluding remarks of this Chapter are presented in Section 6.5.

6.2 Automatic ASSR Detection

6.2.1 Regression Analysis

Before going straight into the discussion on the integration of regression into the proposed ASSR detector, a brief overview on the regression analysis techniques is presented. Regression analysis, or simply known as *regression*, is a statistical technique used to investigate the relationship between variables and to estimate the conditional expectation of the dependent variable, with the given independent variables which usually constant (Hayter, 2002). There are several types of regression analysis models, for instances, Bayesian, robust, nonlinear, multiple linear, simple linear regressions. Selection of the types of regression model will depend and vary on the applications. Typical application ranges from chemical process to biomedicine studies, and also widely used in financial sectors (Draper and Smith, 1981).

Due to the nature of the implementation approach taken, simple linear regression is chosen for its simplicity structurally (since the ASSR detection only involves two sets of variables) and suitability fitted to the idea of predicting the expectation of the background noise (unobservable measurement) at a specify frequency similar to the ASSR signal, where it is unavailable for direct evaluation. As compared to the pre-determined thresholding, the regression-based approach can be viewed to be a self-tune

thresholding module that operates automatically, without the need of subjective ASSR indication (e.g. constant human decision making) and nor the need of any pre-determined thresholds.

Although the simple linear regression operates well generally, with the existence of outliers the regression model may be biased, thus robust regression is preferred for its robustness against outliers. Robust statistics act as the core functionality in robust regression and provide an alternative approach to the classical statistical method. The motivation is to produce estimators that are more resistive to outlying observations from the model assumptions. There are basically three classes of robust estimator methods (i.e. M, L and R type) which commonly used in robust regression analysis (Huber, 1981). As M-type estimator is most widely used, a robust least square approach from the M-type class that known as IRLS with Tukey's Bisquare weight is used in estimating the unobserved background noise. The method is more outlier-resistive than the linear least-squares method and yet still computationally moderate (Fox, 1997).

6.2.2 Simple Regression Linear

A simple linear regression is often viewed as a modelling technique relating two variables with two sets of data, in which the expected value of dependent variable is modelled as a linear combination of a set of explanatory variable (Hayter, 2002). Typically, a data set (or instantaneous sampled population) consisting paired of observations given as

$$(x_1, y_1), (x_2, y_2), \dots, (x_m, y_m) \quad i = 1, 2, \dots, m \quad (6-1)$$

Where the y_i represent the dependent variable and x_i is the explanatory (independent) variable. To consider Eqn. (6-1) in terms of ASSR detection, the (x_i, y_i) pair of Eqn. (6-1) can be re-written as

$$(f_1, \bar{A}_{no,1}), (f_2, \bar{A}_{no,2}), \dots, (f_m, \bar{A}_{no,m}) \quad i = 1, 2, \dots, m \quad (6-2)$$

where f_i is represents a particular frequency of an estimated noise, and $\bar{A}_{no,i}$ would represent the noise amplitude estimated via an ASSR detector with the specific frequency f_i .

A general simple linear regression model is:

$$\bar{A}_{no,i} = \beta_0 + \beta_1 f_i + \varepsilon_i \quad (6-3)$$

where the dependent variable $\bar{A}_{no,i}$ is composed of a linear function $\beta_0 + \beta_1 f_i$ of the independent variable f_i , and the error term ε_i is generally taken to be an independent observation from a normal distribution $N(0, \sigma^2)$. Thus, this implies that vector of $\overline{AA}_{no,i} = [\bar{A}_{no,1}, \bar{A}_{no,2}, \dots, \bar{A}_{no,m}]$ are the observations from the independent random variables of:

$$\overline{AA}_{no,i} \sim N(\beta_0 + \beta_1 f_i, \sigma^2) \quad (6-4)$$

with

$$E(\overline{AA}_{no,i}) = \beta_0 + \beta_1 f_i \quad (6-5)$$

The unknown parameters of σ^2 (error variance), β_0 (intercept parameter) and β_1 (slope parameter), which determine the relationship between the dependent variable and the independent variable can be estimated via fitting the data set with a ‘best fit line’ that best describes the model. Thus, the regression line is given by the equation:

$$\bar{A}_{no} = \beta_0 + \beta_1 f \quad (6-6)$$

The fundamental technique used for determining these unknown parameters is the OLS. These parameters are determined as to minimise the sum of squared residuals (SSR) and given as

$$\begin{aligned} \hat{\beta}_1 &= \frac{\sum_{i=1}^n (f_i - \bar{f})(\bar{A}_{no,i} - \bar{\bar{A}}_{no})}{\sum_{i=1}^n (f_i - \bar{f})^2} \\ &= \frac{S_{XY}}{S_{XX}} \end{aligned} \quad (6-7)$$

where \bar{f} and $\bar{\bar{A}}_{no}$ are the mean of their set variables. While:

$$\beta_0 = \bar{\bar{A}}_{no} - \hat{\beta}_1 \bar{f} \quad (6-8)$$

and

$$\begin{aligned} \hat{\sigma}^2 &= \frac{\sum_{i=1}^m [\bar{A}_{no,i} - (\hat{\beta}_0 + \hat{\beta}_1 f_i)]^2}{m - 2} \\ &= \frac{SSE}{m - 2} \end{aligned} \quad (6-9)$$

As a result, with all the unknown parameters found for the ‘bet fit’ line of Eqn. (6-6), thus any of the expected value, $\bar{A}_{no,i}$ (estimated variables) data set can now be estimated by identifying a specific value of f_i (user defined variables).

Even if the OLS method is performed correctly, there is no guarantee that the estimated parameters are error-free in estimating the best-fitted straight line. In fact, such correspondence is highly unlikely, with the possibility of affected by inevitably sampling error. As a result, a pair of confidence intervals (CI) are constructed around the regression line by taking account of the possible errors.

Denoting a particular of f_i^* of the independent variable, the regression line is:

$$\bar{A}_{no,i}^* = \beta_0 + \beta_1 x f_i^* \quad (6-10)$$

and for considering the interferences of the regression line, the $1 - \alpha$ is the confidence level of the pair of confidence intervals for $\beta_0 + \beta_1 f_i^*$ with α as the error rate, which is the expected value for dependent variable for a particular f_i^* of the independent variable is:

$$\bar{A}_{no,i}^* = (\hat{\beta}_0 + \hat{\beta}_1 f_i^*) \pm t_{1-\alpha, m-2} \hat{\sigma} \sqrt{\frac{1}{m} + \frac{(f_i^* - \bar{f})^2}{\sum_{i=1}^m (f_i - \bar{f})^2}} \quad (6-11)$$

where the standard error is:

$$se(\hat{\beta}_0 + \hat{\beta}_1 f_i^*) = \hat{\sigma} \sqrt{\frac{1}{m} + \frac{(f_i^* - \bar{f})^2}{\sum_{i=1}^m (f_i - \bar{f})^2}} \quad (6-12)$$

and the $t_{1-\alpha, m-2}$ is taken from t -distribution table which can either be single or double sided index with $m - 2$ degree of freedom, m is the sample size. The simple linear regression model is based on the assumption that the distribution is normal but only if the sample size is large ($m \geq 30$). Otherwise, the student's t -distribution should be assumed (based upon the *Sampling Theory*) (Hayter, 2002), which is quite similar to the normal distribution but with heavy tails and if the sample size is infinity it will eventually equal to normal distribution.

On the other hand, if the concern is not about the error or interferences of the regression line but the interferences of the instantaneous sampled population, constructing a set of maximum and minimum boundary is needed for any of the expected value of $\bar{A}_{no,i}$ with value of f_i . In other words, the pair of boundary can be seen as a confident interval (CI) that represents certain percentages of the sampled population, for example, 95% confident that all possible data fall within it. The boundaries can be obtained as:

$$\bar{A}_{no,i}^* = (\hat{\beta}_0 + \hat{\beta}_1 f_i^*) \pm t_{1-\alpha, n-2} \hat{\sigma} \quad (6-13)$$

and again, the $t_{1-\alpha, n-2}$ is taken from t-distribution table to determine the confident of percentages (e.g. $2.024\sigma = 95\%$ with single-sided index used for m equal to 30) in representation of the data set and with $m - 2$ degree of freedom.

6.2.3 Development of Automatic ASSR Detector via Linear Regression

As mentioned in 6.2.2, the unobserved background noise is to be estimated via using linear regression instead of relying on thresholding approach. The main advantage of the regression approach is that of its automatic decision making in terms of ASSR detection. Moreover, it is easily expandable to detect multiple ASSRs with minimum increase in the data samples used for background noise estimation. The proposed ASSR detection so far in the thesis is based on time domain, whereas the linear regression approach is based on frequency domain but can be displayed in time domain via Eqn. (6-14).

The idea of the method is to use the amplitude estimates (signal-channel only) from multiple AKFs at a range of frequencies surrounding the ASSR frequency, to obtain an expected background noise estimate at the same frequency as the ASSR. The operation of the proposed automatic ASSR detection scheme is to be discussed as follows and its schematic diagram of the detection scheme is illustrated in Figure 6.1. The detection scheme is divided into three main parts, and they are signal estimator, background noise estimator and the evaluator. The signal estimator mainly consists of adaptive ASSR filter which is represented by the ASSR detector proposed in Chapter 5 and its schematic of the filter design is illustrated in Figure 5.3 with the evaluation module assumed omitted. As discussed in Chapter 5, the filters-fused AKF has the advantages of having combined elements of artefact-robustness and output efficiency (smaller deviation error). The core part of the objective ASSR detection is about estimating the background noise component of the same frequency as the estimated ASSR, in order to make a direct comparison at the evaluator.

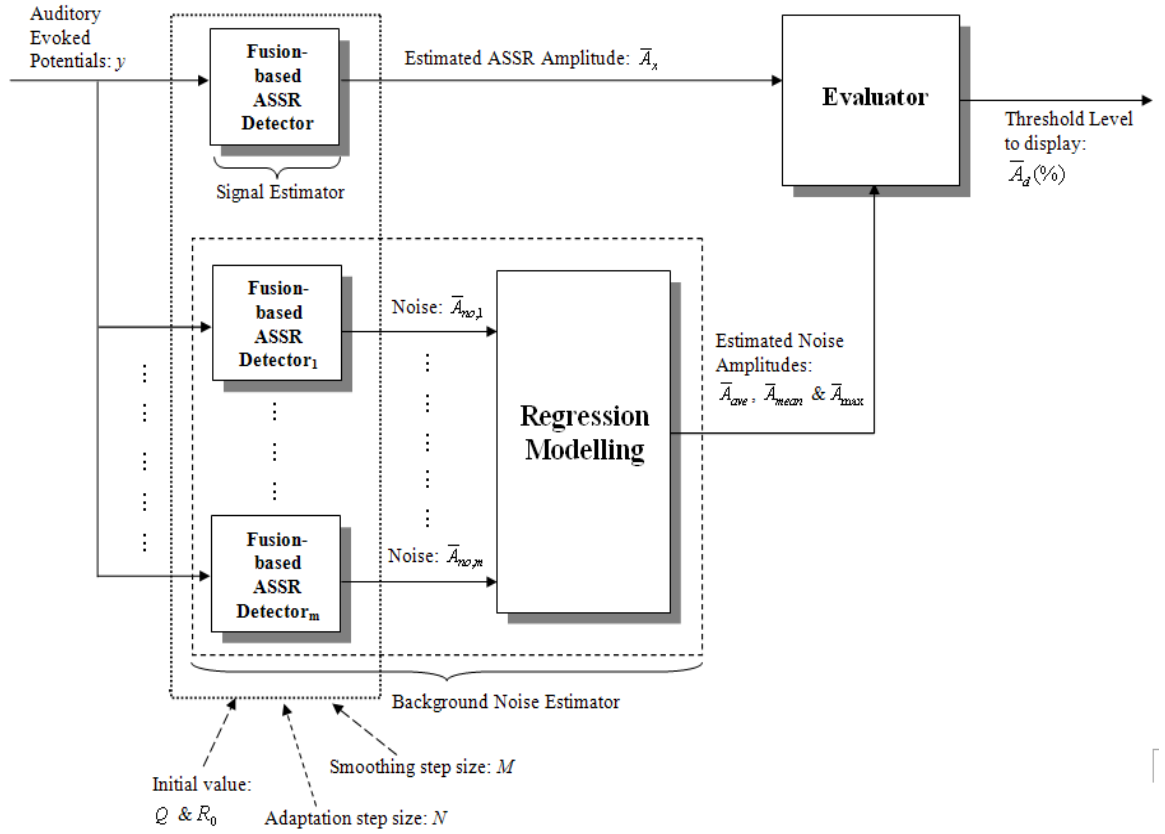


Figure 6.1: Schematic of the automatic ASSR detection scheme.

Several individual fusion-based ASSR detectors (see schematic in Figure 5.3) are used to estimate the surrounding noise amplitudes of the ASSR signal, in order to provide the expected noise amplitude via the regression modelling. The regression used here is based on linear regression approach. With the noise amplitudes provided by a bank of multiple fusion-based ASSR detectors, an estimate of the noise amplitude at the targeted frequency can now be obtained through the regression model calculated via the ordinary least square. The estimated surrounding noise amplitudes is treated as $\hat{A}_{no,i}$ and the frequency band treated as f_i , are the two sets of variables are in Eqn. (6-2). These values are then substituted into the linear regression model (see Eqn. (6-3)) to estimate the expected value of the background noise (same frequency as the ASSR) through fitting of best regression line (see Eqn. (6-6)).

Since the regression modelling is in the frequency domain and for easily comparison to the estimated ASSR, an evaluator is used to display the results from the regression module into the time domain that defined its detection rate via:

$$detection\ rate\ (\%) = \left[\left(\frac{\bar{A}_{x,i}^* - \hat{A}_{ave}}{\hat{A}_{max} - \hat{A}_{ave}} \right) \times \frac{(1 - \alpha)}{2} \right] + Re \quad (6-14)$$

where $1 - \alpha$ is the confidence level of a pair of confidence intervals (single-sided index used) with α as the error rate, $\hat{A}_{x,i}^*$ is the estimated amplitude of ASSR, \hat{A}_{ave} is the estimated noise amplitude at the desired ASSR frequency of regression line and \hat{A}_{max} is the estimated noise amplitude at the upper-bound of the 95% CI of the sampled population at same frequency as the desired ASSR. Re is set to be 50 which represents the location of the regression line, where almost at the middle within the 95% CI of the sampled population (counting from the lower-bound of 95% CI of sampled population).

For demonstration of the purpose Eqn. (6-14), Figure 6.2 illustrates examples on how the regression plot usually in frequency domain can be displayed into the time domain to ease the integration and implementation into the readily real-time ASSR detector proposed, through providing on-line display and decision making to determine the existence or non-existence of ASSR. Denote the generic parameters as:

Variable	\hat{A}_{max}	\hat{A}_{mean}	\hat{A}_{ave}	α	$\hat{A}_{x,1}$ (blue)	$\hat{A}_{x,1}$ (green)	$\hat{A}_{x,1}$ (black)
Index	0.1	0.07	0.06	0.05	0.12	0.07	0.05

Table 6.1: Generic values used for demonstration of the example in Figure 6.2.

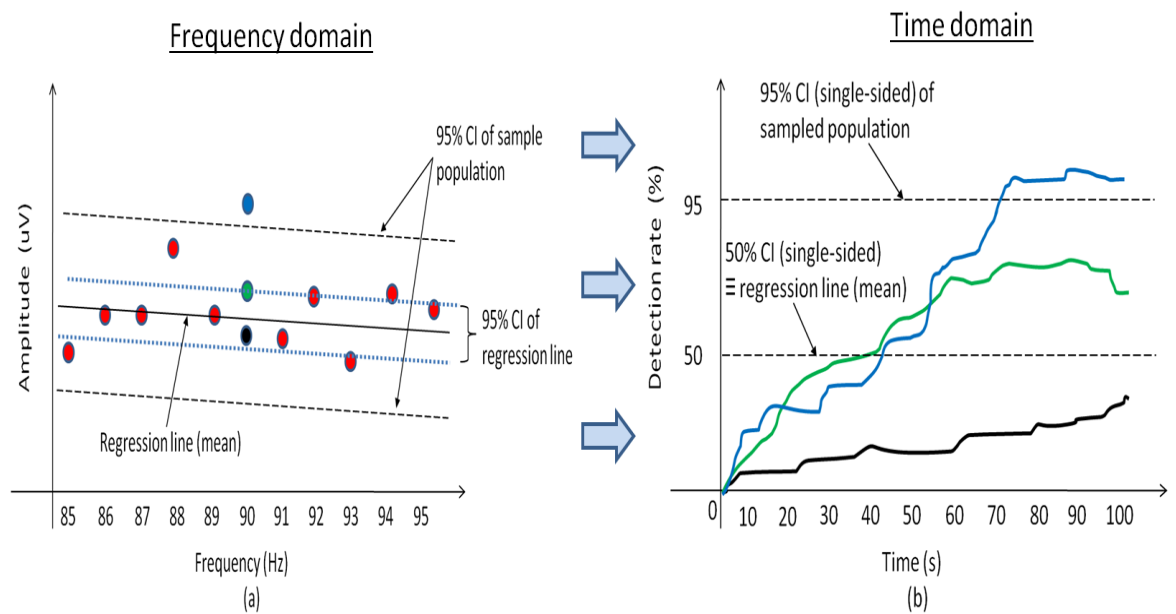


Figure 6.2: Generic example of displaying regression frequency domain plot into time domain response.

According to Eqn. (6-14), the ‘blue estimate’ that exceeded the 95% CI of the sampled population as shown in Figure 6.2a displayed its detection rate as 121.25% at 100s. For the purpose of identifying the existence or non-existence, once the detection rate exceeds 95%, thus ASSR is considered detected (existed). As for the ‘black estimate’, where it is located below the regression line which is at the middle of boundaries of the 95% CI sampled population in Figure 6.2a is display to be at the detection rate of 38.125% in Figure 6.2b via Eqn. (6-14), in which correctly displaying the detection rate from initial frequency domain to the time domain and to be identify to be non-ASSR because it is lower than the 95% CI mark. In addition, the ‘green estimate’ is also at a detection rate of 61.857% that identify as background noise. So far, the detection rate concern in Figure 6.2b is on the boundaries of the sampled population instead if the regression line. If the focus in onto the regression line, similar in steps to the 95% CI boundary are taken except the \hat{A}_{max} in Eqn. (6-14) is now to replace by the \hat{A}_{mean} of the 95% CI of regression line. The ‘blue estimate’ is 335% above the 95% CI of its mean on the regression line, other word meaning expected value of background noise, Hence, the ‘blue estimate’ is not likely to be considered as a background noise based on the mean calculation. In addition, the ‘green estimate’ is also not considered as the background noise because of its detection rate of 97.5% which is higher than the required 95% threshold (probability of being considered as background noise). On the other hand, the likelihood of the ‘black estimate’ with detection rate of only 2.5% is lower than the expected value of background noise, thus the likelihood of the estimate to be considered as ASSR is very low.

With this transformation facility in place, the regression approach can now be analysed in the time domain. As mentioned earlier, single ASSR detection module shown in Figure 6.1 is readily expandable for multiple ASSRs detection. This can be easily done by using m multiple ($m = 10$ in the study) ASSR detection modules of Figure 6.1 for each desired ASSR’s frequency, as shown in Figure 6.3.

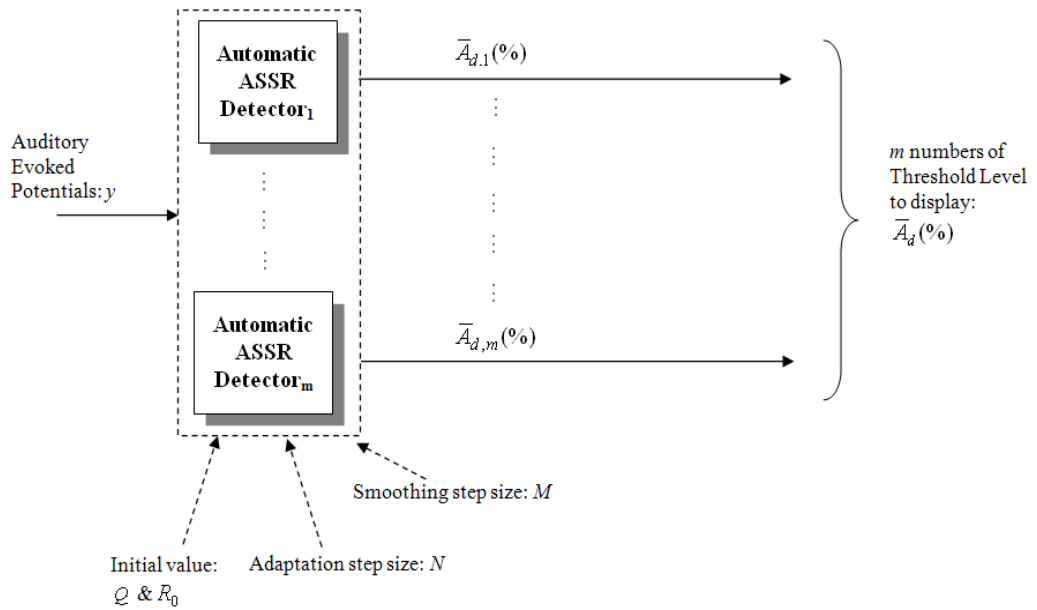


Figure 6.3: Schematic of objective of multiple ASSRs detection scheme.

Although the multiple ASSR detection can be applied based on the schematic structure in Figure 6.3, an alternate way of structuring can further reduce number of automatic ASSR detector in noise estimation. Thus, it reduces design complexity and computation is less intense, but may suffer from a slight drop in terms of output performance. In general, both paths of structuring the multiple ASSRs detection are expected to perform similarly. For example, if eight ASSR signals are to be estimated, the number of AKF module for noise estimation should be $m = 80$ with $m = 10$ associated to each ASSR if according to approach presented in Figure 6.3. However, large numbers of AKF modules could potentially cause delay in processing and intense computational load. As mentioned, a scaled version would be the deployment lower number of AKF ($m = 20$) with carefully placing the noise estimates' frequencies around the desired ASSR signals' frequencies. The schematic layout of the scaled version of the automatic ASSR detection scheme is shown in Figure 6.4. Hence, this would significantly reduce the computation power and processing time, making this approach more appealing in terms of practical implementation.

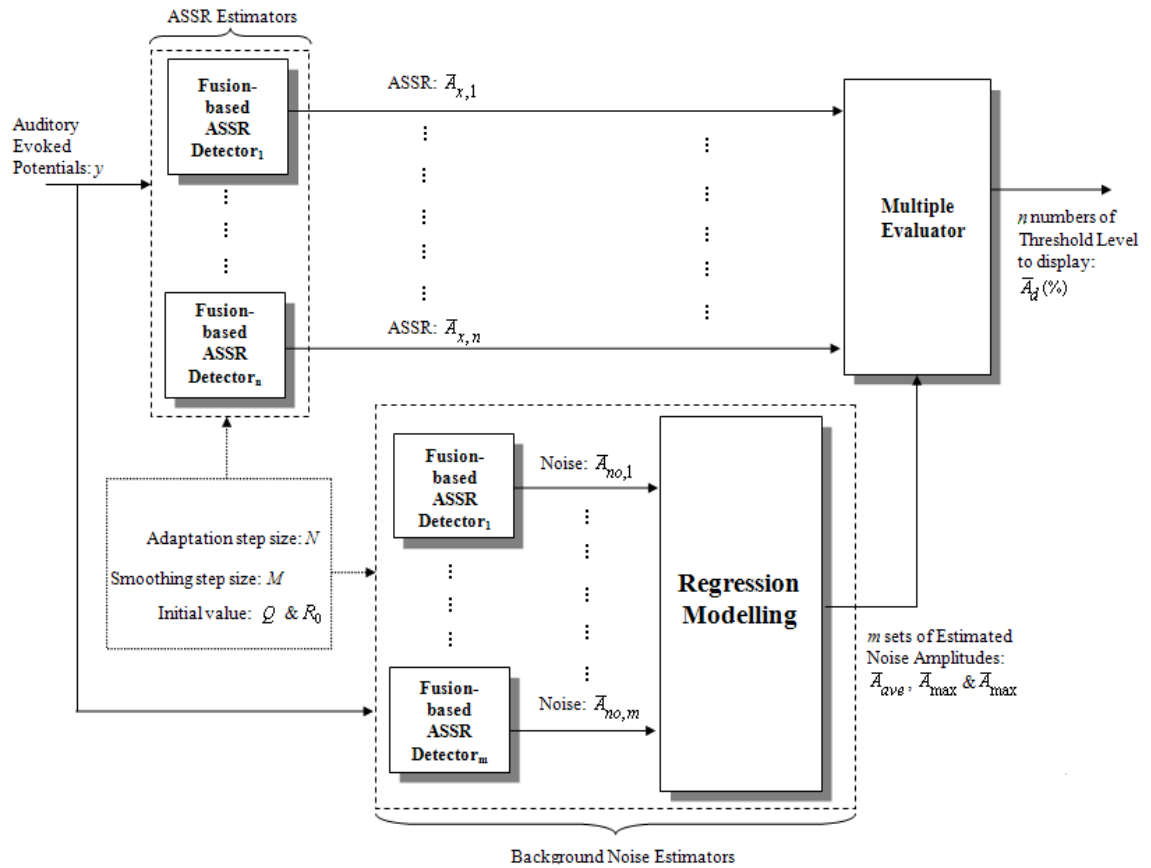


Figure 6.4: Schematic of objective of multiple ASSRs detection scheme (scaled version).

6.3 Outlier-Robust Automatic ASSR Detection

6.3.1 Background

Robust regression is a form of regression analysis designed to circumvent some of the limitation of conventional parametric and non-parametric methods. Unfortunately, the classical least-squares method used in the linear regression model is quite sensitive to outliers which may occasionally occur in real data (Huber, 1981). Therefore, statistical techniques that able to cope with or to detect outlying observations in order to produce better detection rate are to be discussed. This section is mainly concerned with the robust least-squares method in dealing with possible outlier infested data.

The robust issue to be discussed in this section is different from the robust issue discussed earlier. In Chapter 5, the concern is about extracting the ASSR from AEP measurement that potentially contaminated with artefacts (outliers) and the robust method approach used can be seen as univariate robust method with the involvement single variable (covariance $R(j)$ of measurement noise). On the other hand, the

emphasis of the robust approach here is about robustly identifying the existence or non-existence of ASSR via modelling its noise from an estimated set of neighbouring background noise. In order to ensure the accuracy and outlier resilience noise estimation, the linear regression approach is now replaced by a robust regression. This type of robust method is also known as multivariate robust approach because more than one variable (with the involvement of f_i and $\bar{A}_{no,i}$ variables) are taken into account.

There are three basic classes of estimators which commonly used in robust regression, and they are M, L and S estimators. Among these classes, Least Median Square (LMS), Least Trimmed Squares (LTS) and IRLS are the commonly used estimation method in robust regression (Huber, 1981; Rousseeuw and Leroy, 1986). Although they are all outlier-robust, they operate under different principles. The LMS is about minimizing the median of ordered squares of residuals to obtain the regression coefficient, thus more resistive against possible outlier since median is the core of the calculation. On the other hand, the LTS eliminates potential outliers using the winsorized distribution or trimmed principle, thus the approach is robust with possible outliers discard prior to the calculation. The method to be implemented in the robust regression belongs to the widely used M-estimator, known as IRLS with Tukey's Bisquare weight. The IRLS does not operate in the same way as the former two approaches since the calculation takes into account all data samples but allocates weights to them, with heavier weighting on the values with smaller residual while smaller weight on values having larger residual in order to reduce their influences (Huber, 1981). The method is more robust against outlier than the classical least-squares algorithm and is computationally moderate compared to other robust methods.

Despite their superior performance over least-squares estimation in many situations, robust methods for regression are still not widely used. Several reasons may explain their unpopularity (Hampel *et al.*, 1986). For instance, there are several competing robust methods (without unification) and computation of robust estimates is much more computationally intensive than the least-squares estimation (less relevant nowadays as computing power has increased greatly). Moreover, some statisticians believed that the classical method is as sufficiently robust as the robust approaches may be as another vital reason. But having said that, the robust regression approaches does perform better if the recorder data sample is contaminated with outliers especially those with extreme values

6.3.2 Robust Regression

In robust regression, the M-estimators operate under the principle of maximum likelihood, and are widely used because of their high breakdown point and output efficiency (smaller deviation). A robust least-squares method known as IRLS with Tukey's Bisquare weight function is used to perform in the robust regression modelling (Huber, 1981). The Bisquare weight function we_i is as below:

$$we_i = \begin{cases} (1 - u_i^2)^2 & |e| < 1 \\ 0 & |e| \geq 1 \end{cases} \quad (6-15)$$

where u is the standardized adjusted residual and e is standard deviation of u_i .

$$u_i = \frac{r^\#}{K_r s} \quad (6-16)$$

with $r^\#$ being as adjusted residual, K_r is a tuning constant equal to 4.685, s the robust variance. The adjusted residual is initially computed using weighted least-squares and given as:

$$r^\# = \frac{r_i}{\sqrt{1 - he_i}} \quad (6-17)$$

where r_i is the residual from the least-squares calculation and he_i is the leverage that adjusts by down-weighting high-leverage data points, which could have a devastating effect on the non-robust resistive least-squares. Denote the robust variance, s as

$$s = \frac{MAD}{0.6745} \quad (6-18)$$

where MAD is the median absolute deviation of the residual of their median and the constant 0.6745 makes the estimate unbiased for the normal distribution (Huber, 1981).

The process of the robust regression using built-in IRLS in MATLAB's Statistical Toolbox is to fit the regression model via the weighted least-squares method. With the residual obtained, the adjusted residual is then computed (see Eqn. (6-17)). The standardized adjusted residual then is obtained via Eqn. (6-16) with adjusted residual computed. Finally, the Bisquare weight is computed using Eqn. (6-15). The iterative cycle then restarts until the fit convergence is complete. In general, this iterative process is known as IRLS.

With the robust regression line obtained via the IRLS, its confident intervals for the regression line is:

$$\bar{A}_{no,i}^* = (\hat{\beta}_0 + \hat{\beta}_1 f_i^*) \pm t_{1-\alpha, m-2} \hat{\sigma} \sqrt{\frac{1}{m} + \frac{(f_i^* - \bar{f})^2}{\sum_{i=1}^m (f_i - \bar{f})^2}} \quad (6-19)$$

and the boundaries to represent the specific percentages of the sampled data are:

$$\bar{A}_{no,i}^* = (\hat{\beta}_0 + \hat{\beta}_1 f_i^*) \pm t_{1-\alpha, n-2} \hat{\sigma} \quad (6-20)$$

where the $t_{1-\alpha, n-2}$ is taken from t-distribution index with $n - 2$ degree of freedom, n is the sample population size. As mentioned earlier, the t-distribution index is used rather than the normal distribution for any sample size (normally distributed like) smaller than 30 samples. The way of implementing the robust regression in modelling the unobserved noise is similar to the linear regression, as shown in Figure 6.3 and Figure 6.4.

6.4 Evaluation

To demonstrate the performance of the automatic ASSR detection (via regression) and thresholding based ASSR detection, simulations and experimental work were carried out, and their results are illustrated in the following sections.

6.4.1 Simulation Results

To compare the detection rate between the thresholding and the regression approaches in term of ASSR detection. A noisy sinusoidal signal $y(k) = 0.015 \sin(180\pi k) + v(k)$ at sampling rate of 1kHz with initialisation parameters given in Table 4.2, and is corrupted with noise (SNR ≈ -30 dB) is applied to the ASSR detectors.

Figure 6.5a illustrates the amplitude responses of the sinusoid and the noise estimates obtained via thresholding and by regression methods. Both noise estimation methods produced satisfactory results with clear distinctive separation between the sinusoid and the noise estimates. In terms of detection rate response, the thresholding method indicates detection of sinusoid (identified the present of sinusoid) at 20s at pre-defined threshold of 200% (as shown in Figure 6.5d). Whereas the regression method confirmed the detection based upon two different yet interrelated concepts, that is one by comparing the ASSR to the expected (mean) noise value based on the surrounding background noise via Eqn. (6-11), and the other approach considering whether the estimated ASSR is legitimately belong to the sampled population of the background

noise via Eqn. (6-13). Single-sided index is taken from t-distribution table in this case with the assumption that the desired sinusoid or ASSR in particular can only occurred on the positive side of the regression line, where the regression line computed from Eqn. (6-6), and both Eqns. (6-11) and (6-13) are used to compute the error intervals (95% CI) surrounded the regression line.

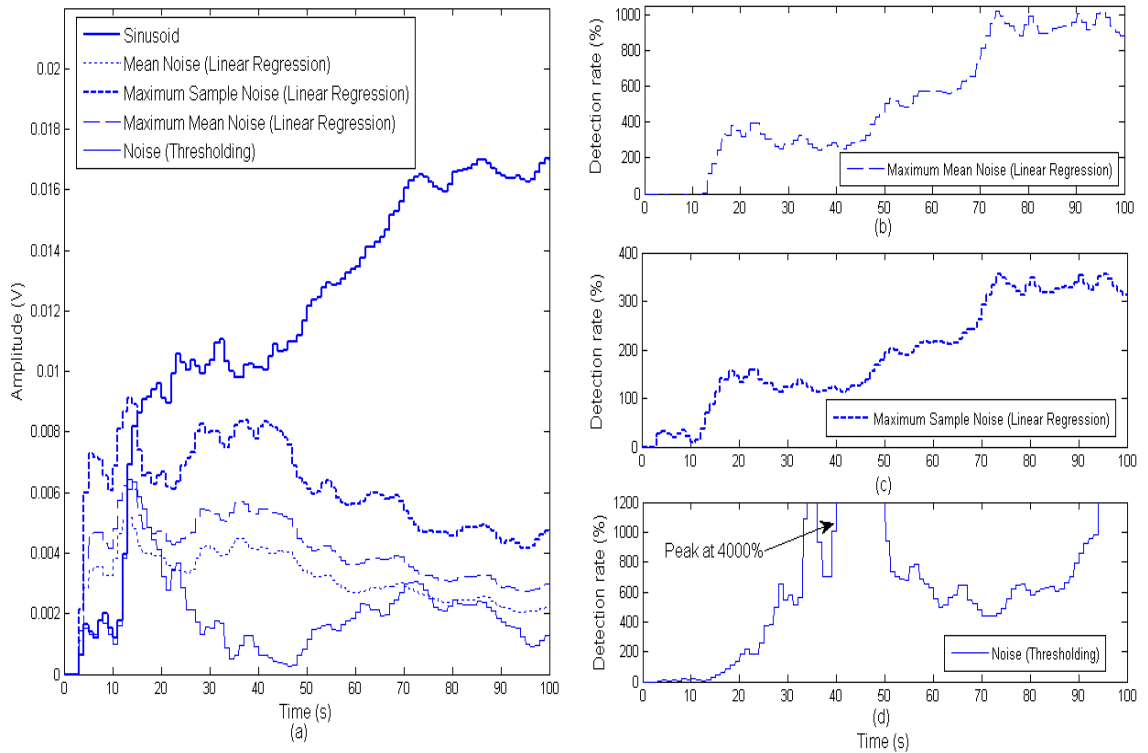


Figure 6.5: Relationship between thresholding and linear regression detection rate responses.

The former approach shown in Figure 6.5b indicated detection rate of 95% achieved at 13s, meaning that at a probability of 95% confident that the ASSR cannot be part of the background noise but with 5% chances of error, hence the 95% mark can be seen as a threshold. Although the 95% CI is defined as the threshold, the threshold is non-stationary but varying from between time interval depending only on the error deviation of the estimated noise amplitudes.

Meanwhile, the second approach displayed detection rate of 95% in Figure 6.5c at 14s, which indicates that the estimated sinusoid is 95% unlikely to be part of the sampled background noise, and again only 5% chances that the decision could be inaccurate.

In other word, both approaches attempt to produce a statistical hypothesis to indicate the likelihood of the estimated sinusoid is not part of the background noise, thus indirectly means that the estimation is a genuine desired signal. In general, both proposed detection methods (i.e. thresholding and regression) are able to distinct the existence and non-existence of the sinusoid at low SNR condition. However, a desirable automatic approach is developed using statistical regression approach, and without *a priori* defined thresholds which is time consuming and can be impractical in some applications.

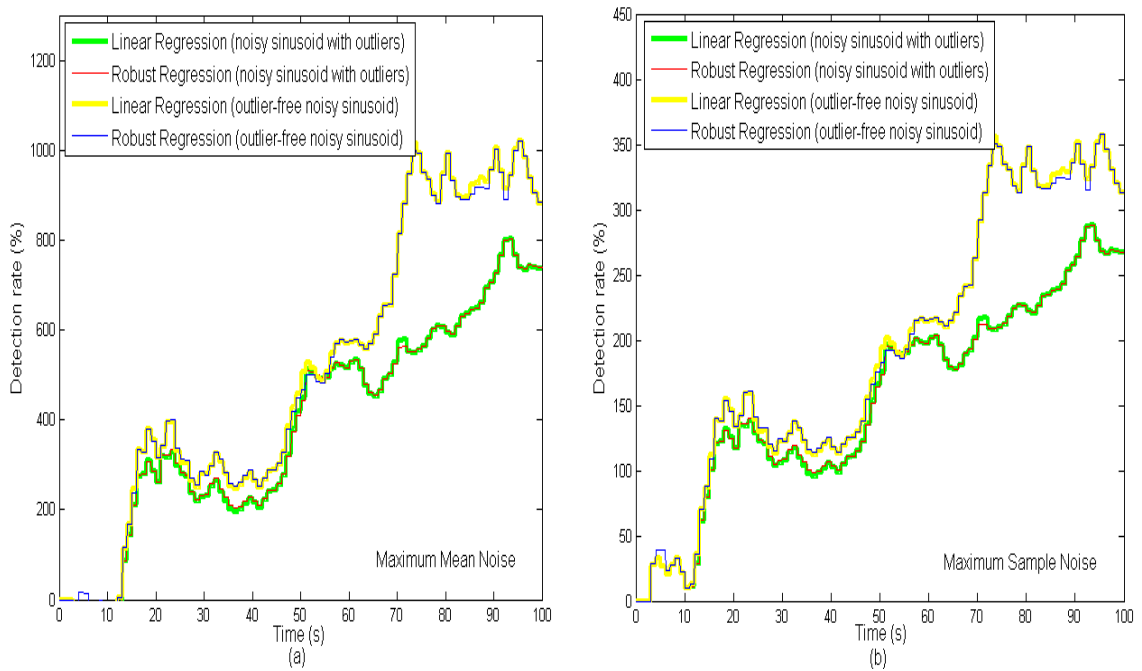


Figure 6.6: Comparative performances between linear and robust regression methods in detection of outlier-free noisy sinusoid and with contamination of outliers.

As seen from Figure 6.5, the linear regression performs satisfactory in identifying the existence of the sinusoid. To demonstrate the performances between the linear and robust regression methods in a more extreme scenario, noisy sinusoidal signals $y(k) = 0.015 \sin(180\pi k) + v(k)$ were generated where one consisted of outliers as shown in Figure 5.4 (having synthesized parameters as in Table 5.1) and the other is outlier-free (similar to Figure 5.4 but without outliers). As illustrated in Figure 6.6, the responses were smaller for the synthetic data with outliers when either of the approach was used in determining the existence of the sinusoid, as in Figure 6.6a and Figure 6.6b. Nonetheless, both regressions methods show capability in identifying the existence of the sinusoids, even in scenario where outliers existed. However, the response via the robust regression method shows close similarity to the response by the linear regression

method without being significant apart from each other in the study. In principle, the robust regression would perform better than the linear regression when outliers exist. This could be because of the background noise estimators were placed symmetrically on both sides of the desired sinusoid (or ASSR) signal, thus the effects of outliers would have been diminished or reduced. In addition, with the fusion-based ASSR detector (from Chapter 5) used instead of the AKF-based ASSR detector (from Chapter 4), improvements were made since the former detector consist of robust capability.

6.4.2 Experimental Results

To illustrate the performances of both thresholding and regression methods practically, real ASSRs data recorded via BIOPAC system were tested. The outcomes from the tests confirmed the simulation remarks regarding the faster detection speed of the regression approaches (linear and robust) and the similarity responses obtained from either linear or robust regression, as shown in Figure 6.7.

As mentioned in Chapter 4, though the thresholding performs satisfactory in identifying the ASSR existence, but with a drawback of the need of empirical trials to pre-determine the level of threshold. Despite the fact that it is time consuming, the threshold may sometimes be viewed as ‘too general’ in a sense it may not properly represent a specific case. No doubt that the estimated ASSR is significantly different from its estimated noise via thresholding as in Figure 6.7a, yet its detection responses (see Figure 6.7d), is close to but yet to exceed or reach the 200% which is the pre-defined threshold via empirical study. On the other hand, the regression approaches provide a self-tune thresholding capability that tuned according to each individual case and without the need or any pre-determined threshold. Moreover, both regression approaches in Figure 6.7b and Figure 6.7c indicate the existence of ASSR in less than 5s, whereas the thresholding is four times slower before pre-defined threshold of 200% is achieved at approximately at 20s.

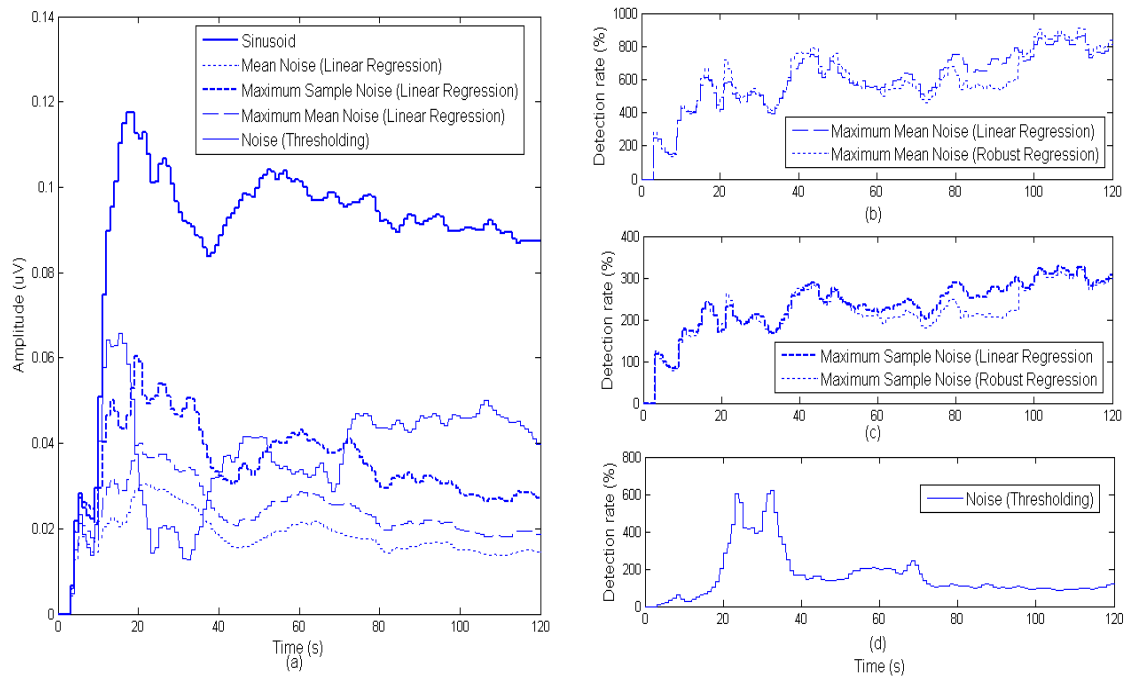


Figure 6.7: ASSR determination via linear regression and by thresholding.

The results presented so far were based on single ASSR detection (using the layout in Figure 6.1), whereas a comparative of multiple ASSRs (8 stimuli are presented simultaneously) detection between the proposed approach (using the layout in Figure 6.4) and the commonly used techniques is illustrated in Table 6.2. These multiple ASSRs data used in the comparison and the simulation of both the averaging techniques (normal and weighted averaging) were obtained from MASTER Demo Tutorial package provided by Rotman Research Institute (2001). Only the linear regression method is presented, because of the insignificance different between the robust and the linear regressions and yet more complex calculation involved. The linear regression approach used is based on the schematic shown in Figure 6.4, which is a scaled version that reduces the number of ASSR detectors used, thus less computation intense. As mentioned earlier in the chapter, there are two ways of indicating the existence of the ASSR statistically via regression approach, one is based on the concept of exceeding the mean of the surrounding noise by the estimated signal and the second approach is based on estimated signal to be located far from the sampled population of background noise, thus hypothetically the likelihood of the estimated signal is not noise but the expected ASSR. For example, if the desired signal achieves 95% marking in the second approach, it will definitely exceed the first approach as it concern is sample noise population than their mean value.

In addition, the second approach is not only used as to identify the existence of ASSR, it also acts as a representation of the estimated signal within the regression boundaries in the time domain instead of the frequency domain. According to the statistical method (F-test) used within MASTER, an expected (average) value is used based upon the surrounding noise. Hence, in principle the first approach proposed which based on the finding the noise amplitude from the regression line with 95% CI is similar to the statistical method used in MASTER, and therefore a more suitable choice for comparison than the boundaries created via 95% CI of the sampled population.

The comparison used is based on the first concept of identifying ASSR on the basis of exceeding the expected (mean value) of the background noise, since this approach can be viewed to be in principle similar to the F-test used by both averaging methods from MASTER. According to Table 6.2, the proposed linear regression method outperforms the averaging methods by 6 out of 8 ASSR detections for the second and third data set but was poor against the first set of data. The key reason for its poor performance is mainly because of the occurrence of excessive extreme artefacts. These were significantly larger in duration which might exceed the limits of fused sample mean ($N=1000$) and median ($N=5000$) operators. Therefore, extreme outliers like these would have caused a significant decrease in Kalman gains within the detector and consequently reduced its convergence rate.

Stimulus (Hz)	MASTER Normal Averaging Time, (s)	MASTER Weighted Averaging Time, (s)	Automatic ASSR Detector (Linear Regression, 95%) Time, (s)	
			N=1k and 5k	N=5k and 5k
			<u>Data set 1</u>	
78.125	180.244	147.456	NA	145
80.078	65.536	81.92	120	24
83.008	65.536	32.768	30	30
84.961	16.384	16.384	18	24
86.914	16.384	16.384	22	26
89.844	16.384	16.384	7	38
91.797	65.536	65.536	NA	54
94.727	32.768	32.768	NA	20
			<u>Data set 2</u>	
78.125	16.384	65.536	7	12
80.078	49.152	98.304	23	24
83.008	16.384	16.384	12	12
84.961	32.768	32.768	40	25
86.914	16.384	16.384	12	12
89.844	32.768	32.768	45	35
91.797	49.152	49.152	14	14
94.727	114.688	131.072	80	90
			<u>Data set 3</u>	
78.125	196.608	196.608	60	87
80.078	163.384	131.072	57	63
83.008	16.384	16.384	17	17
84.961	32.768	32.768	24	25
86.914	16.384	16.384	5	7
89.844	16.384	16.384	4	18
91.797	16.384	16.384	24	27
94.727	49.152	32.768	43	45

Table 6.2: Comparison between proposed method and other conventional methods.

In order counter these artefacts or outliers, the sampled length N (adaptation step size) of Eqn. (4-25) can be increased to allow more data points to be used to improve its variance estimation, thus indirectly improve its resistive against these unanticipated extreme values. According to Table 6.2, improvement were made via increasing N but with a drawback of slower initial convergence rate because of sufficient data points were required before any reliable variance can be estimated. This limits some early detection results obtained when using lower N , but does lead to significant detection rate improvements in some cases where the use of a lower N operator is impossible.

As a result, in extreme cases like data set 1, having larger adaptation step size means improve the detector's breakdown point with larger sampled data point would improve the robust AKF robustness and indirectly making the proposed algorithm more artefacts resilient.

6.5 Concluding Remarks

As shown in this chapter, an automatic ASSR detection can be achieved by using regression modelling to estimate the unobserved background noise, thus to allow direct comparison with the estimated ASSR signal. This is seen as an objective approach because no *a priori* pre-defined threshold is required and it is adaptively self-tuned in real-time. In order to improve its accuracy and reliability in possible outlier-contaminated data sample, robust regression is used instead of linear regression modelling. The robust issue in this Chapter is different from Chapter 5. Chapter 5 is concerned with the existence of outliers when processing the ASSR estimate within an adaptive Kalman filter. On the other hand, the focus here is about improving the reliability in estimating background noise from the regression module.

Although in theory the robust approach should have had the upper hand compared with linear regression, the simulation study does not indicate much difference between both methods. In addition, the linear regression has been selected after taking into account the complexity of the robust regression. The results from the linear regression-based ASSR approach are generally comparable to the averaging methods but with 10 out of 24 trials performing better when using higher data numbers N , as shown in Table 6.2.

7 . Conclusions and Future Research Intentions

7.1 Summary and Conclusion

The ASSR technique is a reliable way to assess hearing thresholds objectively. The most important merit of this technique compared with other objective hearing threshold methods is its frequency specificity. Currently, the technique is mainly used as a follow-up diagnostic protocol of the hearing screening (e.g. OAE or ABR technique) for the “difficult-to-test” group which mainly are from infants. The technique employed in the follow-up protocol provides some vital information for further appropriate measures to be taken, for examples, for middle ear surgery, the application of a hearing aid or the implantation of a cochlear implant. Due to the availability of frequency specific information, hearing aids can be fitted in a more optimal way for subjects with limited or no echo feedback. Unfortunately, the ASSR technique is not without drawbacks. In general, the ASSR amplitudes (in nV) are very small compared to the EEG or seen as the background noise (in uV) where the ASSR is embedded in the measured signal. In addition, the detection of ASSR is more difficult than the ABR detection (hundreds of nVs). Therefore, the duration of the ASSR detection can be quite lengthy due to the nature of the responses and the contamination of unwanted background noise (e.g. EEG

and instrumental interferences) and artefacts (e.g. muscle movement and eye blinking). However, the use of long recording and processing sessions may not always guarantee reliable hearing detection, especially if the subject is not relaxing or non-sedated. Faced with these challenges, proposing a hearing screening protocol based on the ASSR technique can be challenging and not practical, mainly because of its lengthy test duration. Therefore, the focus of the thesis is to develop an ASSR detection technique to reduce the lengthy recording time, increase its robustness against potential occurrence of artefacts and yet without or minimal in compromising its detection rate. Several attempts were conducted in order to tackle the challenges mentioned, which led to the development of automatic ASSR detection scheme which operates adaptively in real-time, artefacts-robust and automatic in identification.

Chapter 1 introduced and addressed the importance of the ASSR technique and the challenges faced for its limited use so far. In order to understand the ASSR, an overview on the topic is provided in Chapter 2 and together with the discussion on the existing conventional detection methods. The most popularly use combination of approaches or detection protocol so far is based upon artefacts-rejection, averaging, FFT and statistical test. This combined detection protocol performs better among other existing methods, but the issue regarding the lengthy test time remains an open research topic with rooms for improvements.

A new route is taken to further improve the ASSR detection by addressing the detection from the viewpoint of filtering or state estimation. The detection of the weak ASSR embedded within an overwhelm background noise (including potential artefacts interferences) is seen as detection of a noisy sinusoid oscillating at a known frequency as the ASSR is a sinusoid-like signal. Chapter 3 initially presented the simulation trials with synthetic data conducted using the observer-based detector to validate its performance and followed up with the detection with experimental recorded AEP. BIOPAC data acquisition system is used for AEP recording in the project and has not been reported so far its usage in ASSR recording elsewhere. In general, BIOPAC data acquisition had been used in many education and research institutions, and it is a reliable system at moderate costs. Preliminary studies on the ASSR in responses to its variable characteristics (e.g. relation to stimulus intensity, modulation frequency and etc.) are carried out by using BIOAPC data acquisition system and processed by the

observer-based ASSR detector. The purpose is to verify and evaluate the performances of both the BIOPAC system and the proposed observer-based ASSR detection scheme.

Chapter 4 introduced an adaptive state estimation technique (discrete type) known as adaptive Kalman filtering into the ASSR detector. The key advantages of this approach to the observer-based method are its adaptive gain tuning and noise statistic estimation capability. This is vital in practical AEP processing, where the background noise statistics is unknown and may be time-varying. Both the observer and Kalman techniques are structurally equivalent and comparable in terms of performances, with one commonly implemented in continuous time (observer-based) and the other in discrete time (KF-based). However, the discrete version enables easier adaptable parameters updating for digital implementation in modern days applications. According the results presented in Chapter 4, the AKF-based ASSR detection scheme performed satisfactory in determining the existence and non-existence of ASSR. Moreover, by combining the output responses of both ASSR (fundamental frequency) and its harmonic (first), thus this can further reduce the test time needed.

An artefacts-robust ASSR detection based on MSDF method was developed in Chapter 5. The concept of this approach is to fuse the output responses from the ASSR detection scheme in Chapter 4 with respectively the sample mean operation and sample median operation. In nature, the sample mean operator is more efficient in producing higher consistency outputs (less deviation from the true mean) than the sample median operator if the data samples are without outliers, whereas the sample median is highly robust against artefacts (outliers) as compared to the sample mean. The breakdown point of the sample mean is 0% which means its measurement is very vulnerable even to a single extreme value or outlier. On the other hand, the sample median has a breakdown point of 50%. This means that at least half of the data points must be artefacts for its measurement to be inaccurate and biased. Since both operators have their advantages and disadvantages, the MSDF approach is used in order to obtain the best from the two. Through fusion, the MSDF-based ASSR detection achieved faster detection rate and more artefact-robust as compared to the non-fused ASSR detection algorithm in Chapter 4.

In Chapter 6, a regression modelling based method has been developed to provide an automatically tuned threshold level. Before that, determination of the existence or non-

existence of ASSR had been based upon empirically pre-defined constant threshold level throughout a test. The approach generally works well under the assumption that the background noise statistics and its SNR are stationary, but this is not without drawbacks. If the assumption is violated, the ASSR detection is no longer operating appropriately (assumed slight variation) due to the fact if the SNR is lower than empirically expected and if the threshold remained unchanged, this would cause an increase in false alarm in detection. On the other hand, if the SNR is higher than initially expected, this would lead to delay in detection or identification. Therefore, the proposed automatically tuned thresholding is adaptively tuned on-line, thus objective thresholding can be achieved. Generally speaking, linear regression approach is reliable and performs well but a more outlier-resistive method known as robust regression is introduced. The performance of the robust regression method is comparable to the linear regression if the data set is not contaminated with outliers or when the number of data samples used is large (with limited numbers of outliers). If otherwise, the robust regression approach should be more suitable because of its robustness against outliers. However, no significant difference as initially expected for these cases had been observed in the simulations carried out in this study.

In accordance to the results obtained in this thesis, it is clear that the proposed real-time ASSR detection algorithm based on the combination of AKF and MSDF is comparable to if not better than the most widely used averaging approach (i.e. used in MASTER). The proposed detector has its advantages in terms of

- Real-time adaptability- operates in real-time with shorter ‘window’ or data length in estimating the noise covariance. On-line covariance estimation allowed adaptive detection via self-tuneable gains.
- Detection rate- improved the detector’s ability to operate under very poor SNR environment and yet with reliable response.
- Artefact-robustness- improved the robustness of noise covariance estimation against unprecedented artefacts that could bias the reliability of the detection.
- Objective decision making-ability to automatically identify the existence or non-existence of ASSR objectively via self-tuning threshold.

On the other hand, the existing sequence of methods used in MASTER required sophisticated processing protocol in terms of hardware and acquisition unit. Moreover, the averaging and FFT involved demanded specific minimum length of recorded data for reasonable output resolution.

Although advanced signal processing techniques (e.g. detection scheme proposed in this thesis) improve the ASSR detection rate and reduce the test time required, others factors (e.g. types of stimuli chosen, choices of electrodes placement, selection of test environments and etc.) may also affect the ASSR detection. As a result, to further enhance the detection rate of the ASSR, all possible influencing factors have to be taken into consideration while conducting ASSR assessment through combining different approaches (e.g. advanced signal processing techniques, types of stimuli modulation and etc.) and optimising their conditions (e.g. use of multiple stimuli, control test environment and etc.).

As discussed in the thesis, ASSR technique shows promising merits against other objective hearing tests due to its valuable frequency specific information. So far, the ASSR is mainly used as a hearing diagnostics tool because of the lengthy test duration needed, and still the time required in running the audiometric diagnosis is lengthy. In order to implement the ASSR as a hearing screening tool, the lengthy test time is the primary concern. This thesis aims to reduce the ASSR test duration, and to improve its robustness against background noise or unwanted artefacts with reliable detection rate, by developing an autonomous ASSRs detection scheme that performs in real-time. In addition, sophisticate hardware requirements that normally associated with the standard averaging method are avoided, which would ensure structurally simpler ASSR detection system to be implemented. To summarise, the implementation of the ASSR technique as a hearing screening tool will become a reality with the long standing challenges faced overcome. As a result, patients from the “difficult population” will be directly benefited.

7.2 Future Research Direction

Although the proposed ASSR detection framework (single-channel measurement) demonstrated improvement in shortening the test duration while being robust against possible artefacts, there is still room for improvements. Further research intentions are addressed as follows.

AEP modelling: Due to the challenges faced in ASSR detection and the nature of its response, generation of an ASSR model will help to predict the pattern of the response more effectively, such a model can also be used in the development of new detection

algorithms. Thus, further reducing the lengthy test time and improving the capability of ASSR detection are possible.

Generalization of the detection algorithm: The ASSR detection problem can be seen as a classical signal estimation or filtering. This means the proposed ASSR detection scheme can be applied to other applications through specific ad-hoc modification tailored to particular applications. The key merit of the proposed detection algorithm is of its detection rate performance within low SNR condition (i.e. -30dB).

For instance, the current proposed ASSR detection scheme can also be adapted and tailored specifically to detect distortion product otoacoustic emission (DPOAE) which is also a type of objective hearing screening technique, but its main focus is to screen human cochlear function in which is the main source of sensorineural hearing loss. In general, DPOAE and ASSR both provide frequency specific and quantitative assessment of the hearing capability. With the acoustically measured DPOAEs evaluate the activity of the cochlea's outer hair cell (OHC), whereas the electrically measured ASSRs evaluate the responses of the auditory nervous system. DPOAE test is often view as a fast, efficient and reliable test of cochlear function. In addition, the DPOAE are steady-state responses evoked using two tones of frequencies f_1 and f_2 , where $f_1 < f_2$, $f_2/f_1 = 1.2$, and the most robust DPOAE appears at the frequency $f_{dp} = 2f_1 - f_2$. The greatest advantage of DPOAE compared to ASSR is its fast detection and is widely accepted as part of a standard hearing screening tool. However, its biggest concern would be its robustness against background noise, where typically DPOAE is one of few hearing tests conducted under non-controlled environments.

Other potential applications of the detection algorithm are for examples in extracting electrocardiogram (ECG) from noise interferences (e.g. power-line and other physiological noise), and deploy as an estimator in the field of brain-computer interface (BCI) to detect human physiological signal (e.g. muscle movement) that is vital in bio-feedback or rehabilitation in healthcare applications.

References

Abidi, M. A., and Gonzalez, R. C. (1992), *Data Fusion in Robotics and Machine Intelligence*, Boston: Academic.

Ahn, J. H., Lee, H. S., Kim, Y. J., Yoon, T. H., and Chung, J. W. (2007), “Comparison pure-tone audiometry and auditory steady state response for the measurement of hearing loss”, *Otolaryngology-Head and Neck Surgery*, 136, 966-971.

Alspach, D. L., and Abiri, A. (1974), “A Bayesian solution to the problem of the state estimation in an unknown noise environment”, *International Journal of Control*, 19.

Anderson, B., and Moore, J. (1979), *Optimal Filtering*, New Jersey: Prentice-hall.

Aoyagi, M., Kiren, T., Furuse, H., Fuse, T., Suzuki, Y., Yokota, M., and Koike, Y. (1994), “Pure-tone threshold prediction by 80-Hz amplitude-modulation following response”, *Acta. Otolaryngol. Suppl.*, 511, 7-14.

Bar-Shalom, Y. and Li, X. (1995), *Multitarget–Multisensor Tracking: Principles and Techniques*, Storrs: YBS Publishing.

Belanger, P. R. (1974), “Estimation of noise covariance matrices for linear time-varying stochastic process”, *Automatica*, 10, 267-275.

Bess, F. H., and Humes, L. E. (1995), *Audiology: the fundamentals*, Baltimore: Williams & Wilkins.

Brookhouser, P. E., Gorga, M. P., and Kelly, W. J. (1990), “Auditory brainstem response results as predictors of behavioral thresholds in severe and profound hearing impairment”, *Laryngoscope*, 100(8), 803-810.

Brown, M. D. (2005), Genetic Mutation Links Diabetes and Hearing Loss, Hearing Health [Online]. Available at: http://www.drf.org/hearing_health/archive/2005/winter05_geneticmutation.htm.

Brown, R. G., and Hwang, P. Y. C. (1997), *Introduction to Random Signals and Applied Kalman Filtering*, 3rd edition, New York: John Wiley & Sons.

Campbell, F. W., Atkinson, J., Francis, M. R. and Green, D. M. (1977), "Estimation of auditory thresholds using evoked potentials: A clinical screening test", *Progress in Clinical Neurophysiology*, 2, 68–78.

Carrew, B., and Bellanger, P. (1973), "Identification of optimum filter steady state gain for systems with unknown noise parameters", *IEEE transactions on Automatic Control*, 18(6), 582-587.

Chang, K. C., Saha, R. K., and Bar-Shalom, Y. (1997), "On optimal track-to-track fusion", *IEEE Transactions on Aerospace and Electronic Systems*, 33, 4, pp1271-1276.

Chong, C. Y., Mori, S., Baker, W. H., and Chang, K. C. (2000), "Architectures and Algorithms for Track Association and Fusion", *IEEE Aerospace and Electronic Systems*, 15(1), 5-13.

Clark, G. (2003), *Cochlear implants, fundamentals & applications*, New York: Springer-Verlag.

Clopton, B. M., and Viogt, H. F. (2006), *Auditory System*, In: Bronzino J D (ed), *The Biomedical Engineering Handbook: Biomedical Engineering Fundamentals*, 3rd ed., Taylor & Francis.

Cohen, B. C., and Sances, Jr. A. (1977), "Stationary of the human encephalogram", *Med. Biol. Eng. Comput.*, 15, 515-518.

Cohen, L. T., Rickards, F. W. And Clark, G. M. (1991), "A comparison of steady-state evoked potentials to modulated tones in awake and sleeping humans", *Journal of the Acoustical Society of America*, 90(5), 2467–2479.

Cone-Wesson, B., Dowell, R. C., Tomlin, D., Rance, G., & Ming, W. J. (2002a), "The auditory steady-state response: comparison with the auditory brainstem response", *J. Am. Acad. Audiol.*, 13(4), 173-187.

Cone-Wesson, B., Parker, J., Swiderski, N., & Rickards, F. (2002b), "The auditory steady-state response: full-term and premature neonates", *J.Am. Acad. Audiol.* 13(5), 260-269.

Dalzell, L., Orlando, M., MacDonald, M., Berg, A., Bradley, M., Cacace, A., et al. (2000), "The New York State universal newborn hearing screening demonstration project: ages of hearing loss identification, hearing aid fitting, and enrolment in early intervention", *Ear and Hearing*, 21(2), 118-130.

Dario, P. (1988), *Sensors and Sensory Systems for Advanced Robots*, Springer-Verlag.

Dee D P, Cohen, S. E., Dalcher, A., and Ghil, M. (1985), "An efficient algorithm for estimating noise covariances in distributed systems", *IEEE Transactions on Automatic Control*, 30(11), 1057-1065.

Dillon, H. (2001), *Hearing aids*, New York: Thieme Publishers.

Draper, N. R., and Smith, H. (1981), *Applied Regression Analysis*, London: Wiley.

Drimitrijevic, A., John, M. S., Van Roon P, Purcell, D. W., Adamonis, J., Ostroffs J, et al. (2002), Estimating the audiogram using multiple auditory steady-state responses, *J. Am. Acad. Audiol.*, 13(4), 205-224.

Drolet, L., Michaud, F., and Cote, J. (2000), Adaptable Sensor Fusion using Multiple Kalman Filters, *Proc. IEEE/RSJ Intl. Conf. on Intelligent Robots and System*, Takamatsu, Japan.

Dunn, K. P., Wilner, D., and Chang, C. B. (1976), Kalman Filter Algorithm for a Multisensor System, *Proc 15th IEEE Conf. Decision Control*.

Fox, J. (1997), *Applied Regression Analysis: Linear Models and Related Methods*, Sage.

Friedland, B. (1982), "Estimating noise variances by using multiple observers", *IEEE transactions on Aerospace and Electronic Systems*, 18, 442-448.

Friedland, B. (1990), On estimation of noise variance in linear dynamics systems by multiple observer, *Proceedings of 5th International Symposium on Intelligent Control*, Philadelphia, PA.

Fulton, T. R., and Lloyd, L. L. (1969), *Audiometry for the Retarded*, Baltimore: The Williams & Wilkins Company.

Galambos, R., Makeig, S., and Talmachoff, P. J. (1981), "A 40-Hz auditory potential recorded from the human scalp", *Proceedings of the National Academy of Science USA*, 78(4), 2643-2647.

Gao, J. B. and Harris, C. J. (2001), "Some Remarks on Kalman Filters for the Multisensor Fusion", *Elsevier Information Fusion*, 3, 191-201.

Geisler, C. D. (1960), *Average response to clicks in man recorded by scalp electrodes*, *Technical Report*, Cambridge: M.I.T.

Gelb, A. (1974), *Applied Optimal Estimation*, MIT Press.

Goodman I R, Mahler, R. P., and Nguyen, H. T., (1997), *Mathematics of Data Fusion*, London: Kluwer Academic Publishers.

Hall, D. L., and Linn, R. J. (1991), Survey of commercial software for multisensor data fusion, *Proc. SPIE Conf. Sensor Fusion and Aerospace Applications*, Orlando, FL.

Hall, D. L. and Llinas, J. (1997), "An Introduction to Multisensor Fusion", *Proc. IEEE*, 85(1), 6-23.

Hall, J. W. (1992), *Handbook of Auditory Evoked Responses*, Needham: Allyn & Bacon.

- Hall, J. W. (2000), *Handbook of Otoacoustic Emissions*, San Diego: Singular Publishing Group.
- Hampel, F. R. (1971), “A general qualitative definition of robustness”, *Annals of Mathematics Statistics*, 42, 1887–1896.
- Hampel, F. R. (1974), “The influence curve and its role in robust estimation”, *Journal of the American Statistical Association*, 69, 382–393.
- Hampel, F. R., Ronchetti, E. M., Rousseeuw, P. J., Stahel, W. A. (1986), *Robust Statistics: The Approach Based on Influence Functions*, London: Wiley.
- Harris, C., Bailey, A., and Dodd, T. (1998), “Multisensor data fusion in defense and aerospace”, *Journal of Royal Aerospace Society*, 162(1015), 229–244.
- Hashemipour, H. R., Roy, S., and Laub, A. J. (1988), “Decentralized structures for parallel Kalman filtering”, *IEEE Trans. Automatic Control*, 33(1), 88-93.
- Haughton, P. (2002), *Acoustics for Audiologists*, London: Elsevier Academic Press.
- Hayter, A. J. (2002), *Probability and Statistics: For Engineers and Scientists*, Duxbury and Thomson Learning.
- Heardman, A. T. and Stapells, D. R. (2001), “Thresholds determined using the monotic and dichotic multiple auditory steady-state response technique in normal-hearing subjects”, *Scand. Audiol.*, 30, 41-49.
- Heardman, A. T. and Stapells, D. R. (2003), “Auditory steady-state response thresholds of adults with sensorineural hearing impairment”, *Int. J. Audiol.*, 42, 237-248.
- Herdman, A., Lins, O., Van Roon, P., Stapells, D. R., Scherg M and Picton, T. W. (2002), “Intracerebral sources of human auditory steady-state responses”, *Brain Topography*, 15(2), 69–86.

Hilborn, Jr. C. G., and Lainiotis, (1969), “Optimal estimation in the presence of unknown parameters”, *IEEE Transactions on Syst. Sci. Cyben.*, 5, 38-43.

Hou, M. (2005), “Amplitude and frequency estimator of a sinusoid”, *IEEE Trans. Automat. Contr.*, 50, 855-858.

Hsu, Y C, Younger, J., and Balakrishnan, S. N. (1991), Estimation of process noise covariance in home guidance, *Proceedings of 1991 American Control Conference*, Boston, MA, 2309-2310.

Huber, P. J. (1981), *Robust Statistics*, New York: Wiley.

International Organization for Standardization (1998), Acoustics-Reference zero for the calibration of audiometric equipment [Online], Available at: <http://www.iso.org>.

John, M. S., and Picton, T. W. (2000a), “MASTER: a Windows program for recording multiple auditory steady-state responses”, *Computer Methods and Programs in Biomedicine*, 61, 125-150.

John, M. S. and Picton, T. W. (2000b), “Human auditory steady-state responses to amplitude-modulated tones: Phase and latency measurements”, *Hearing Research*, 141, 57-79.

John, M. S., Dimitrijevic, A., and Picton, T. W. (2001a), “Weighted averaging of steady-state responses”, *Clin. Neurophysiol*, 112, 555-62.

John, M. S., Dimitrijevic, A., Van Roon, P., and Picton, T. W. (2001b), “Multiple auditory steady-state responses to AM and FM stimuli”, *Audiology & Neuro-Otology*, 6, 12-27.

John, M. S., Dimitrijevic, A., and Picton, T. W. (2002), “Auditory steady-state responses to exponential modulation envelopes”, *Ear & Hearing*, 23 (X), 106-117.

John, M. S., Brown, D. K., Muir, P. J., and Picton, T. W. (2004), “Recording Auditory Steady-State Responses in Young Infants”, *Ear & Hearing*, 25(6), 539-553.

Johnson, R. (1992), *Applied Multivariate Statistical Analysis*, London: Prentice Hall.

Joint Committee on Infant Hearing (2000), “Year 2000 position statement: Principles and guidelines for early hearing detection and intervention programs”, *Pediatrics*, 106, 798-817.

Kailath, T. (1968), “An Innovations Approach to Least-Squares Estimation Part I: Linear Filtering in Additive White Noise”, *IEEE Transactions on Automatic Control*, 13(6), 646-655.

Kalman, R. E. (1960), “A new approach to linear filtering and prediction problems”, *Trans. ASME Journal of basic Engineering*, 82, 35-45.

Kalman, R. E., and Bucy, R. (1960), “New results in linear filtering and prediction theory”, *ASME Journal of basic Engineering*, 83, 95-108.

Kashyap, R. L. (1970), “Maximum Likelihood identification of stochastic linear systems”, *IEEE Transactions on Automatic Control*, 15, 25-34.

Kemp, D. T. (1979), “Evidence of mechanical nonlinearity and frequency selective wave amplification in the cochlea”, *Arch. Otorhinolaryngol.*, 224, 37-45.

Kuwada, S., Anderson, J. S., Batra, R., Fitzpatrick, D. C., Teissier, N., and D’Angelo, W. R., (2002), “Sources of the scalp-recorded amplitude-modulation following response”, *Journal of the American Academy of Audiology*”, 13(4), 188–204.

Kwakernaak, H., and Sivan, R. (1972), *Linear optimal control systems*, New York: Wiley-Interscience.

Linden, R. D., Chambell, K. B., Hamel, G., and Picton, T. W. (1985), “Human auditory steady-state evoked potentials during sleep”, *Ear and Hearing*, 6(3), 167–174.

Lins, O. G., and Picton, T. W. (1995), “Auditory steady-state responses to multiple simultaneous stimuli”, *Electroencephalography and Clinical Neurophysiology*, 96, 420-432.

Lins, O. G., Picton, T. W., Boucher, B. L., Durieux-Smith, A., Champagne, S. C., Moran L M, *et al.* (1996), "Frequency specific audiometry using steady-state responses", *Ear and Hearing*, 17(2), 81-96.

Llinas, J., and Waltz, E. (1990), *Multisensor Data Fusion*, Boston, MA: Artech House.

Loizou, P. C. (1998), "Mimicking the Human Ear", *IEEE Signal Processing Magazine*, 101-130.

Luenberger, D. G. (1971), "An Introduction to Observers", *IEEE Trans. Automat. Contr*, 16, 596-602.

Luts, H. and Wouter, J. (2005), "Comparison of MASTER and AUDERA for measurement of auditory steady-state responses", *Int. J. Audiology*, 44, 244-253.

Luts, H. (2005), Diagnosis of hearing loss in newborns: Clinical application of auditory steady-state responses, PhD thesis, Katholieke Universiteit Leuven, Leuven, Belgium.

Luts, H., and Wouters, J. (2004), "Hearing assessment by recording multiple auditory steady-state responses: the influence of test duration", *Int. J. Audiology*, 43(8), 471-478.

Luts, H., Desloovere, C., Kumar, A., Vandermeersch, E., and Wouters, J. (2004), "Objective assessment of frequency-specific hearing thresholds in babies", *Int J Pediatr Otorhinolaryngol*, 68(7), 915-26.

Luts, H., Desloovere, C., and Wouters, J. (2006), "Clinical application of dichotic multiple-stimulus auditory steady-state responses in high-risk newborns and young children", *audiol. Neuro-Otol.*, 11, 24-37.

Magill, D. T. (1965), "Optimal adaptive estimation of sampled stochastic process", *IEEE Transactions on Automatic Control*, 10, 434-439.

Maiste, A. and Picton, T. (1989), "Human auditory evoked potentials to frequency modulated tones", *Ear and Hearing*, 10, 153-160.

Malmivuo, J. and Plonsey, R. (1995), *Bioelectromagnetism: principles and applications of bioelectric and biomagnetic fields*, New York: Oxford University Press.

Mason, J. A., and Herrmann, K. R. (1998), "Universal infant hearing screening by automated auditory brainstem response measurement", *Pediatrics*, 101, 221-228.

Mason, S. (1993), *Electric response audiometry*, In: McCormick B (Ed.), Paediatric audiology 0-5 years, 2nd Edition, Whurr Publishers Ltd.

Maybeck, P. (1979), *Stochastic Model, Estimation, and Control-Volume 1*, New York: Academic Press.

McNamara, D. M., and Ziarani, A. K. (2004), A new adaptive technique of estimation of steady state auditory evoked potentials, *Conf Proc IEEE Eng Med Biol Soc.*, 6, 4544-4547.

Mehra, R. K. (1970a), "On the identification of variances and adaptive Kalman filtering", *IEEE transactions on Automatic Control*, 15(2), 175-184.

Mehra, R. K. (1970b), "An algorithm to solve matrix equation $PHT=G$ and $P=\Phi P \Phi^T + \Gamma \Gamma^T$ ", *IEEE Transactions on Automatic Control*, 15, 600.

Mehra, R. K. (1971), "On-line identification of linear dynamic with applications to Kalman filtering systems", *IEEE transactions on Automatic Control*, 16(1), 12-21.

Mehra, R. K. (1972), "Approaches to adaptive filtering", *IEEE Transactions on Automatic Control*, 17(5), 693-698.

Meyers, K. A., and Tapley, B. D. (1976), "Adaptive sequential estimation with unknown noise statistics", *IEEE Transaction on Automatic Control*, 21(4), 520-523.

Moghaddamjoo, A. (1986), Robust adaptive Kalman filtering with unknown inputs, *Proceedings of 1986 American Control Conference*, Seattle, WA.

Moore, B. C. J. (2003), *An introduction to the psychology of hearing*, 4th edn, Amsterdam: Academic Press,

Moore, D. S., and McCabe, G. P. (1999), *Introduction to the Practice of Statistics*, WH. Freeman & Company.

Morein, R., and Kalata, P. (1990), A polynomial algorithm for noise identification in linear system, *Proceedings of 5th International Symposium Intelligent Control*, Philadelphia, 595-600.

NHS (2008), Your Baby's Hearing Screening Test [Online], Newborn Hearing Screening Programme, Available at: <http://hearing.screening.nhs.uk/leaflets>.

Niedwiecki, M. (1988), Identification of nonstationary stochastic system using parallel estimation schemes, *Proceedings of 27th Conference Decision and Control*, Austin, TX, 258-263.

Niedwiecki, M. (1990), "Identification of time-varying system using combined parameters estimation and filtering", *IEEE transaction on Acoustic, Speech and Signal Processing*, 38(4), 679-686.

Nolte, J. (1988), *The human brain: an introduction to its functional anatomy*, 2nd edn, St. Louis: CV Mosby.

Northern, J. L., and Downs, M. P. (1991), *Hearing in Children*, 4th edn, Baltimore: Williams & Wilkins.

Oussalah, M., and De Schutter, J. (2000), Adaptive Kalman filter for noise identification, *International Conference on Noise and Vibration Engineering (ISMA25)*, 13-15 September.

Parker, D. J. and Matsebula, D. (1992), "The period evoked potential: a rapid technique for acquisition of phase-locked responses to continuous pure-tone stimulation", *Br. J. Audiol.*, 26, 335-8.

Perez-Abalo, M. C., Savio, G., Torres, A., Martin, V., Rodrigue, E., and Galan, L. (2001), "Steady-state responses to multiple amplitude-modulated tones: An optimized method to test frequency-specific thresholds in hearing-impaired children and normal-hearing subjects", *Ear Hear.*, 22, 220-211.

Petitot, C., Collett, L., and Durrant, J. D. (2005), "Auditory steady-state responses (ASSR): effects of modulation and carrier frequencies", *Int. J. Audiol.*, 44(10), 567-573.

Pickles, J. O. (1988), *An introduction to the physiology of hearing*, 2nd edn, London: Academic Press.

Picton, T. W. (1991), "Clinical usefulness of auditory evoked potentials: A critical evaluation", *JSLPA*, 15(9), 3-18.

Picton, T. W. (2006), *Audiometry Using Auditory Steady-State Responses*, In: Burkard R F, Don M and Eggermont J J (ed), *Auditory Evoked Potentials: Basic Principles and Clinical Application*: Lippincott Williams & Wilkins.

Picton, T. W. and John, M. S. (2004), "Avoiding electromagnetic artefacts when recording auditory steady-state responses", *Journal of the American Academy of Audiology*, 15, 541-554.

Picton, T. W., Dimitrojevic, A., John, M. S. And Van Roon, P. (2001), "The use of phase in the detection of auditory steady-state responses", *Clin. Neurophysiol.*, 112(9), 1698-1711.

Picton, T. W., John, M. S., Dimitrijevic, A., and Purcell, D. (2003a), "Human auditory steady-state responses", *International Journal of Audiology*, 42, 177-219.

Picton, T. W., John, M. S., Purcell, D. W. and Plourde, G. (2003b), "Human auditory steady-state responses: The effects of recording technique and state of arousal", *Anesthesia Analgesia*, 97(5), 1396-1402.

- Picton, T. W., Dimitrijevic, A. Perez-Abalo, M. C., and Van Roon, P. (2005), "Estimating audiometric thresholds using auditory steady-state responses", *J. Am. Acad. Audiol.*, 16(3), 143-156.
- Plourde, G., and Picton, T. W. (1990), "Human auditory steady state responses during general anesthesia", *Anesth Analg*, 71, 460–468.
- Plourde, G., Villemure, C., Fiset, P., Bonhomme, V., and Backman, S. B. (1998), "Effect of isoflurane on the auditory steady-state response and on consciousness in human volunteer", *Anesthesiology*, 89(4), 844-851.
- Qiang, G., and Harris, C. J. (2001), "Comparison of two measurement fusion methods for Kalman-filter-based multisensory data fusion", *IEEE Transactions on Aerospace and Electronic Systems*, 37(1), 273-280.
- Rance, G., Rickards, F. W., Cohen, L. T., De Vidi, S., and Clark, G. M. (1995), "The automated prediction of hearing thresholds in sleeping subjects using auditory steady-state evoked potentials", *Ear and Hearing*, 16(5), 499–507.
- Regan, D. (1966), "Some characteristics of average steady-state and transient responses evoked by modulated light", *Electroencephalogram Clinical Neurophysiology*, 20, 238-248.
- Regan, D. (1989), *Human brain electrophysiology: evoked potentials and evoked magnetic fields in science and medicine*, Amsterdam: Elsevier.
- Rickards, F. W. and Clark, G. M (1984), *Steady-state evoked potentials to amplitude-modulated tones*, Boston.
- Roecker, J. A. and McGillem, C. D. (1988), "Comparison of two-sensor tracking methods based on state vector fusion and measurement fusion", *IEEE Transactions on Aerospace and Electronic Systems*, 24(4), 447-449.

Rotman Research Institute (2001), MASTER: Multiple-Auditory-Steady-State-Evoked-Response [Demo], Available at: http://www.rotman-baycrest.on.ca/users/sasha_j/Masterdl.htm

Rousseeuw, P. J. and Leroy, A. M. (1986), *Robust Regression and Outlier Detection*, London: Wiley.

Sage, A. P., and Husa, G. W. (1969), Adaptive filtering with unknown prior statistics, *Proceedings of 1969 Joint Automatic Control Conference*, 1969, 760-769.

Saha, R. K. (1996), "Track-to-track with dissimilar sensors", *IEEE Transactions on Aerospace and Electronic Systems*, 32(3), 1021-1029.

Saha, R. K. and Chang, K. C. (1998), "An efficient algorithm for multisensory track fusion", *IEEE Transactions on Aerospace and Electronic Systems*, 34(1), 200-210.

Scharf, L. L., and Alspach, D. L. (1972), On stochastic approximation and an adaptive filter, *Proceedings of IEEE Conference on Decision and Control*, New Orleans, LA, 253-257.

Seikel, J. A., King, D. W., and Drumright, D. G. (2000), *Anatomy and physiology for speech, language, and hearing*, 2nd edn, San Diego: Singular Publishing Group.

Sharbrough, F., Chatrian, G. E., Lesser, R. P., Lüders, H., Nuwer, M. and Picton, T. W. (1991), "American Electroencephalographic Society Guidelines for Standard Electrode Position Nomenclature", *J. Clin. Neurophysiol*, 8(2), 200-202.

Sherwood, L. (1993), *Human Physiology: From Cells to Systems*, Minneapolis: West Publishing Co.

Simon, D. (2006), *Optimal State Estimation: Kalman, H_∞ and Nonlinear Approaches*, New York: Wiley.

Sinha, N. K. (1973), "Adaptive Kalman filtering using stochastic approximation", *Electronics Letters*, 9, 177-178.

Sinha, N. K., and Tom, A. (1977), "Adaptive state estimation for systems with unknown noise covariances", *International Journal of system sciences*, 18(4), 377-383.

Smith, D. and Singh, S. (2006), "Approaches to Multisensor Data Fusion in Target Tracking: A Survey", *IEEE Transaction on Knowledge and Data Engineering*, 18(12), 1696–1710.

Stapells, D. R., Linden, D., Suffield, J. B., Hamel, G., and Picton, T. W. (1984), "Human auditory steady state potentials", *Ear and Hearing*, 5(2), 105–113.

Stapells, D. R., Markeig, S., and Galambos, R., (1987), "Auditory Steady-State Responses– Threshold Prediction Using Phase Coherence", *Electroencephalography and Clinical Neurophysiology*, 67(3), 260-270.

Stapells, D. R., Herdman, A., Small, S. A., Dimitrijevic, A. and Hatton, J. (2004), Current Status of the Auditory Steady-State Responses for Estimating an Infant's Audiogram, In: Seewald RC, Bamford JM, eds. *A Sound Foundation Through Early Amplification 2004*. Basel, Switzerland: Phonak AG, pp. 43-59.

Stapells, D. R., Galambos, R., Costello, J. A., and Makeig, S. (1988), "Inconsistency of auditory middle latency and steady-state responses in infants", *Electroencephalography and Clinical Neurophysiology*, 71(4), 289–295.

Staudte, R. G. and Sheather, S. J. (1990), *Robust Estimation and Testing*, New York: Wiley.

Stueve, M. P., and O'Rourke, C. (2003), "Estimation of Hearing Loss in Children: Comparison of Auditory Steady-State Response, Auditory Brainstem Response, and Behavioral Test Methods", *Am J Audiol*, 12, 125-136.

Suzuki, T., and Kobayashi, K. (1984), "An evaluation of 40-Hz event-related potentials in young children", *Audiology*, 23, 599–604.

Swanepoel, D., and Hugo, R. (2004), “Estimations of auditory sensitivity for young cochlear implant candidates using the ASSR: preliminary results”, *Int J Audiol*, 43(7), 377-382.

The Hearing Research Trust (2005), Deafness the facts [Online], Available at: <http://www.deafnessresearch.org.uk/factsheets/hearing-tests-for-babies.pdf>.

Tlumak, A I., Durrant, J. D., and Collet, L. (2007), “80 Hz auditory steady-state responses (ASSR) at 250 Hz and 12,000 Hz”, *Int. J. Audiol.*, 46(1), 26-30.

University of Michigan Health System (2003), Test Methods: Summary Chart [Online], Available at: <http://www.med.umich.edu/childhearinginfo/test/summaryChart.pdf>.

van der Reijden C. S., MJens, L. H., and Snik, A. F. (2005),” EEG derivations providing auditory steady-state responses with high signal-to-noise ratios in infants”, *Ear Hear.*, 26(3), 299-309.

van der Reijden, C. S., Mens, L. H. and Snik, A. F. (2006), “Frequency-specific objective audiometry: Tone-evoked brainstem responses and steady-state responses to 40 Hz and 90 Hz amplitude modulated stimuli”, *Int. J. Audiol.*, 45,40-45.

Van Dun, B., Wouters, J., and Moonen, M. (2007a), “Improving auditory steady-state response detection using independent component analysis on multichannel EEG data”, *IEEE Trans. Biomed. Eng.*, 54(7), 1220-1230.

Van Dun, B., Wouters, J., and Moonen, M. (2007b), Multi-channel Wiener filtering based auditory steady-state response detection, *Proc. Int. Conf. Acoustic., Speech Signal Processing (ICASSP)*, vol II, Honolulu, HI, pp. 929-932.

Van Dun, B., Rombouts, G., Wouters, J. and Moonen, M. (2009), “A Procedural Framework for Auditory Steady-State Response Detection”, *IEEE Transactions on Biomedical Engineering*, 56(4), 1098-1107.

Van Maanen, A., and Stapells, D. R. (2005), “Comparison of multiple auditory steady-state responses (80 vs. 40Hz) and slow cortical potentials for threshold estimation in hearing-impaired adults”, *International Journal of Audiology*, 44, 613-624.

Wilcox, R. R. (2004), *Introduction to Robust Estimation and Hypothesis Testing*, 2nd Edition, San Diego: Academic Press.

Willsky A S, Bello, M., Castanon, D., Levy, B., and Verghe, G. (1982), "Combining and updating of local estimates and regional maps along sets of one-dimensional tracks", *IEEE Trans. Automatic Control*, vol. 27(4), 799-812.

Wright, F. (1980), "The fusion of multi-source data", *Signal*, 39-43.

Yetter C J (2006), How to Read an Audiogram [Online], Western Oregon University. Available at:
<http://www.wou.edu/education/sped/wrocc/HT%20Read%20Audiogram%20web.pdf>.

Yoshinaga-Itano, C., Sedey, A. L., Coulter, D. K., and Mehl, A. L. (1998), "Language of early- and later-identified children with hearing loss", *Pediatrics*, 102(5), 1161-1171.

Yost, W. A. (2000), *Fundamentals of hearing: An introduction*, 4th edn, San Diego: Academic Press.